

**HEAVY MINERAL CHARACTERIZATION OF BEACH SAND  
ALONG THE CANAGUINIM-POLEM STRETCH,  
SOUTH GOA**

A Dissertation

Course code and Course Title: GLO-301 Dissertation

Credits: 16

Submitted in partial fulfillment of Master's Degree in Applied Geology

By

**MELDRIN TITAN AFONSO**

Seat Number: 22P0450010

ABC ID-377461457178

PR.NO:20190322

Under the Supervision of

**Dr. POORNIMA ROHAN SAWANT**

School of Earth, Ocean and Atmospheric Science  
Goa University



**GOA UNIVERSITY**

**MAY 2024**




Examined by:

Seal of the School

### DECLARATION BY STUDENT

I hereby declare that the data presented in this Dissertation report entitled, "**Heavy Mineral Characterization of Beach Sand along the Canaguinim-Polem Stretch, south Goa**" is based on the results of investigations carried out by me at Goa University at the School of Earth, Ocean, and Atmospheric Science, Goa University under the supervision of Dr. Poornima Rohan Sawant and the same has not been submitted elsewhere for the award of a degree or diploma by me. Further, I understand that Goa University or its authorities will not be responsible for the correctness of observations / experimental or other findings given the dissertation.

I hereby authorize the University authorities to upload this dissertation to the dissertation repository or anywhere else as the UGC regulations demand and make it available to anyone as needed.

  
meidwin.Titan. Afonso

Signature and Name of Student

Seat no: 22P0450010

Date: 02/05/2024

Place: Goa University

### COMPLETION CERTIFICATE

This is to certify that the dissertation report "**Heavy Mineral Characterization of Beach Sand along the Canaguinim-Polem Stretch, south Goa**" is a bonafide work carried out by Mr. Meldrin Titan Afonso under my supervision in partial fulfillment of the requirements for the award of the degree of Masters in Applied Geology in the Department of Earth Sciences at the School of Earth, Ocean and Atmospheric Sciences Goa.

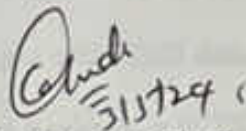


Dr. Poornima Rohan Sawant

Assistant professor

Goa University

Date: 02/05/2024



Senior Prof. Sanjeev Ghadi

Goa University

Dean School of Earth, Ocean and Atmospheric Science

Date:

Place: Goa University



School Stamp

**HEAVY MINERAL CHARACTERIZATION OF BEACH SAND  
ALONG THE CANAGUINIM-POLEM STRETCH,  
SOUTH GOA**

A Dissertation

Course code and Course Title: GLO-301 Dissertation

Credits: 16

Submitted in partial fulfillment of Master's Degree in Applied Geology

By

**MELDRIN TITAN AFONSO**

Seat Number: 22P0450010

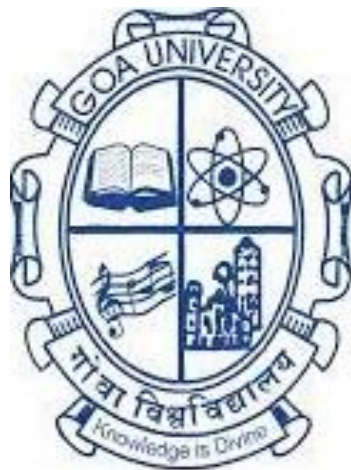
ABC ID-377461457178

PR.NO:20190322

Under the Supervision of

**Dr. POORNIMA ROHAN SAWANT**

School of Earth, Ocean and Atmospheric Science  
Goa University



**GOA UNIVERSITY**

MAY 2024

**HEAVY MINERAL CHARACTERIZATION OF BEACH SAND  
ALONG THE CANAGUINIM-POLEM STRETCH,  
SOUTH GOA**

A Dissertation

Course code and Course Title: GLO-301 Dissertation

Credits: 16

Submitted in partial fulfillment of Master's Degree in Applied Geology

By

**MELDRIN TITAN AFONSO**

Seat Number: 22P0450010

ABC ID-377461457178

PR.NO:20190322

Under the Supervision of

**Dr. POORNIMA ROHAN SAWANT**

School of Earth, Ocean and Atmospheric Science  
Goa University



**GOA UNIVERSITY**

MAY 2024

Examined by:

Seal of the School

### **DECLARATION BY STUDENT**

I hereby declare that the data presented in this Dissertation report entitled, “**Heavy Mineral Characterization of Beach Sand along the Canaguinim-Polem Stretch, south Goa**” is based on the results of investigations carried out by me at Goa University at the School of Earth, Ocean, and Atmospheric Science, Goa University under the supervision of Dr. Poornima Rohan Sawant and the same has not been submitted elsewhere for the award of a degree or diploma by me. Further, I understand that Goa University or its authorities will not be responsible for the correctness of observations / experimental or other findings given the dissertation.

I hereby authorize the University authorities to upload this dissertation to the dissertation repository or anywhere else as the UGC regulations demand and make it available to anyone as needed.

.

Signature and Name of Student

Seat no: 22P0450010

Date:

Place: Goa University

**COMPLETION CERTIFICATE**

This is to certify that the dissertation report “**Heavy Mineral Characterization of Beach Sand along the Canaguinim-Polem Stretch, south Goa**” is a bonafide work carried out by Mr. Meldrin Titan Afonso under my supervision in partial fulfillment of the requirements for the award of the degree of Masters in Applied Geology in the Department of Earth Sciences at the School of Earth, Ocean and Atmospheric Sciences Goa.

Date:

Dr. Poornima Rohan Sawant  
Assistant professor  
Goa University

Senior Prof.Sanjeev Ghadi

Goa University

Dean School of Earth, Ocean and Atmospheric Science

Date:

Place: Goa University

School Stamp

## ACKNOWLEDGEMENT

I would like to take this occasion and acknowledge everyone important in accomplishing my dissertation. First of all, I sincerely thank my guide Dr. Poornima Rohan Sawant for her remarkable support, motivation, and feedback throughout the completion of the work. Her positive, encouraging, and active leadership in this project helped me grow into an autonomous researcher.

I would like to thank Dean Dr. S. C. Ghadi, former Dean C. U. Rivonker, and Vice Dean (Academics) Dr. Anthony A. Viegas, for permitting me to work on my dissertation at Goa University

I would like to thank all the faculty members, Dr. Nicole Sequiera, Mr. Mahesh Mayenkar, Dr. Pooja P. Ghadi, and Dr. Niyati Kalangutkar for their encouragement and constant support, and a sincere thanks to our laboratory assistant Rajesh Mangeshkar along with the Administrative staff of the School of Earth, Ocean and Atmospheric Sciences for their support in completing all the official procedures.

Also like to thank Dr. Digamber G. Porob and his PhD student Mr. Pranav Valvaikar for helping out with XRD data at Goa University. I would also like to thank Jyothi Yarram, a Technical Assistant at BITS Pilani Goa campus who helped me with SEM and EDX data.

Finally, an immense thank you to my family for their unfailing support, care, and continuous encouragement throughout my dissertation work. Finally, I would like to express my gratitude towards my friends Sakshi Tukaram Parwar, Meldroy Vas, Juyee Priolkar, Simran Shecar, Mohammad Kaif Jamkhandi, Aaron Pereira, Yadnesh Vazarkar, K.M. Dharni and all



those who have supported me in ways both seen and unseen. Without your contributions, this project would not have been possible.

## TABLE OF CONTENTS

Sl.No	TITLE	PgNo
	CHAPTER I	1
1.1	Introduction	2
1.1.1	Where to find heavy minerals	3-5
1.1.2	Types of heavy Minerals	6-9
1.1.3	Distribution of heavy minerals	10-12
1.1.4	Why study heavy minerals	13
1.2	Scope	14
1.3	Physiography of Goa	15-17
1.4.1	General geology of Goa	18-19
1.4.2	Previous study in Goa	20-22
1.4.3	Proposed revision of the Goa group	23-24
1.4.4	Lithological characteristics	25-27
1.5	Study Area	28-29
1.6	Aim and Objectives	30
1.7	Brief structure of the dissertation	31
	CHAPTER II	32
2.0	Literature Review	33-42
	CHAPTER III	43
3.0	Methodology and Material	44
3.1	Sampling	44

Sl.No	TITLE	PgNo
3.2	Sieve sand size analysis	46
3.3	Preparing samples	48
3.4	Heavy magnetic separation of heavy magnetic minerals	48-49
3.5	Heavy non-mineral separation	50
3.5.1	Density separation	50-51
3.6	Under stereo-zoom microscope	52
3.7	SEM analysis	53
3.7.1	Principle of SEM	53
3.7.2	SEM with EDX	54
3.7.3	SEM for Heavy minerals	54
3.8	XRD analysis	55
3.8.1	Principle of XRD	55
3.8.2	XRD in earth science	57
3.8.3	Sample preparation for XRD	57
	CHAPTER IV	59
4.0	Observation	60
4.1.1	Sieve size analysis observation	60-65
4.1.2	Range selection for heavy minerals	66
4.1.3	Observation in size distribution	66
4.2	Heavy mineral distribution	67
4.3	Stereozoom observation	68-74
4.4.1	XRD analysis for non-magnetic minerals	75-79

Sl.No	TITLE	PgNo
4.4.2	XRD analysis for magnetic minerals	80-83
4.5	SEM – EDX analysis	84-91
4.6	Discussion and interpretation	92-98
4.7	Conclusion	99
4.8	References	100-105

### LIST OF FIGURES

Chapter	List of Figures		Pg.No
Chaper1: Introduction	figure 1	Photomicrographs of some heavy minerals	2
	figure 2	Minerals weather from a vein deposit, move downhill and are concentrated by flowing water into a stream placer	4
	figure 3	Placer deposits formation	5
	figure 4	Beach placers	5
	figure 5	Zircon minerals	6
	figure 6	Ilmenite mineral	7
	figure 7	Garnet mineral	8
	figure 8	Global distribution of heavy mineral deposits of the world. Note that such deposits are restricted to tropical subtropical belts of the world (After Krishnamurthy 2012)	10
	figure 9	Heavy mineral distribution map of India ( world thorium occurrences, deposits, and resources)	11
	figure 10	Major Beach and Inland Placer deposits of India. ( world thorium occurrences, deposits, and resources)	12
	figure 11	Map showing broad physiographic divisions of Goa ( Natural Resources of Goa: A geological perspective)	16

	figure 12	GEOLOGY OF GOA (revised after GSI, 1996, by integrating arguments based on the field, petrological, geochemical, and isotope data following the works of Dhoundial et al. 1987; Devaraju et al. 2007; 2010; Dessai et al. 2009)	24
	figure 13	Study area map South Goa	29
Chapter 3 Methodology	figure 14	Diagram showing beach profile along the shore of Betul	45
	figure 15	A)the core tube is pushed into the sediments with the head of the plunger remaining on the surface. B). sample collection for sieve size analysis C). sample storage	45
	figure 16	. A. sample collection.B. sample cleaning. C. arrangement of sieves. D. sieve shaker.	47
	figure 17	A- Coning and quartering of samples, B- addition of H <sub>2</sub> O <sub>2</sub> for removal of organic matter, C- addition of HCL	48
	figure 18	magnetic minerals aligned with magnetic directions	49
	figure 19	diagram showing an arrangement for Density separation	51
	figure 20	Minerals Under Sterozoom Microscope	52

	figure 21	A- samples were placed on Studs. B- Quanta FEG 250	55
	figure 22	A. powdered samples were placed in the rectangular cavity sample holder of dimension 2x1.5 x0.2cm <sup>2</sup> . B. Rigaku XRD machine	58
Chapter IV Observation and conclusion	figure 23	Grain size distribution in A - Backshore sample, B- foreshore sample	60
	figure 24	Bar graph showing Heavy minerals and Magnetic mineral Weight percentage	67
	figure 25	Diopside image from sample M1BS	68
	figure 26	Tourmaline images from sample M3.1BS	68
	figure 27	Mg Hornblende Images from sample M1BS	68
	figure 28	Rutile Grain from sample M5BS	69
	figure 29	The Garnet grain from the sample M3.1BS	69
	figure 30	Epidote grain from sample M3.1BS	69
	figure 31	Staurolite grain from sample M3.1BS	70
	figure 32	Actinolite grain from Sample M4BS	70
	figure 33	Tremolite Grain from sample M5BS	70

	figure 34	Goethite Grains from sample M10BS	71
	figure 35	Geothiot Grains from sample M3.1BS	71
	figure 36	A- XRD graph for M1BS , B- Quantification Pie chart for M1BS	75
	figure 37	A- XRD graph for M3.1BS , B- quantification Pie chart for M3.1BS	76
	figure 38	A - XRD data for M4BS , B- quantification Pie Chart M4BS	77
	figure 39	A- XRD data for M5.1BS , B- Quantification pie chart for M5.1BS	78
	figure 40	A- XRD graph of M10BS , B- Quantification chart of M10BS	79
	figure 41	A- XRD of M1BS magnetic minerals, B- Quantification Pie Chart of M1BS magnetic	80
	figure 42	A-XRD of M10BS magnetic minerals, B- Quantification Pie chart of M10BS magnetic minerals	81
	figure 43	FSEM image of Tourmaline in Image (A and B), Image C - EDX Graph of tourmaline showing Element composition	84



	figure 44	FSEM image of Hornblende in Image (A,B, C&D), Image E - EDX Graph of Hornblende showing Element composition	85
	figure 45	FSEM image of Tremolite in Image (A,B, C&D), Image E - EDX Graph of Tremolite showing Element composition	86
	figure 46	FSEM image of Garnet in Image (A,&B ), Image C - EDX Graph of Garnet showing Element composition	87
	figure 47	FSEM image of Actinolite in Image (A,B,C,D ), Image E - EDX Graph of Actinolite showing Element composition	88
	figure 48	FSEM image of Goethite in Image (A,B,C,D ), Image E - EDX Graph of Goethite showing Element composition	89

### List of Tables

Chapters	Tables		Pg.No
Chapter I Introduction	Table 1	Heavy minerals with their density, stability in weathering and diagenesis, and possible provenance	9
	Table 2	Lithostratigraphic Classification Of Rocks From Goa (Ater Gokul Et Al. 1985 And The Proposed Revision) Journal Geological Society Of India	27
	Tables 3	Showing sample number along with name and Coordinates	29
Chapter IV Observation and conclusion	Table 4	M1BS and M1FS table for grain size distribution	62
	Table 5	M3.1BS and M3.1FS grain size distribution	63
	Table 6	M4BS and M4FS grain size distribution	63
	Table 7	M5.1BS and M5.1FS Grain size distribution	64
	Table 8	M10BS and M10FS grain size distribution	65
	Table 9	Heavy mineral and magnetic mineral weight percentage	

# CHAPTER I

## INTRODUCTION

## 1.0 Introduction

A naturally occurring solid with a distinct chemical composition and crystal structure is referred to as a mineral in geology. Most minerals are inorganic, yet some mineralogists accept those composed of organic materials or formed by living things as opposed to geological processes. The Latin term mineral, which means ore or mine, is where the word mineral originated in the Middle Ages. There are thousands of known minerals. There are many minerals and they have their significance. In the same way, there is a group of minerals known as (heavy minerals) with a density greater than 2.9 grams per cubic centimeter ( $\text{g/cm}^3$ ). This means they are significantly denser than common rock-forming minerals like quartz and feldspar, which have densities of around  $2.65 \text{ g/cm}^3$  and  $2.54\text{--}2.76 \text{ g/cm}^3$ , respectively.

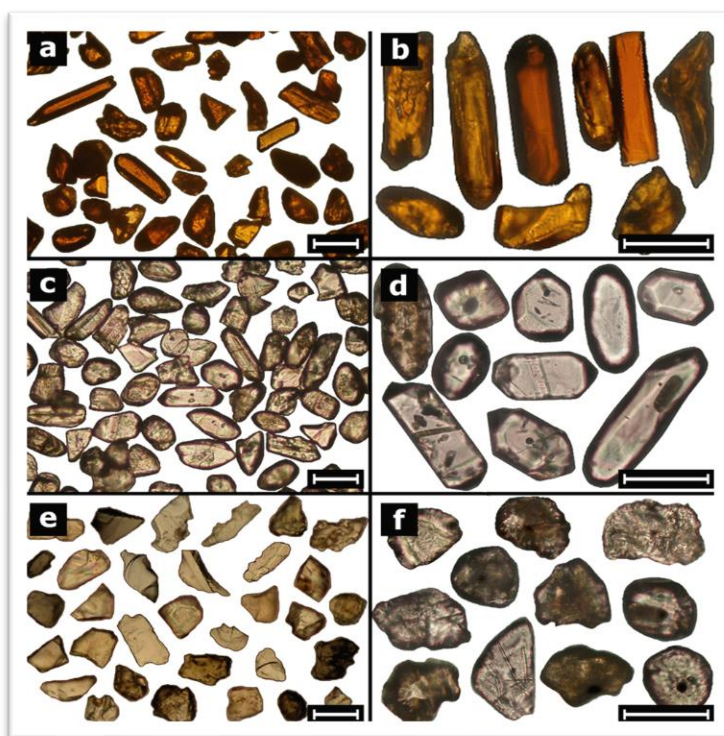


**Figure 1 Photomicrographs of some heavy minerals:**

[https://www.researchgate.net/figure/fig-2-Photomicrographs-of-some-heavy-minerals-a-b-rutile-c-d-zircon-e\\_fig2\\_355887821](https://www.researchgate.net/figure/fig-2-Photomicrographs-of-some-heavy-minerals-a-b-rutile-c-d-zircon-e_fig2_355887821)

Why are heavy minerals heavy and light minerals light reason is that heavy minerals contain metals like iron (Fe) or titanium (Ti) that have a lot of mass packed into their atoms. A higher density is the result of these components working together with the arrangement of atoms in the crystal structure and light minerals contain elements like silicon (Si) or oxygen (O) that have fewer massive atoms. Their reduced overall density can also be attributed to the way these atoms are arranged in the crystal structure. In Figure 1 there are some of the heavy minerals listed, (a, b) rutile; (c, d) zircon; (e) garnet; (f) monazite.

### **1.1.1 Where to find heavy minerals**

The natural concentration of heavy minerals is brought on by the motion of particles through gravity. Weathering processes release heavy, stable minerals from their matrix, which are then gradually carried downslope into streams where they rapidly winnow the lighter matrix as shown in Figure 2. Thus, in stream, beach, and lag (residual) gravels, the heavy minerals concentrate and produce workable ore deposits. Minerals such as gold, platinum, cassiterite, magnetite, chromite, ilmenite, rutile, native copper, zircon, monazite, and other gemstones have a high specific gravity, are robust, and are chemically resistant to weathering.

Placer deposits come in many forms: eluvial, or stream placers; beach placers; and eolian, or eolian, placers. The most placer gold, cassiterite, platinum, and gemstones have been found in stream placers, which are by far the most significant

Stream placers require swift water flow to concentrate. Heavy minerals are deposited much more quickly than light minerals where the velocity declines because the flow rate plays a significant role in the ability to transport solid material. Rich gold deposits are found in Alaska and the Klondike, platinum placers in the Urals, tin (cassiterite) deposits in Malaysia,

Thailand, and Indonesia, and diamond placers in the Congo (Kinshasa) and Angola are a few examples of stream placers.

Beach placers are created on shorelines where shore currents and wave activity move materials, concentrating the lighter elements more quickly than the heavier ones. The heavy minerals are deposited on the strand line shown in Figure 4. Among the examples of beach placers are the gold deposits of Nome, Alaska; the zircon sands of Brazil and Australia; the black sands (magnetite) of Oregon and California; and diamond-bearing marine gravels of Namaqualand, South Africa.

eluvial placers are created by weathered deposits. Since the light materials are carried away by wind and rain rather than by streams, they can be regarded as intermediates in the production of stream placers. Examples are Malaysia's placers of cassiterite and Australia's earlier exploited gold resources.

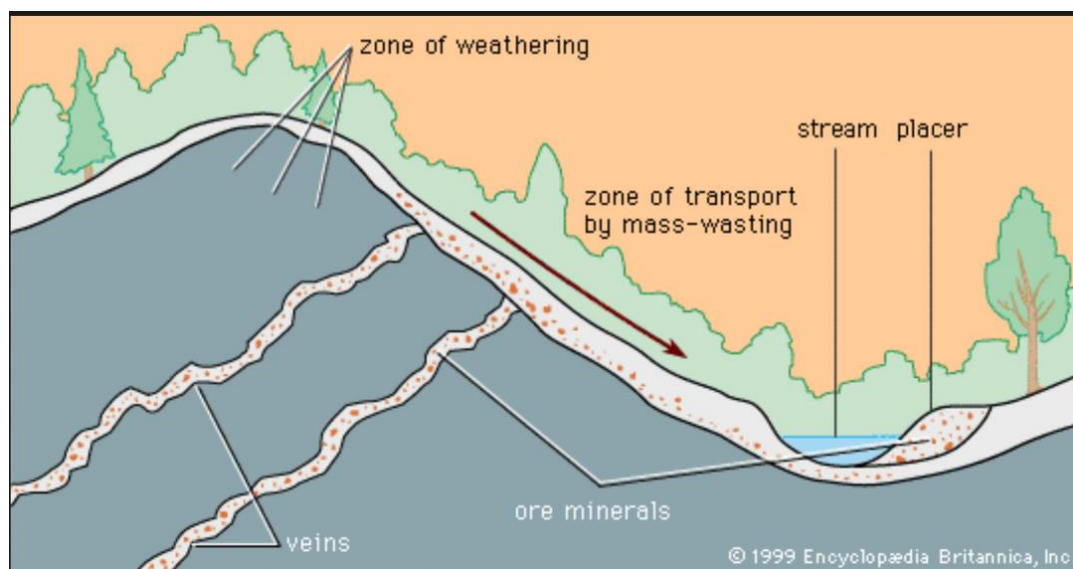


**Figure 2 : Minerals weather from a vein deposit, move downhill, and are concentrated by flowing water into a stream placer**

<https://www.britannica.com/media/1/462598/1515>

Residual placers originate at or close to the location where the parent rock's minerals were first liberated. Weathering and erosion are the processes that lead to this concentration. Picture a vein of gold piercing a rock. The lighter elements are swept away by wind and rain as the granite weathers over time. Gold and other heavier, more resilient minerals are left behind. Although residual placer deposits are typically not very large, they can contain a significant amount of minerals. Examples of placer deposits are shown in Figure 3 Residual placers are only stable in flat morphologies because steeper slopes induce soil creep and with it a down-slope displacement of ore fragments (resulting in colluvial placers).

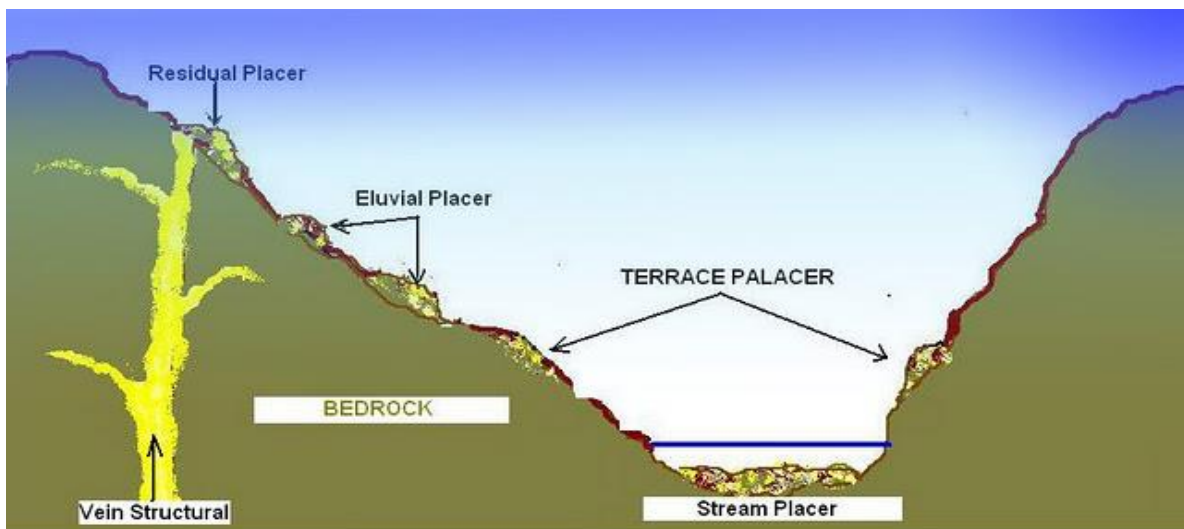


**FIGURE 3: Placer deposits formation:-**

<https://www.google.com/url?sa=i&url=https%3A%2F%2Fwww.911metallurgist.com%2Fblog%2Flist-types>

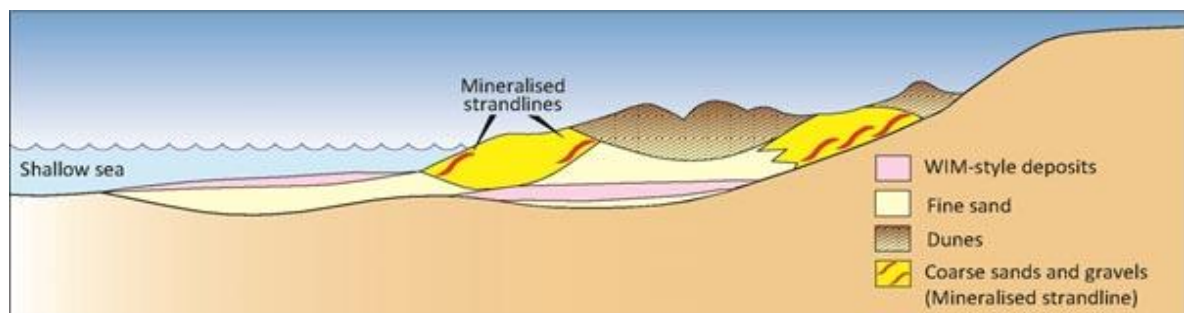


**FIGURE 4 :Beach placers**

[https://www.google.com/url?sa=i&url=http%3A%2F%2Fearthsci.org%2Fmineral%2Fmindep%2Fmindsand%2Fmindsand.html&psig=AOvVaw3Ym\\_3x-B-iWgicsD9UbpT&ust=1714209607725000&source=images&cd=vfe&opi=89978449&ved=0CBiQjRxqFwoTCLjSp-jG34UDFQAAAAAdAAAAABAL](https://www.google.com/url?sa=i&url=http%3A%2F%2Fearthsci.org%2Fmineral%2Fmindep%2Fmindsand%2Fmindsand.html&psig=AOvVaw3Ym_3x-B-iWgicsD9UbpT&ust=1714209607725000&source=images&cd=vfe&opi=89978449&ved=0CBiQjRxqFwoTCLjSp-jG34UDFQAAAAAdAAAAABAL)

### 1.1.2 Types of heavy minerals

- 1) Zircon ( $\text{ZrSiO}_4$ ) is a zirconium silicate (figure 5) with a high specific gravity (4.2-4.86), making it a heavyweight among minerals. This allows it to concentrate with other heavy minerals during natural sorting processes. It's also very hard (7.5 on the Mohs scale), making it resistant to weathering and erosion. In igneous and metamorphic rocks, zircon is formed at the initial stages of rock formation. These microscopic zircon crystals, which preserve a record of previous geological events, can be extraordinarily old. Although zircon is found in igneous and metamorphic rocks, placer deposits such as beaches, riverbeds, and occasionally even dunes valuable quantities of the mineral can be found. A rich concentration of heavy minerals like zircon has been left behind in this area where water currents have wrung out lighter materials.

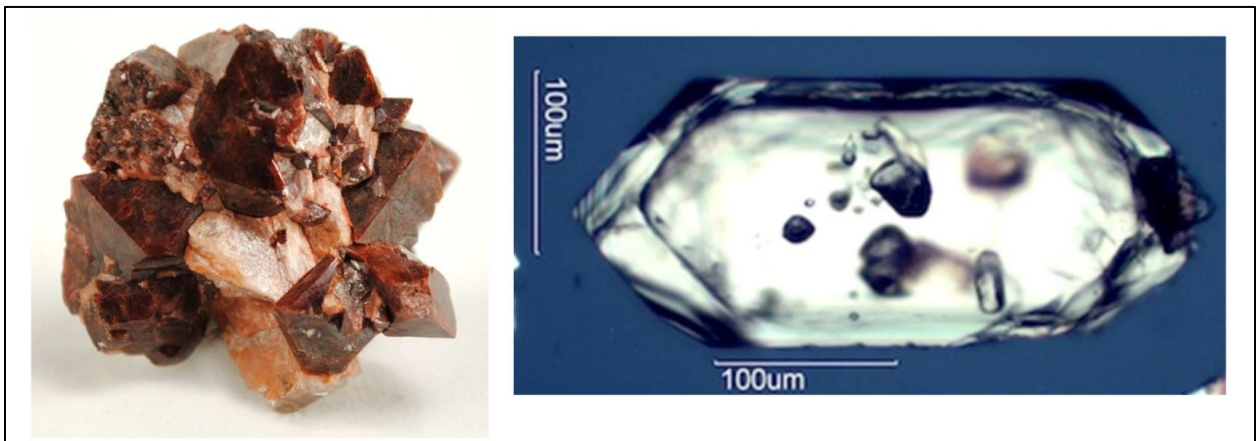


**FIGURE 5 : Zircon minerals**

<https://cdn.irocks.com/storage/media/57844/conversions/t10469a-large.jpg>

- 2) Ilmenite ( $\text{FeTiO}_3$ ) is an iron-titanium oxide mineral (figure 6) It forms during the solidification of magma (igneous rocks). Ilmenite resists weathering very well. Ilmenite grains weather with the sediment in rocks that contain them. These grains separate during



stream transit due to their high specific gravity, accumulating as "heavy mineral sands."

Ilmenite is the number one ore of titanium metal.



**FIGURE 6 : Ilmenite mineral**

<https://th.bing.com/th/id/OIP.e0rNGZHQYO-TPz3mmkTHvAHaFj?rs=1&pid=ImgDetMain>

- 3) Garnets aren't formed specifically as heavy minerals, but rather during igneous or metamorphic rock formation. They exist within these rocks until weathering and erosion release them. garnets are a set of minerals having the generic formula  $X_3Y_2(SiO_4)_3$ , where X and Y can be any element, including chromium, calcium, magnesium, iron, and aluminum. Figure 7 shows garnets. This variance produces various varieties of garnet with unique colors. Despite their differences, garnets are all heavy minerals due to their high density (more than 2.9). They can concentrate during natural sorting processes because of their density. Water transportation (rivers, waves) removes garnets from rocks when weathering releases them according to density. Due to its weight, garnet can settle in placer deposits next to other heavy minerals in slower-moving waters or along the coast. Table 1 will show the list of heavy minerals with their density range along with their stability in diagenesis and weathering and their possible provenance.



**FIGURE 7: Garnet**

[https://th.bing.com/th/id/OIP.K9iLQncDPCw-byX\\_dZLUCAHaHh?rs=1&pid=ImgDetMain](https://th.bing.com/th/id/OIP.K9iLQncDPCw-byX_dZLUCAHaHh?rs=1&pid=ImgDetMain)

Table 1 will show the list of heavy minerals with their density range along with their stability in diagenesis and weathering and their possible provenance.

Mineral	Density	Stability in weathering	Stability in diagenesis	Provenance
Anatase	3.82-5.77	High	High	Felsic igneous rocks, hydrothermal veins, alteration product of titanite or ilmenite.
Andalusite	3.13-3.16	High	Low	Metamorphic rocks.
Amphibole	3.02-3.50	Low	Low	Igneous and metamorphic rocks.
Apatite	3.1-3.35	Low	High	Igneous and metamorphic rocks.
Cassiterite	6.9-7.07	High	High	Felsic plutonic rocks, hydrothermal deposits.
Chloritoid	3.51-3.80	Moderate	Moderate	Metamorphic rocks.
Chromite	4.43-5.09	High	High	Mafic and ultramafic igneous rocks.
Clinopyroxene	2.96-3.52	Low	Low	Igneous and metamorphic rocks.
Epidote	3.12-3.52	Low	Low	Mostly metamorphic rocks, less igneous rocks.
Garnet	3.59-4.32	Moderate	Moderate	Mostly metamorphic but igneous also.
Ilmenite	4.70-4.79	Moderate	Moderate	Igneous and metamorphic rocks, sometimes hydrothermal veins.
Kyanite	3.53-3.65	High	Moderate	Metamorphic rocks, rarely in igneous rocks.
Magnetite	5.17-5.20	Low	High	Igneous and metamorphic rocks, hydrothermal veins.
Monazite	5.00-5.30	High	High	Igneous and metamorphic rocks.
Olivine	3.22-4.39	Low	Low	Mostly mafic and ultramafic igneous rocks, some metamorphic rocks also.
Orthopyroxene	3.21-3.96	Low	Low	Mafic and ultramafic igneous rocks, high grade metamorphic rocks.
Rutile	4.23-5.50	High	High	Igneous and metamorphic rocks.
Sillimanite	3.23-3.27	High	Low	Metamorphic rocks, sometimes granite.
Staurolite	3.74-3.83	High	Moderate	Metamorphic rocks.
Titanite	3.45-3.55	Moderate	Moderate	Igneous and metamorphic rocks.
Tourmaline	3.03-3.10	High	High	Granitic pegmatites, some metamorphic rocks.

Table 1 :- Heavy minerals with there density , stability in weathering and diagenesis and there possible provenance

### 1.1.3. Distribution of heavy minerals

It is recognized that there are placer mineral deposits along the coasts of many nations worldwide. However, the distribution of significant beach placer deposits is restricted to tropical-subtropical belts of the world. Reason being -

- a) warmer climate:- Higher rates of chemical and physical weathering are observed in warmer climates. Rocks are broken down by this weathering process, releasing minerals that can be eroded and carried by water.
- b) Higher erosion rates;- Tropical and subtropical regions tend to have more rainfall and intense storms, which can lead to higher rates of erosion. deposits occur in the east and west coasts of Australia, the southern part of China, Sri Lanka, Malaysia, Madagascar, Vietnam Egypt, Sierra Leone, the Republic of South Africa, Guinea, Ivory Coast, Brazil, the south-eastern United States, and Canada as shown in figure 8 The majority of heavy mineral.



Figure 8: Global distribution of heavy minerals deposits of the world. Note that such deposits are restricted to tropical subtropical belts of the world (After Krishnamurthy 2012)

Ilmenite, sillimanite, garnet, zircon, rutile, and monazite (REEs, thorium) are the minerals that make up the mineral assemblage of heavy mineral deposits. The sources for the heavy minerals vary from deposit to deposit, depending on the lithological composition of the hinterland or coastal area. Generally speaking, highly metamorphosed rocks that are exposed in the terrain have been the source of significant mineral accumulations along the coast. Typically, the source rocks undergo severe tropical weathering, or lateralization, from which denudation (fluvial, pluvial, and aeolian) transports the heavy mineral portion. Given below in Figure 9 is the heavy mineral distribution map of India.

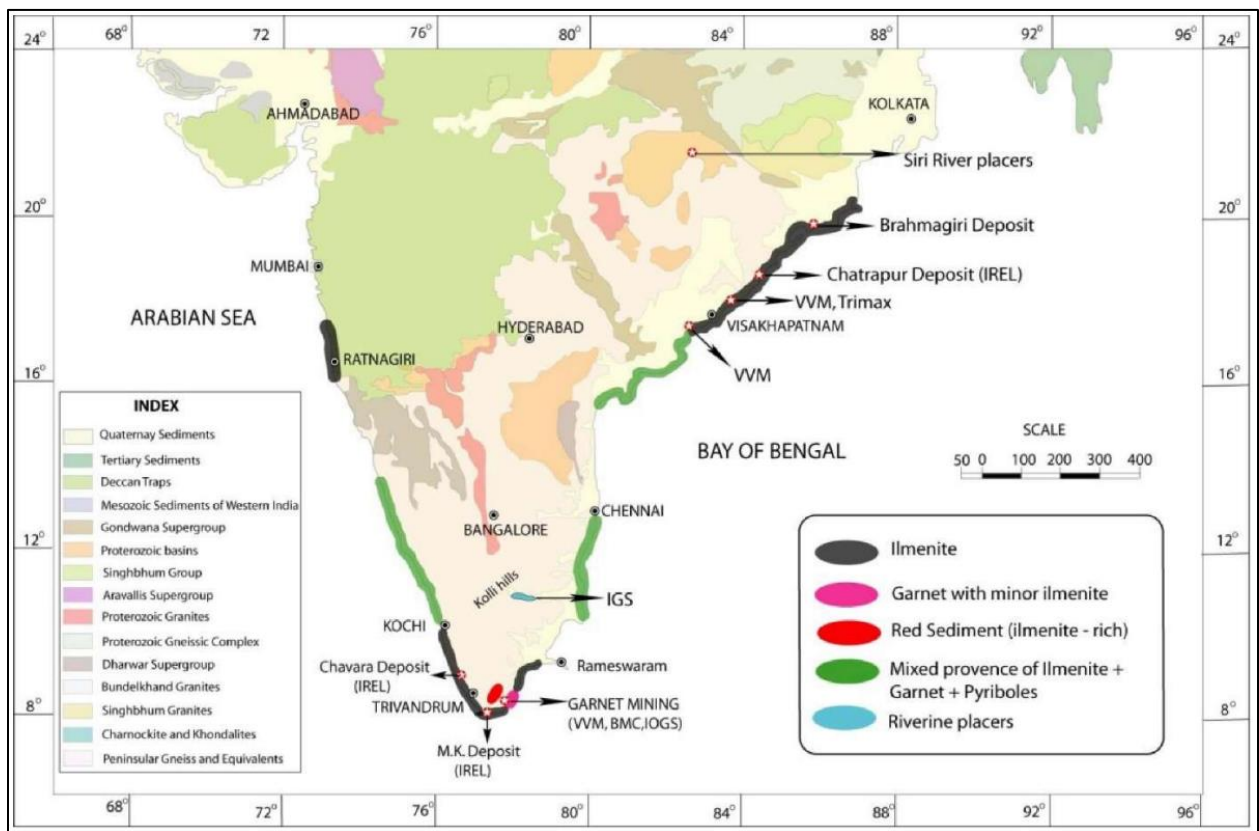


**Figure 9 :- Heavy mineral distribution map of India ( world thorium occurrences, deposits, and resources)**  
**Harikrishnan Tulsidas July 2019**

The finest places to develop coastal placers are on the beaches of Tamil Nadu, Kerala, Andhra Pradesh, and Odisha. The deeper portions have not yet been investigated because beach placer deposits can only be studied down to a depth of 10 m. While beaches on the east coast, in the states of Tamil Nadu, Odisha, and Andhra Pradesh, are well-developed and stretch over several kilometers in width with a well-developed dunal system, beaches on the west coast, in Kerala and the southwest coast of Tamil Nadu, are narrow or barrier deposits that appeared with the development of dunes generated by prominent aeolian action during dry months. Figure 10 shows the Major Beach and Inland Placer deposits of India.

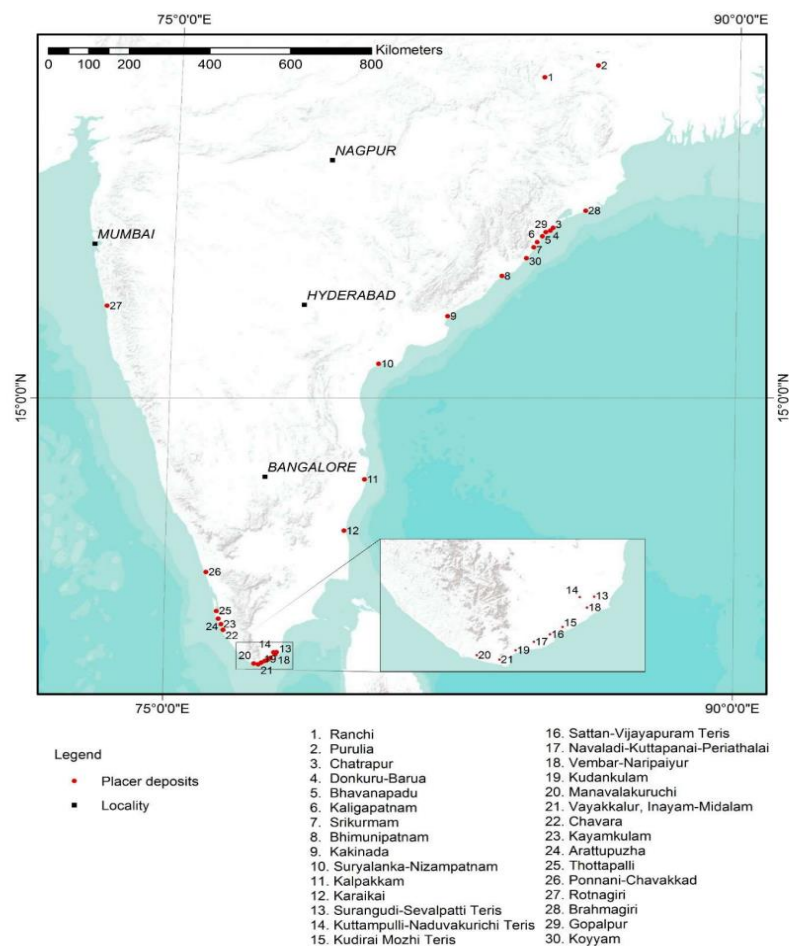


**Figure 10 :- Major Beach and Inland Placer deposits of India. ( world thorium occurrences, deposits, and resources) Harikrishnan Tulsidas July 2019**

#### **1.1.4 .Why to study heavy minerals?**

**Provenance studies:** Heavy minerals are useful to study the provenance of sand or sandstone. How do we study provenance? Think of heavy minerals as little investigators. Because they're durable and hold onto their characteristics, they act as tracers. By examining the types and proportions of heavy minerals in rocks, geologists can pinpoint the source rock from which the sediments originated. Heavy minerals are useful indicators of sediment source rocks because different types of source rocks yield different suites of heavy minerals.. Alkaline igneous source rocks are indicated by a suite of heavy minerals that includes rutile, titanite, apatite, biotite, hornblende, monazite, zircon, and rutile. A group of minerals known as the andalusite, garnet, staurolite, topaz, kyanite, sillimanite, and staurolite suite is indicative of metamorphic rocks.

**Determining the sediment's origin:** Geologists can use this information to trace the origin of sediments since distinct source rocks typically have distinct assemblages of heavy minerals. This is helpful for research such as reconstructing historical rivers and figuring out how landscapes have evolved throughout time.

## 1.2 .Scope

The primary focus of this research is to comprehensively investigate heavy mineral assemblages along the coast of Goa, India, unraveling their geological patterns, distribution, and economic potential. The study aims to shed light on the specific heavy mineral species present, their concentrations, and the factors influencing their distribution in the coastal sediments of Goa.

This research project seeks to meticulously explore the intricate details of heavy mineral assemblages along the coastal expanse of Goa, India. The scope encompasses a multifaceted investigation into the mineralogical composition, spatial distribution, environmental influences, and economic significance of heavy minerals in this region. Through extensive field surveys and sample collections at selected sites along the Goan coastline, a detailed examination of heavy mineral species and their variations across different stretches will be undertaken. The spatial distribution will be analyzed, considering factors such as beach morphology, proximity to river mouths, and geological formations, while environmental influences, including seasonal changes, monsoons, and potential anthropogenic activities, will be assessed. Moreover, an economic evaluation will focus on identifying economically valuable species like ilmenite, rutile, and zircon, exploring their potential industrial applications and contribution to Goa's economic landscape. Comparative analyses with existing studies in Goa and other coastal regions will provide a broader geological context. Utilizing advanced laboratory techniques, including X-ray diffraction, scanning electron microscopy, and EDS, this research aims to enhance our understanding of the geological processes influencing heavy mineral distribution along the Goan coast from Canaguinim Beach in Quepem to Polem Beach in Karnataka. The insights gained will not only contribute



valuable information for sustainable resource management but also establish a baseline for future studies on coastal dynamics and mineral exploration in the region.

### **1.3 Physiography of Goa**

The coastal state of Goa lies on the West Coast of India between N 14° 53' and N 15° 48'. The State is wider in the north and has a coastline that stretches over 100 kilometers in length. The approximate coordinates of the Western and Eastern extents are E 73° 39' and E 74° 20', respectively. From a physiological perspective, the state can be divided into three terrain types: low-lying coastal-estuarine plains to the west, an undulating region in the center, and steep Western Ghats slopes on the state's eastern boundary. As shown in figure 11 . The three terrain types can be delineated roughly longitudinally, except in the far South of the State, where all three types seem to merge.

The western coastal-estuarine plains with tablelands: Low-lying characteristics such as farms, settlement areas, mangroves, saltpans, Kazan lands, sandy beaches, and estuary mudflats make up this landscape. The two main estuaries in the state, the Mandovi and Zuari, have lower basins where the estuary plains stretch over 10 to 12 km inland. In North Goa, the plains are more extensive and prominent but they are not continuous and are separated by low, laterite-topped plateaus (tablelands) that are less than a hundred meters high. The coastal estuarine plains are considerably smaller, more isolated, and have a more constrained area in the state's far south ( (the Quepem and Canacona coast ). Even in this vicinity of the coast, the terrain is frequently rugged and mountainous.

The central undulating region (midlands): This area, primarily consisting of relict hills with elevations between 100 and 600 meters, is a transition between the steeper, higher

topography of the Western Ghats and the lower coastal plain and plateau terrain. This midland region is broader to the north, because the Western Ghats are situated much further inland in North Goa. The hills and valleys of this undulating region are generally aligned (elongated) in an NW-SE direction (as are the Western Ghat ranges in North Goa). The trend of the hills and the ghats in North Goa is controlled by the structure (folding and schistosity) of the rock formations in the region. In North Goa the fold axis and schistosity of the rock formations is NW-SE. The coastline of Goa is also NW-SE and therefore the inland hill ranges remain almost parallel to the coast.

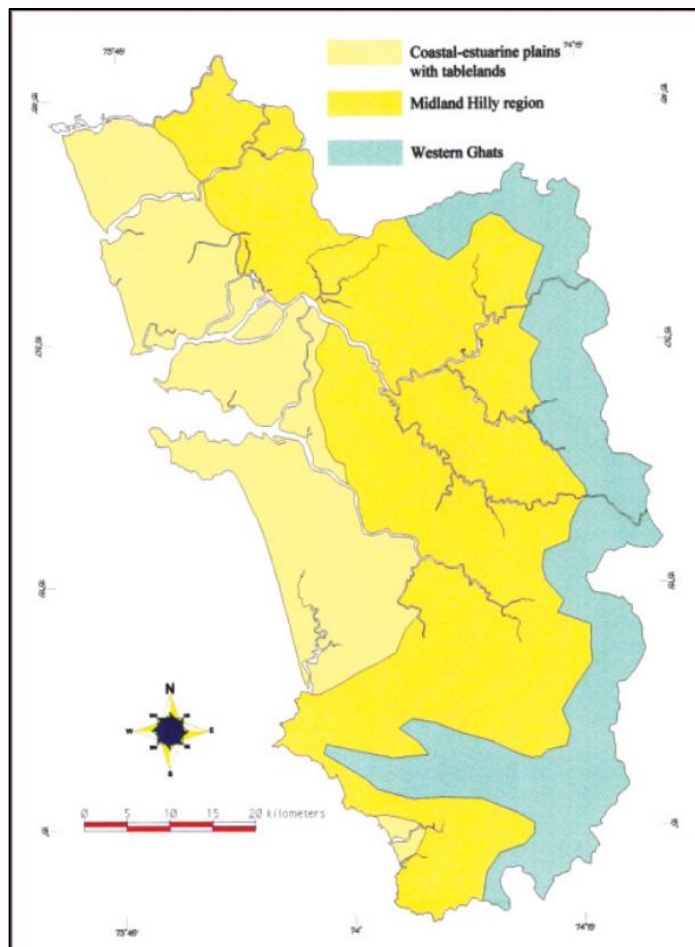


**Figure11 :- Map showing broad physiographic divisions of Goa ( Natural Resources of Goa: A geological perspective)**

However, in South Goa the structure (folding and schistosity) of the underlying rock formations is WNW-ESE and therefore the hill ranges and the ghats have a trend closer to East-West. As the coastline is almost North-South (NW-SE) the East-West trending hills and ridges encounter the sea at their Western ends. In this Southern region of Goa, it is difficult to demarcate (with precision) midlands from the Western Ghats because the transition from the rugged (hilly cliffs) coastline to mountain ridge tops is sharp.

The Western Ghats: This hilly area, which covers the eastern and southern parts of Goa, is made up of steeper, higher mountains that reach elevations of 600 to 1000 meters. The Western Ghats (Sahyadris) have a general NW-SE trend (except for the ranges in south Goa). In north Goa, they are more than 40 km away from the sea. In the south, however, the trend of the hills, which is related to the underlying rock structure, is almost East-West (WNW-ESE). A western arm of the Ghats (the Karmal Ghat) meets the sea in its lower reaches, As a result, the talukas of Quepem and Canacona have very limited areas of the coastal estuarine plain and the midland region translates very sharply into the ghat region.

All the rivers that flow within the state are estuarine the tidal waters reaching several kilometres inland. These estuary systems split the remnant landforms of the plains and midlands between the Sahyadri and the coast. The rivers have their source in the Western Ghat range, but they rapidly lose their force as they flow through the estuary plains and the midlands before emptying into the sea. Along with a few smaller coastal inlets, these estuaries include the Tiracol, Chapora, Mandovi, Zuari, Sal, Talpona, and Galgibag.

### 1.4.1 GENERAL GEOLOGY OF GOA

Geologically speaking, the state of Goa, which is located on India's west coast and has an area of roughly 3700 square kilometers, is a portion of the Indian Precambrian Shield. In this region, there are greenschist supra crustal rocks that overlie a basement consisting of trondhjemitic (Peninsular) gneiss and are intruded by mafics, ultra-mafics, and granites. Only the northeastern corner of the state has the late Cretaceous Deccan Traps. Most of the geological formations are covered in laterite (of varying thickness on remnant hills) and alluvium and sand (on the coastal-estuarine plains), as would be expected in a wet tropical environment.

The complex combination of the Western and Eastern Dharwar cratons (WDC, EDC) is found in the southern half of the Indian shield, namely in the granite-greenstone terrain of the Dharwar craton.

Goa is situated in the northwestern part of the WDC where the Shimoga-Goa supracrustal belt extends contiguously until it is concealed beneath the Arabian Sea and the Deccan Traps in the north. The belt possibly continues beneath the Traps up to the Narmada, where the Narmada-Son lineament terminates this supracrustal belt. The Shimoga-Goa belt extends NNW-SSE over a length of approximately 250 km and has a maximum width of about 120 km at Dharwar. The western margin of the belt is marked by large domal masses of gneissose rocks such as the Chandranath granite gneiss and the Canacona granite. The eastern margin is faulted, whereas the southern section appears to have been deposited in shallow waters. The latter is associated with subaerial mafic volcanic rocks at Kumbharwada and north of Karwar and Ankola. The thickest accumulation of mafic volcanic of this schist belt is, however, centered at Bababudan and Kudremukh which form the southern extensions of this

belt (Harinadha Babu et al. 1981a). A thick sequence of greywackes occupies the northern section of the basin. The southern section in general, is characterized by orthoquartzite/basic lava association that denotes subaerial environments and intermittent volcanic activity in a coastal sand environment under stable conditions. The limestone-iron-manganese ore sequence of Goa and north Kanara (Castlerock band) in the northern part (Maclaran, 1904) of the Shimoga belt is in physical continuity with that in the southern part and serves as the marker horizon to show the continuity of the rocks over the entire length of the belt. The granitic-gneisses from Goa were assigned either a syntectonic or post-tectonic status (Harinadha Babu et al. 1981a; Gokul et al. 1985) about the deformational episodes exhibited by the supracrustals. However, there is a considerable lack of clarity as regards the interrelationship among the granitic gneisses on the one hand and between the gneisses and the supracrustal greenstones on the other. The supra crustal sequences in particular, consist of metavolcanics and clastics each with peculiarities of its own, yet both have been included under one stratigraphic group namely the Goa Group (e.g. Gokul et al. 1985).

### 1.4.2 Previous Study in Goa

The litho units from Goa were geologically examined by Fermor (1909) and later by Dunn (1942). A formal stratigraphic classification was, however, provided by Oertal (1958) who divided the rocks into two groups: (i) the lower infra conglomerate group and (ii) the upper metalliferous group. The granitic rocks occurring at Quepem, Canacona, and Dudhsagar were considered by him to be intrusive into the schistose rocks. The Goa region in general, is largely occupied by schistose rocks (Pascoe, 1950; Dhepe, 1954) but for the northeastern corner of the State where Deccan Traps (late Cretaceous to Eocene) overlie the Dharwar metasediments. Recent geological mapping (GSI, 1996) has shown that the basal sequences are made of metavolcanics with intercalations of metasediments overlain by a larger proportion of clastics, dominated by greywackes. In these respects, they are similar to the Dharwar-type greenstones of Radhakrishna and Vaidyanadhan (1997). Gokul et al. (1985) proposed a modern scheme of stratigraphic classification and grouped the litho-units of Goa into four formations. The stratigraphic succession proposed by Gokul et al. (1985) is presented in Table 2 . along with the proposed revision. In their scheme of classification, all the granitic gneisses and the granites from Goa were considered coeval and intrusive into the metasediments (e.g. Harinadha Babu et al. 1981b; Gokul et al. 1985). The basement for the supracrustal sequence was not identified. The GoaGroup typically has a greenstone dominated sequence at the base which is overlain by a meta conglomerate over which rests a dominantly clastic sequence. The metaconglomerate (tilloid) was assigned the status of a para-conglomerate. The granitic gneisses in Goa are exposed at four different localities and are referred to as (i) Chandranath granite gneiss, (ii) Tamdi felspathic gneiss, (iii) Dudhsagar granite, and (iv) Canacona granite. They are all considered intrusives into the supracrustals (greenstones) by Gokul et al. (1985). The Chandranath granite gneiss was considered to be

syntectonic with the first phase of folding, the Tamdi felspathic gneiss and the Dudhsagar granite were considered to be synkinematic with the second phase, whereas the Canacona granite was considered to be post-tectonic (Gokul et al. 1985). In light of the recent work (Dhondial et al. 1987; Devaraju et al. 2007, 2010; Dessai et al. 2009) especially on the granitic gneisses, greenstones, and intrusive granites from representative sections, it is proposed to revisit the classification of the greenstones from this area. The Goa Group of Gokul et al. (1985) needs to be integrated (see also Devaraju et al. 2010) with the contiguous Dharwar Supergroup of WDC, as otherwise, it would give an erroneous impression of forming a separate stratigraphic entity within the Dharwar craton. The Goa Group (e.g. Gokul et al. 1985) denotes a local classification confined to Goa and is here divided into two groups namely the Barcem Group and the Ponda Group which correspond respectively to the Bababudan and Chitradurga Groups of the Dharwar Supergroup in the unified regional classification. The proposed stratigraphic scheme is listed in Table 2.

After Gokul et al. (1985)			Proposed Revision		
Basic Intrusives		Metadolerite	Basic Intrusives		Metadolerite/Dolerite
			Canacona Granite	2395±390 (?) Ma	Porphyritic potassic granite
			Mafic-ultramafic layered complex	Peridotite-Gabbro	Dunite-peridotite-gabbro complex and equivalents
				Vagheri Formation	Metabasalt Argillite and metagreywacke
Basic Intrusives		Dolerite, Gabbro	Ponda Group (= Chitradurga Group)	Bicholim Formation	Banded ferruginous quartzite Manganiferous chert breccia with pink ferruginous phyllite Limestone Pink ferruginous phyllite Quartz-chlorite-amphibolite-schist
				Sanvordem Formation	Metagreywacke Argillite, quartzite, tilloid
Chandranath Granite Gneiss	2600±100 Ma	Granodiorite	~~~~~ Unconformity ~~~~~		
Goa Group	Vagheri Formation	Metabasalt Argillite and metagreywacke	Barcem Group (= Bababudan Group)	Barcem Formation	Matagabbro Peridotite, talc-chlorite schist Quartzite, quartz-sericite-schist Red Phyllite Quartz porphyry Massive, schistose and vesicular metabasalt
	Bicholim Formation	Banded ferruginous quartzite Manganiferous chert breccia with pink ferruginous phyllite Limestone Pink ferruginous phyllite Quartz-chlorite-biotite-schist			~~~~~ Unconformity ~~~~~
	Sanvordem Formation	Argillite, quartzite, tilloid			
	Barcem Formation	Metagabbro Peridotite, talc-chlorite-schist Quartzite, quartz-sericite-schist Phyllite Quartz-porphyry Massive, schistose and vesicular basalt			
Basement: not identified			Chandranath Granite Gneiss	2700-2900 Ma	Granodiorite
			Anmode Ghat trondhjemite gneiss	3300-3400 Ma	Basement: trondhjemite-tonalite-granodiorite

**Table 2 :- . Lithostratigraphic Classification Of Rocks From Goa (After Gokul Et Al. 1985 And The Proposed Revision) Journal Geological Society Of India.**



### 1.4.3 Proposed Revision of the Goa Group

In light of the aforesaid, a revision of the classification of the Goa Group (e.g. Gokul et al. 1985) is warranted. The lithological characteristics of the supracrustal rocks permit the subdivision of the Goa Group (e.g. Gokul et al. 1985) into two sequences of greenstones Figure 12. The lower sequence that rests on the TTG gneisses with a quartz-pebble conglomerate is largely dominated by mafic volcanics with intercalated clastics. It was designated as the Barcem Formation of the Goa Group by Gokul et al. (1985). This sequence is elevated to the status of a 'Group' which is formally named the Barcem Group. The 'Group' as per the provisions of the international stratigraphic guide (Hedberg, 1976, p.34) should consist of more than one Formation. However, considering the lithological and the facies variation within the Barcem Formation, it is felt that detailed mapping may eventually lead to its division into more than one Formation. It bears many similarities with the lower part of the Kalaspura Formation of the Bababudan Group. The upper sequence of supracrustals, which makes up the three formations namely the Sanvordem, Bicholim, and Vagheri, is assigned to a new stratigraphic group for which the formal term Ponda Group is proposed. This seems to be appropriate and reasonable. Moreover, the correlation of this group with the Chitradurga Group of the Dharwar Supergroup is justified in agreement with Gokul et al. (1985).

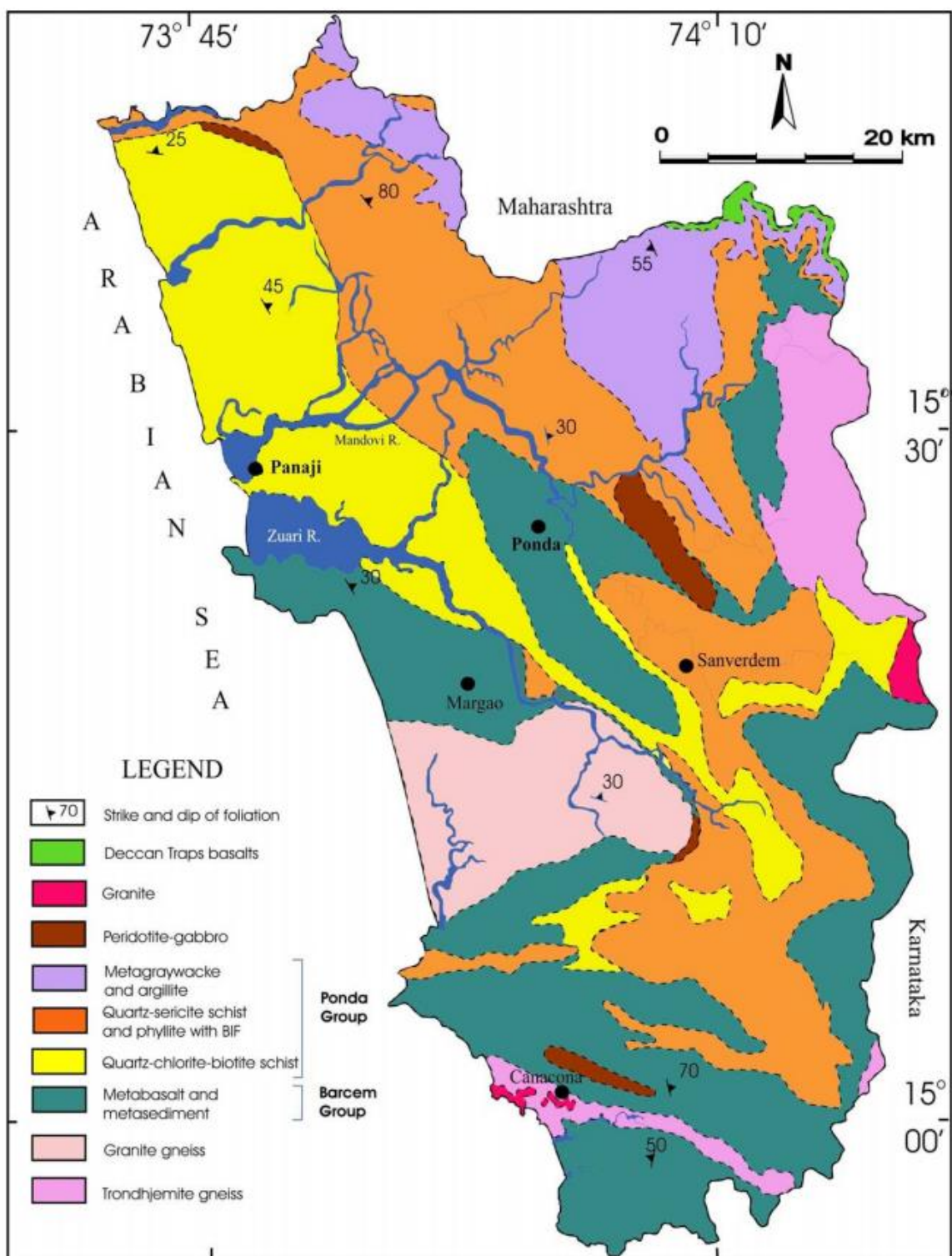


Figure 12 :- GEOLOGY OF GOA (revised after GSI, 1996, by integrating arguments based on the field, petrological, geochemical, and isotope data following the works of Dhoundial et al. 1987; Devaraju et al. 2007; 2010; Dessai et al. 2009)

#### **1.4.4 Lithological characteristics**

The typical characteristics of the Formations of the Barcem and Ponda Groups are described below.

##### **Barcem Group**

The newly identified Barcem Group is best developed to the southeast of Barcem village and accounts for a thickness of over 2 km, however, in the northwest between Margao and Vasco-da-Gama the rocks attain a thickness of about 2.5 km. It has a quartz pebble conglomerate at the base and the litho units consist of metavolcanic with intercalations of quartzites and pelites. The volcanics are represented by basic and felsic lavas, agglomerates, and tuffs. The metasediments consist of quartzites, quartz-sericite-schists, quartz-chlorite-schists, and minor phyllites. Non-vesicular metabasalts are exposed around Astagal, Polem, Padi, and Subdalem in the south and Tisk (Usgao)-Dharbandora in central Goa. Vesicular metabasalts are exposed to the north of Gulem, at Barcem, and along the Saleri-Vagon road in Canacona taluka. Those from Bogmalo are vesicular, amygdaloidal and are dominated by pyroxene and at places contain olivine. The basalts in general, consist of saussuritised plagioclase and uralitised pyroxene forming actinolite, chlorite, epidote, clinozoisite along with opaques.

##### **Ponda Group**

The Ponda Group is best developed around Ponda town where most of the lithologies are well exposed. It comprises three formations which in ascending order are the Sanvordem Formation, the Bicholim Formation, and the Vagheri Formation, all of which are dominated by clastics with very subordinate mafics only in the Vagheri Formation. Around Ponda, the total thickness of this group is about 8.8 km.

### **Sanvordem Formation**

The Sanvordem Formation rests on the Chandranath granite gneiss with a polymict meta conglomerate at the base and comprises metagreywacke and argillites. The conglomerate consists of stretched and elongated pebbles of quartzite and gneiss in a schistose.

chlorite matrix. The proportion of lithologies varies considerably from place to place, so much so that one single lithology may be present to the complete exclusion of the other members. The best section of this formation is exposed along the railway track between Sanvordem railway station and Periudoc. In this section, it has a thickness of over 1.2 km. The exposures across River Mandovi between Aguada and Baga are dominated by thinly bedded (laminated) argillites. The meta-conglomerate consists of stretched lenticular pebbles and boulders of quartzite and granite gneiss, The metagreywackes are faintly schistose and show graded bedding. The rock consists of sub-angular quartz, plagioclase, and lithic fragments in a matrix of sericite, chlorite, and quartz. The argillites are light to deep grey and consist of quartz in a sericite-chlorite matrix with opaques. Rarely biotite has formed at the expense of chlorite.

### **Bicholim Formation**

This Formation can be traced over the entire length of Goa (~ 185 km) in an NW-SE direction from Naibag in the northwest to Salgini in the southeast. The average true thickness of the Formation is about 1.4 km (Gokul et al. 1985). It consists of amphibole schists, ferruginous and manganiferous phyllites, limestones, and banded ferruginous quartzites (BHQ) that occur as intercalations within the phyllites. The BHQs serve as the protores for the iron ore deposits that are extensively developed in this formation. The BHQs are thinly

laminated and consist of alternate laminae of hematite/magnetite and chert. The banded iron formation (BIF) consists of two subfacies- the haematite sub-facies and the magnetite sub-facies, both of which show an interdigitated relationship. ). Calcareous (carbonate facies of BIF) and carbonaceous (sulfide facies) intercalations are common. Manganese being an inseparable associate of iron in almost all BIF the world over, both these exhibit a zonal distribution pattern. The dominant lithology is represented by quartz-chlorite-tremolite schists followed by ferruginous phyllites.

### **Vagheri Formation**

The topmost formation of this Group is represented by Vagheri Formation which conformably overlies the Bicholim Formation. It is best exposed to the northeast of Valpoi. It comprises metagreywacke-argillite with intercalated metabasalts, The metagreywackes are grey to greyish green, compact, and exhibit poorly developed schistosity. The rock consists of angular to sub-angular cryptic- and lithic fragments in a fine-grained mesostasis made up of quartz, feldspar, and chlorite. The metabasalts occur as narrow, lenticular intercalations within the metagreywacke and exhibit a poorly developed foliation at places. The rock is grey to greenish grey, hard, compact, and has faint schistosity. It consists of chlorite, tremolite/actinolite, plagioclase, epidote, zoisite, opaques, and quartz which may be secondary.

## 1.5 Study Area

The long coastline of Goa is complex Figure 13. The coast in general is oriented in NNW and SSE direction. The coasts of Salcete and much of Bardez and Pernem are made up of long sandy beach stretches, and it is quite tempting to classify them as emerging but if you compare it with the coasts of Canacona-Quepem and Marmagoa could well be classified as submerging or submergent. All the rivers that flow across the state are estuarine and tidal waters penetrate several kilometers inland. This fact leads us to believe that the coastal zone of Goa is sinking. Wave action and current directions play their role as do coastal rock formations. The shape of the coastline and many of the coastal features are controlled by a variation in rock types and rock structures. Many of these rock types and structures are exposed in the coastal headlands along the coast.

The present study mainly focuses on the sand sediments present on coastal areas/beaches in Goa. The area under investigation lies on the southern portion of the coast of Goa along the western coast of India. The area of interest is around a 40 km coastal stretch from Canaguinim Beach to Palm Beach. Canaguinim Beach is located at Latitude 15° 7'36.38" N and 73°56'25.55"E longitude which falls in the Quepem taluka And Polem Beach is located at Latitude 14°54'27.56"N and 74° 4'56.59"E longitude which lies in Canacona taluka. In the south of Goa (Quepem and Canacona) the coast is rather hilly and mountainous. In this region, hill ranges of the Western Ghats extend up to the sea and, therefore, sandy beaches and coastal plains are limited in size, while headlands with sea cliffs abound. As compared to the northern part of the state, low lateralized plateau-topped hills occur within and between coastal-estuarine plains. In south Goa, the rocks are folded with a WNW-ESE trend (direction of fold axis). The intensity of folding is strong and the metamorphic layering

(schistosity and gneissosity) of the exposed rocks is often vertical or steeply dipping with the same WNW-ESE strike. The sea from the west attacks the varied rock layers almost at right angles to the schistosity. The frequently differing rock layers are the cause of variation in erosion rates and the result is a very indented and crenulated coastline, as observed particularly in Quepem and Canacona.

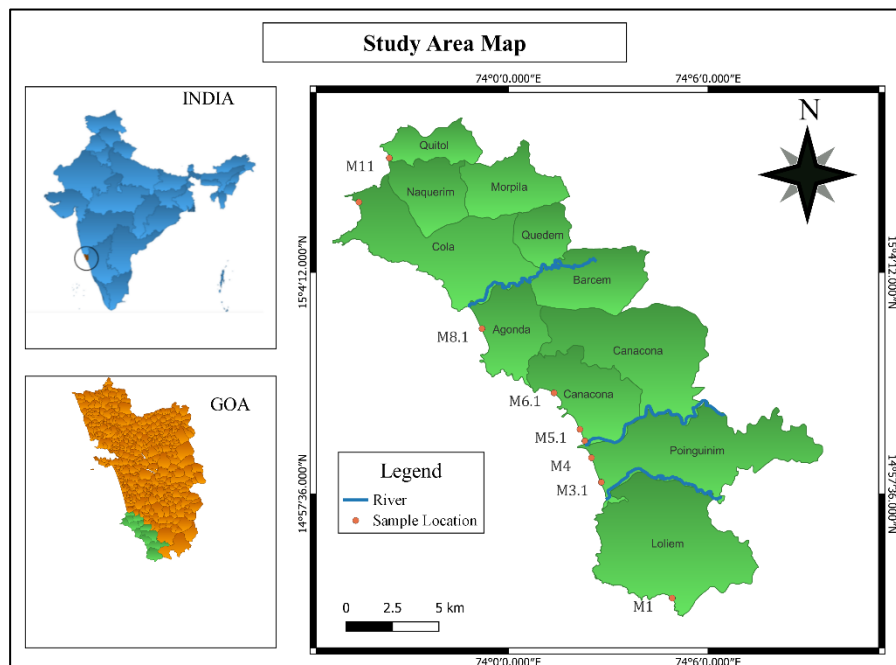


**FIGURE13 : Study area map South Goa**

SAMPLES	NAME	COORDINATION
M1FS	POLEM	14°54'29.69"N 74° 4'55.34"E
M1BS		
M3.1 FS	GALGIBAGA	14°57'56.85"N 74° 2'47.59"E
M3.1BS		
M4 FS	TALPONA	14°58'40.54"N 74° 2'29.74"E
M4 BS		
M5.1 FS	RAJBAG	14°59'31.32"N 74° 2'8.97"E
M5.1 BS		
M6.1FS	PALOLEM	15° 0'36.45"N 74° 1'22.40"E
M6.1 BS		
M8.1FS	AGONDA	15° 2'31.35"N 73°59'12.58"E
M8.1BS		
M10FS	CAB DE RAM	15° 6'17.39"N 73°55'30.73"E
M10BS		

**Table 3 Showing sample number along with name and Coordinates**

### **1.6. Aim and Objectives**

- Determine the abundance and distribution of individual mineral species, with particular attention to heavy minerals.
- Measure the size distribution of the particles along the shoreline.
- Utilize mineralogical analysis and transportation history of surficial texture to unravel the provenance of these minerals.
- To estimate and quantify the heavy mineral of the study area.



### **1.7 Brief Structure of Dissertation**

Heavy minerals are defined as minerals with a density exceeding 2.9 grams per cubic centimeter ( $\text{g/cm}^3$ ), significantly higher than common rock-forming minerals such as quartz and feldspar. They are valuable for studying the origin of sand or sandstone and serve as an exploration tool for identifying nearby ore deposits. Extensive research has been conducted on heavy minerals globally, particularly in India. The coastal areas of Tamil Nadu, Kerala, Andhra Pradesh, Odisha, and Karnataka are prime locations for developing placer deposits, with numerous studies focusing on these regions.

Notably, studies on heavy minerals along the northern coast of Goa have been reported by G. N. Nayak in 1997 and A. Sreenivasa et al. in 2014, although research on South Goa remains limited. To conduct our current research, samples were collected following standard procedures from South Goa beaches. These samples underwent density separation using bromoform. X-ray diffraction (XRD) analysis was performed on the separated minerals to identify their crystal structure, aiding in mineral identification and providing insights into the bulk heavy mineral composition. Additionally, selected samples were examined using a stereo zoom microscope, while some mineral grains underwent scanning electron microscope (SEM) analysis to reveal their surface texture.

Furthermore, 300-gram sand samples were processed for grain size analysis to determine the average sand size on South Goa beaches. Changes in these parameters can indicate variations in energy conditions and sedimentary deposition patterns.

# CHAPTER II

## LITERATURE REVIEW

## 2.0 Literature review

Heavy minerals being Higher in density the majority of heavy minerals are deposited in particular settings where they can gather and concentrate. Embarking on a global exploration of heavy minerals, the collective body of literature paints a comprehensive panorama, illuminating the multifaceted dimensions of these mineralogical treasures. Studies conducted across diverse regions provide insights into the intricate interplay of geological processes, sedimentary dynamics, and the economic significance of heavy mineral deposits. Here is an elaborative synthesis of key literature from various corners of the globe:

Australia - Roy et al. (2016): Roy et al.'s investigation along the expansive Australian coastline delves into heavy mineral deposits, spotlighting the economic prowess of minerals like ilmenite, rutile, and zircon. Their study not only unravels the geological processes shaping Australia's coastal sediments but also underscores the pivotal role these minerals play in the country's economic landscape.

South Africa - Cawthorn et al. (2019): Venturing into the mineral-rich sands of South Africa, Cawthorn et al.'s research meticulously identifies and characterizes heavy minerals such as ilmenite, rutile, zircon, and garnet. Beyond their geological insights, the findings offer a historical narrative and shed light on the economic value encapsulated within these coastal deposits.

Brazil - Dillenburg et al. (2017): Dillenburg et al.'s exploration along the Brazilian coast unravels the tapestry of heavy mineral occurrences, bringing to the forefront the prevalence of ilmenite, rutile, and zircon. The study not only contributes to understanding coastal

dynamics and sedimentary processes but also enriches the global discourse on the complexities of heavy mineral distribution.

India - Kurian et al. (2012): In the vast expanse of the Indian coastline, Kurian et al.'s review stands as a beacon, offering a broad panorama of heavy mineral occurrences. Discussing geological settings, sedimentary processes, and economic significance, the work extends its implications globally, emphasizing the necessity for detailed studies to unlock the full economic potential of coastal heavy mineral resources.

USA - Van Gosen (2014): Van Gosen's meticulous exploration of heavy mineral occurrences within the United States provides a targeted focus on titanium and zircon minerals. The study not only contributes to the understanding of these resources within the U.S. but also acts as a beacon for global comparisons, enriching the collective knowledge of heavy minerals.

Mozambique - Lousada et al. (2020): In the captivating landscapes of Mozambique, Lousada et al.'s study delved into heavy mineral deposits, spotlighting the economic potential encapsulated within ilmenite, rutile, and zircon. Their research not only adds nuance to the understanding of mineral resources in East Africa but also contributes to the global tapestry of heavy mineral studies.

Norway - Stamsø et al. (2018): Stamsø et al.'s exploration of heavy mineral occurrences along the Norwegian coast offers a glimpse into the mineralogical richness, characterizing minerals like ilmenite, rutile, and garnet. The study not only contributes to Norway's coastal geology but also provides a comparative lens for understanding global variations in heavy mineral content.

China - Feng et al. (2013): Feng et al.'s intricate research in China unravels the intricacies of heavy mineral deposits, honing in on ilmenite, rutile, and zircon occurrences. Their study not only offers insights into the mineralogical composition of Chinese coastal areas but also becomes a valuable piece in the mosaic of global heavy mineral literature.

Senegal - Cisse et al. (2015): In the West African context, Cisse et al.'s investigation into heavy mineral sands in Senegal identifies economically valuable minerals such as ilmenite and zircon. Beyond the local perspective, their research contributes to a broader understanding of mineral potential in the West African region, enriching the global discourse on heavy minerals.

Brazil- Maria Augusta M. da Silva (1978) conducted a comprehensive heavy minerals study in southeastern Brazil, covering the stretch from Rio Grande to Chui, focusing on beach sands and river sediments. The research primarily explored heavy mineral species, their concentrations, distribution along beaches, origin, concentration methods, and potential mineral exploration sites. The findings suggest a combination of local sources (Rio Grande do Sul Shield and Paraná Basin) and distant sources (Andean province) contributing to heavy minerals in beach sands, transported by rivers and coastal currents. Concentration processes involved sediment buildups during spring tides or storms, continuous washing in backshore channels, and erosion caused by wind on the offshore surface.

Eastern Mediterranean Mustafa Ergin et al.,( 2005) the research investigated grain size and heavy mineral distribution in backshore silt samples from beaches around the Finike and Antalya Gulfs in the eastern Mediterranean. The majority of beaches exhibited medium- to

well-sorted sand as the predominant mean particle size. The heavy mineral concentrations, reaching up to 86% of bulk sediment, and significant element concentrations suggested an ultramafic origin, primarily from the ophiolitic rocks of the Antalya–Tekirova nappe on the coastal hinterland. The study highlighted the importance of understanding particle size, chemical makeup, and heavy mineral composition in these modern beach sediments.

Worldwide Overview - Jones et al. (2021): Jones et al.'s panoramic synthesis provides a truly global perspective, summarizing heavy mineral occurrences, economic importance, and exploration methods worldwide. Serving as a compendium of insights from various regions, this review acts as a cornerstone for a comprehensive understanding of heavy mineral resources on a global scale, underlining the imperative for sustainable resource management and ongoing research endeavors.

In essence, the worldwide literature on heavy minerals not only serves as a repository of regional studies but also weaves a collective narrative that transcends geographical boundaries. These investigations collectively contribute to our evolving understanding of the mineralogical diversity, distribution patterns, and economic potential of heavy minerals on a global scale. The findings resoundingly underscore the imperative for sustainable resource management and advocate for continued research to unlock the full economic potential of these valuable coastal deposits, forging a path towards a shared global understanding of these geological treasures.

A thorough examination of the literature on heavy minerals in India reveals a comprehensive body of research that spans diverse coastal regions, providing a nuanced understanding of the mineralogical intricacies, distribution patterns, and economic potentials associated with these deposits. The studies outlined below contribute significantly to this knowledge base:

Overview of Coastal Regions - Kurian et al. (2012): Kurian et al.'s expansive review offers a holistic perspective on heavy mineral occurrences along the vast Indian coastline. Delving into the geological settings and sedimentary processes, the work emphasizes the economic significance of heavy minerals. It advocates for more detailed studies to unlock the full economic potential embedded within these coastal resources.

Odisha Coast - Sahoo et al. (2019): A focused study along the Odisha coast provides valuable insights into heavy mineral distribution and concentration. The research exposes a diverse suite of

heavy minerals, ranging from ilmenite and garnet to zircon, rutile, and magnetite. The findings underscore the economic promise of these minerals, particularly in beach placer deposits.

West Coast - Padmalal et al. (2007): Padmalal et al.'s investigation into the southwestern continental shelf of India enriches our understanding of heavy mineral distribution. The study identifies major heavy minerals, including ilmenite, rutile, zircon, garnet, and sillimanite. These findings contribute significantly to unraveling the geological processes shaping the sediments along the West Coast.

Eastern Coast - Chakraborty et al. (2014): Focusing on the Mahanadi delta region, Chakraborty et al.'s study delves into the distribution of heavy minerals in sediments. Identifying minerals such as ilmenite, magnetite, garnet, and zircon, the research underscores the impact of fluvial processes on the concentration and distribution of heavy minerals in this region.

Kerala Coast - Chandramohan et al. (2010): An in-depth investigation along the Kerala coast explores the intricate heavy mineral assemblages. Key minerals such as ilmenite, garnet, rutile, zircon, and sillimanite are identified. The study emphasizes the critical role of understanding sediment dynamics for effective exploration and exploitation of heavy minerals.

Gulf of Mannar - Rao et al. (2014): The study by Rao et al. provides a detailed examination of heavy mineral distribution in the ecologically sensitive Gulf of Mannar. Noteworthy occurrences of ilmenite, garnet, zircon, and rutile are identified, contributing to a broader understanding of heavy mineral deposits in this unique region.

Tamil Nadu Coast - Thangadurai et al. (2011): Thangadurai et al.'s study scrutinizes the coastal sediments of Tamil Nadu, unraveling the content of heavy minerals. Prominent minerals such as ilmenite, garnet, zircon, and rutile take center stage, contributing to the characterization of coastal sediments and shedding light on their economic potential.

Karnataka- G. Shalini et.al -2023: In India, studies were also done on Provenance and Implications of Heavy Minerals in the Beach Sands of India's Central West Coast (G. Shalini et.al 2023) The study was carried out on the estuarine beach sands of the Mulki-Pavanje River system, which is located close to the town of Mulki in Udupi District, Karnataka, India, along the CWC of India. This research discusses the heavy mineral assemblage and mineral chemistry of the beach sands in Mulki, Karnataka, on the central west coast of India, to determine their origin. The sands of Mulki Estuarine Beach have a heavy mineral assemblage that includes rutile, zircon, ilmenite, magnetite, hornblende, epidote, kyanite, and tremolite. The mineral chemistry and heavy mineral assemblage point to a mixed provenance of high-grade metamorphic, acidic, and basic igneous rocks. The presence of kyanite, tremolite, and



rutile indicates the presence of high-grade metamorphic source rocks. The Mulki Pavanje River emerges from a metamorphic terrain of modest grade. Monazite is one of the minerals which is characterized as heavy minerals and a special study were done by (J. K. Anitha et.al) in Kerala, India along the coast of the Neendakara–Kayamkulam belt. study aims to shed light on the chemistry and distribution of monazite minerals throughout. An effort is made to look into the texture and mineralogy of beach sediments, and then the mineral monazite is recovered for in-depth structural and chemical analysis. The research concluded that an efficient way to ascertain the monazite mineral's chemical composition and surface morphological features is to combine ED-XRF and SEM-EDS. The texture and mineralogy of beach sediments give a clear picture of the distribution of strategic heavy minerals along the coast, which can guide potential target exploration. The principal chemical components of monazite minerals, such as  $\text{Ce}_2\text{O}_3$ ,  $\text{La}_2\text{O}_3$ , and  $\text{P}_2\text{O}_5$ , are 26.658, 13.421, and 23.649%, in that order. The chemical and mechanical weathering mechanisms that happened in the monazite mineral are shown by the SEM

In summary, the collective literature on heavy minerals in India provides a mosaic of insights derived from various coastal regions. These investigations deepen our understanding of the diverse mineralogical compositions and distribution patterns of heavy minerals across the country. The findings underscore the imperative for sustainable resource management and advocate for continued research to fully harness the economic potential embedded within these valuable coastal deposits.

The coastal region of Goa, India, has been a focal point for comprehensive studies delving into the intricate mineralogical composition of beach sands, unraveling the geological characteristics and potential economic importance of these deposits. A series of pivotal

investigations conducted along the Goa coastline have illuminated the rich tapestry of heavy minerals, shedding light on their diverse assemblages and contextualizing them within the geological landscape.

One noteworthy study, led by Sreenivasa et al. in 2014, focused its attention on the captivating Vagator Beach in North Goa. Employing a sophisticated array of techniques, including heavy mineral separation, X-ray diffraction (XRD) analysis, and optical microscopy, the researchers unveiled a tapestry of minerals. Among them, opaque minerals like magnetite and ilmenite took center stage, alongside transparent heavy minerals, including hornblende, epidote, garnet, rutile, zircon, and enstatite. Emphasizing the significance of advanced tools like XRD and Scanning Electron Microscopy (SEM), the study provided an intricate exploration into the mineralogical nuances of Vagator Beach.

Venturing further along the Goa coastline, the Morjim - Arambol Beach became a subject of interest for researchers Kidwai and Wagle (1975), and Kidwai et al. (1981). This stretch, extending NNW-SSE from the Chapora River mouth, unfolded a geological narrative characterized by heavy minerals such as garnet, staurolite, epidote, chlorite, hornblende, tourmaline, augite-diopside, hypersthene, and zircon. These early studies provided foundational insights into the diversity of minerals along the Goa coastline, setting the stage for subsequent research endeavors.

The narrative extended further to the Tila-Mati Beach, dissected by Mislankar and Iyer (1996) and Nayak (1997). Nestled between Polem and Majali, this north-south trending sheltered black sand beach displayed an exceptional composition rich in amphiboles,

primarily consisting of tremolite-actinolite. The heavy minerals identified, including hornblende, tremolite, magnetite, ilmenite, pyroxenes, and epidote, painted a unique picture of the mineral wealth embedded in this coastal enclave. G.N Nayak 1997 published a paper on a case study of beach sediments from Goa using grain size parameters and heavy minerals as indicators of the depositional environment studied between the Tiracol and Chapora Rivers. Heavy mineral suite identified in this area proves the provenance to be mainly the catchment area of the two rivers. There are essentially two categories for heavy minerals: low density and high density. Low-density minerals are located farther away from river mouths, while high-density heavy minerals are concentrated closer to them. The opaques (magnetite and ilmenite), hornblende, augite/diopside, staurolite, hypersthene, garnet, actinolite/tremolite, and rutile are the heaviest minerals that were successfully identified. They discovered that the grain size varied throughout the coast, suggesting various energy levels and transport processes at various points. Furthermore, the particular kinds of heavy minerals found in the sediments offered hints regarding their origin, indicating that the surrounding rivers were their primary source. Overall, the study shows that examining the heavy mineral content and grain size

might be useful methods for learning about the processes that have shaped beach habitats in the past and today.

Collectively, these studies underscore the captivating heterogeneity of heavy mineral deposits along the Goa coastline, revealing a mosaic of mineralogical variations and concentrations. While Vagator Beach stood out with notable concentrations of magnetite and ilmenite, other locales showcased a diverse array of heavy minerals, including amphiboles, garnet, tourmaline, and zircon. The application of advanced analytical techniques, such as

XRD and SEM, added layers of precision to the characterization of these minerals, offering profound insights into their geological genesis and potential economic significance. As the exploration continues, further research endeavors are essential to broaden the knowledge base and pave the way for sustainable resource management in this ecologically significant region.

# CHAPTER III

## METHODOLOGY

### **3.0 Methodology and Materials**

Sampling for heavy mineral analysis: The value of heavy mineral analyses largely depends on the accuracy of sampling; it must be planned with great care. The sampling technique will be determined in part by the study's objectives and the characteristics of the depositional environment. However, it is crucial to plan a dense sample procedure and gather untethered material. Random sample collection will almost definitely produce useless and unsatisfactory results. Samples should be taken at regular intervals. The best heavy mineral assemblages are typically found in fine-to-medium-grained sands or sandstones, while grain size can have an impact on heavy mineral compositions.

#### **3.1. Sampling**

The entire study workflow consists of four steps apart from field investigation including sample collection: a) grain size analysis b) Preparation of samples c) Heavy and light mineral separation technique, and d) Identification by a petrographic microscope and stereo zoom.

The quantitative sampling of exposed sandy beaches was achieved by using a piston corer. Piston corers can be easily made by cutting the end off a plastic syringe of 60 ml and PVC pipe of 5 cm in diameter with 2 replicates of each Figure 15. A total of nine stations were marked at an interval of 4km which was divided into sub-samples that is the backshore and foreshore Figure 14. The samples were collected during the pre-monsoon season. About 100g samples were collected from each station.

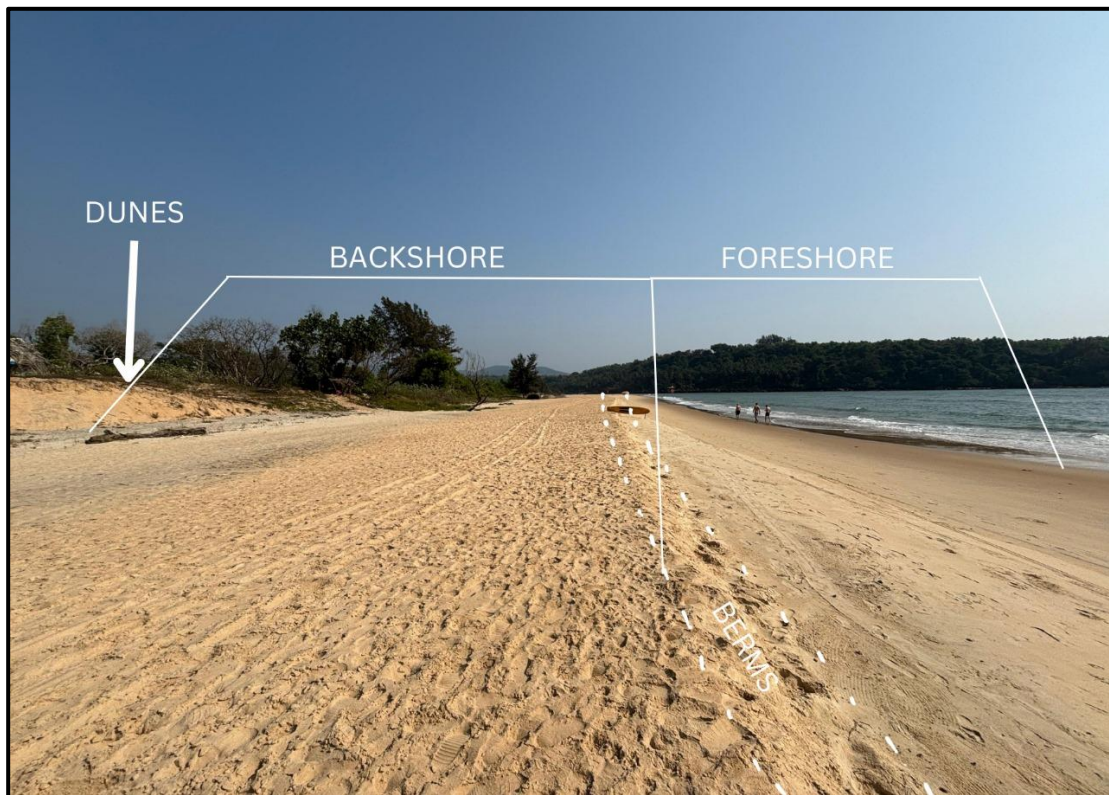


**FIGURE 14** Diagram showing beach profile along the shore of Betul



**FIGURE 15** a) the core tube is pushed into the sediments with the head of the plunger remaining on the surface. b. sample collection for sieve size analysis c. sample storage.

### 3.2 Sieve Sand Size Analysis

The grain size analysis test is performed to determine the percentage of each size of grain that is contained within a soil sample, and the results of the test can be used to produce the grain size distribution curve. This information is used to classify the soil and to predict its behavior. As per the present study beach sand was taken into consideration and distribution was done within the sand size itself. Once the sieve size analysis is done the following data distribution graph can be plotted along with further calculation of the mean size value.

Procedure :-

- 1) Samples were collected on the coast of south Goa with the use of a shovel and sample bag.
- 2) Backshore and foreshore samples were collected with 15 mt interval
- 3) Samples were then kept for oven drying and let all the water dry.
- 4) Samples were later cleaned where large shells and rock fragments were hand-picked and a few medium size shells were removed with the help of sieves.
- 5) After corning and quartering 300 grams of samples were measured for sieve size analysis
- 6) A range of 10 sieves were selected and they were concerning different sand sizes such as (850 microns, 710 microns, 600 microns – Coarse sand size ), ( 500 microns & 300 microns – Medium sand size ), ( 250 microns & 180 microns – fine sand size ) , ( 106 microns, 90 microns & 75 microns – very fine sand size ).
- 7) The sieves were kept on the sieve shaker machine in and descending order of numbers.the sieves were vibrating and rotating for 15 min. Samples. were then removed from the sieves and were weighted.





**FIGURE 16 . A. sample collection. B. sample cleaning. C. arrangement of sieves. D. sieve shaker.**

50 grams of sample were selected from coarse sand to fine sand fraction and was further gone under the sample preparation process. The reason for taking coarse sand to very fine sand fractions through mash was to keep the size under sand fraction also taking a single sand fraction would allow us to do heavy mineral analysis in all sizes under sand rather than taking only fine sand or medium sand.

### 3.3. Preparing Samples

To dry out the sediment samples, they were roasted at 60°C. An approximately 50g sediment sample is extracted using coning and quartering. Figure 2.2 A This was done to reduce bias samples. The samples were then treated with H<sub>2</sub>O<sub>2</sub> to remove the organic matter which include things like decomposing plant debris or organic contaminants. Then Acid digest is applied to dissolve unwanted carbonate material. The technique can facilitate the removal of calcareous particles from unconsolidated sediments by adding dilute HCl (10%) Figure 17.

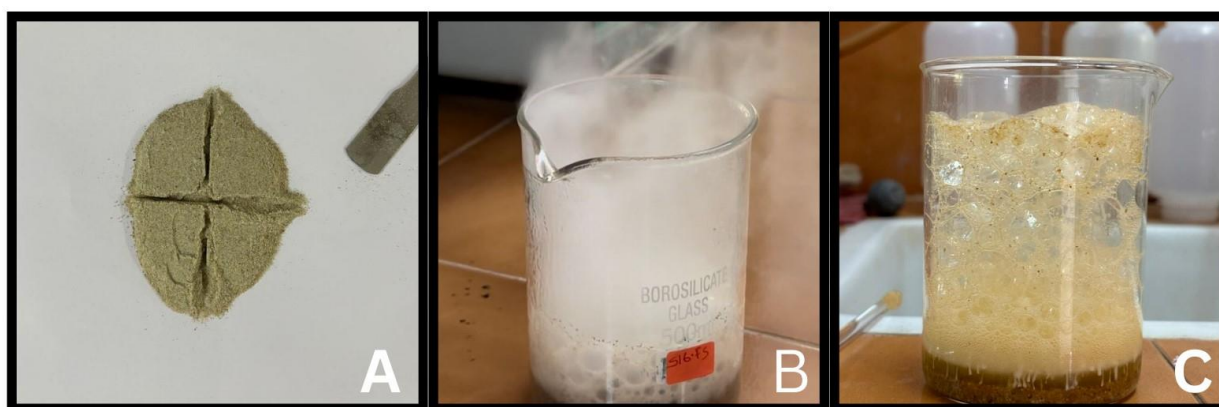


**FIGURE 17** A- Coning and quartering of samples, B- addition of H<sub>2</sub>O<sub>2</sub> for removal of organic matter, C- addition of HCL

### 3.4 Magnetic separation of heavy minerals

This method is used to separate minerals that are magnetically susceptible from those that are not. A magnet is passed over the sample, and the magnetic minerals are attracted to the magnet. This method is often used in conjunction with gravity separation. The magnetic minerals are seen in Figure 17 This method was used before the addition of HCL so that the grains don't corrode.

Procedure:

1. The sample was evenly spread on clean paper (a thin layer allows the magnet better access to individual particles).
2. Wrap the magnet in a paper.
3. The hand magnet was held close to the surface of the sample, but not touching it, it glided slowly across the sample.
4. The magnetic minerals in the sample attracted to the magnet. Take away the magnet as the magnetic minerals will come along with it.
5. Unwrap the paper, and collect the magnetic minerals in a clean dish.
6. step 2 was repeated 3 times to catch any magnetic minerals that may not have been captured in the first pass.
7. Weight the magnetic minerals.

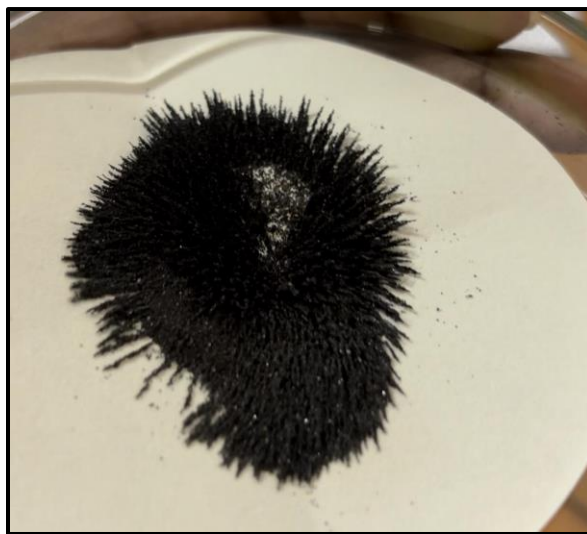


**FIGURE 18** magnetic minerals aligned with magnetic directions

### 3.5. Heavy Mineral Separation

Heavy minerals are minerals with a specific gravity greater than that of quartz i.e. 2.65 or feldspar i.e. 2.76. A specific gravity of 2.8 is accepted as a lower limit so any mineral with a specific gravity of more than 2.8 is a heavy mineral. The method by which heavy minerals are separated in the laboratory is the separation by heavy liquid and magnetic separation. The principle for liquid separation is that “minerals with different specific gravities can be separated from each other by liquid whose specific gravity lies between the two minerals. The heavy mineral sink to the bottom and lighter

minerals float at the surface”. The apparatus used is known as the separating funnel. Liquid separation is that “minerals with different specific gravities can be separated from each other by liquid whose specific gravity lies between the two minerals. The heavy minerals sink to the bottom and lighter minerals float at the surface”. The apparatus used is known as the separating funnel.

#### 3.5.1 . Density separation.

Density separation is based on the different minerals have different densities. Thus, if a mixture of minerals with different densities is placed in a liquid with an intermediate density, the grains with less densities than that of the liquid will float, and grains with densities greater than the liquid will sink. Typical mineral densities range from about 2.2 g/cc to as much as 8 g/cc but are generally between 2.5 and 3.5 g/cc for silicate minerals. Suitable liquids for density separation include bromoform (density = 2.84 g/cc) and diiodomethane (density = 3.31 g/cc). Because of the use of high-density liquids, density separation is often referred to as heavy liquid separation. Heavy liquid separations are generally done in separatory funnels. Figure (2.3) illustrates the arrangement of equipment used for separation by gravity settling.

Procedure:

1. Samples were served to obtain material in the 500 to 75-micron range.
2. Weigh samples were weighted about 25 g was used for the analysis. Recorded sample weight, heavy liquid.
3. Pour bromoform into the upper (separatory) funnel (see Fig. 3). The funnel should be about 1/2 full. This experiment was carried out in a well-ventilated fume hood.
4. Samples were poured into bromoform and stirred thoroughly to wet all particles and disperse air bubbles.
5. Allowed particles to settle; stirring was done periodically so that particles would not adhere to the funnel wall. The funnel was covered with watch glass/foil paper to reduce heavy-liquid evaporation loss.

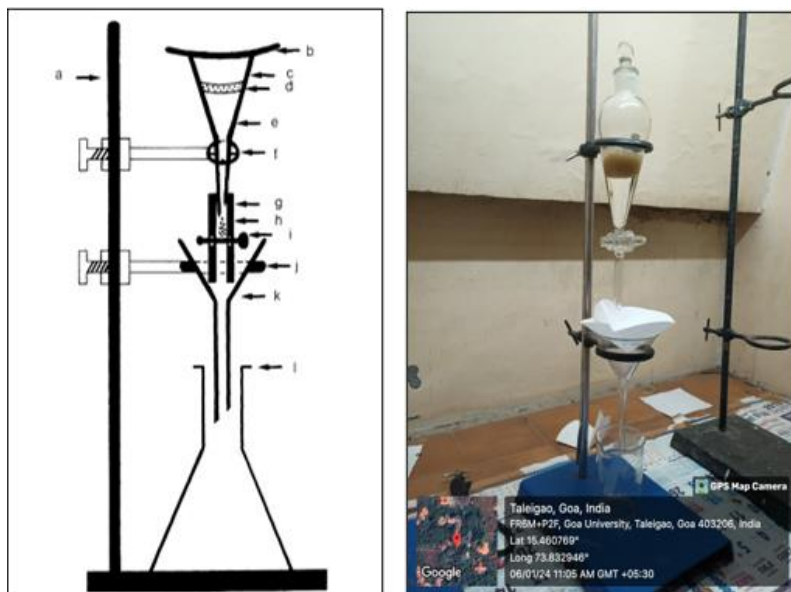


**FIGURE 19 A- Diagram showing an arrangement for Density separation.**

6. When heavy minerals are settled to the bottom of the separatory funnel, open pinch-cock and allow heavy mineral particles to drop onto the filter paper in the lower funnel. Close pinch-cock so that minerals floating in the remaining heavy liquid will remain in the separatory funnel.

7. After the heavy liquid has drained from the filter paper into used heavy-liquid bottle below, remove the paper and place it upside down in a porcelain dish or large watch glass containing a plastic squeeze bottle containing acetone was used to wash the dish in case any particle is adhere to the filter paper and also to remove the coating of bromoform.

8. The heavy minerals fraction was dried and their weight was recorded.

### 3.6. Under stereo zoom microscope

The heavy mineral which was obtained by density Separation was observed in the stereo zoom microscope. Hand-picking of grains was done with the help of a needle. Different mineral species can be recognized, and easily selected, under the stereo binocular microscope using their color or morphology. heavy mineral grains were separated for SEM–EDX analysis and the remaining sample was given for XRD analysis.

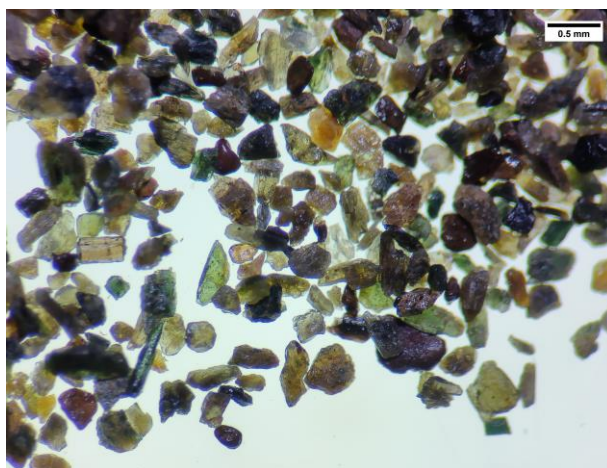


**FIGURE 20 Minerals Under Sterozoom Microscope**

### **3.7 . SEM ANALYSIS**

The scanning electron microscope, or SEM, is a kind of electron microscope that uses a low-energy electron beam to focus and scan specimens. It is used to examine the surfaces of microorganisms. The development of electron microscopes was due to the inefficiency of the wavelength of light microscopes. Compared to light microscopes, electron microscopes have far shorter wavelengths, which allows for higher resolution power.

#### **3.7.1. Principle of SEM**

The Scanning electron microscope works on the principle of applying kinetic energy to produce signals on the interaction of the electrons. These electrons are secondary electrons, backscattered electrons, and diffracted backscattered electrons which are used to view crystallized elements and photons. Secondary and backscattered electrons are used to produce an image. The secondary electrons emitted from the specimen play the primary role of detecting the morphology and topography of the specimen while the backscattered electrons show contrast in the composition of the elements of the specimen.

Scanning Electron Microscopy (SEM) is a powerful tool widely used in Earth science for analyzing the microscopic world of rocks, minerals, and other geological samples. SEM excels at producing detailed images of a sample's surface features, allowing researchers to examine textures, shapes, and sizes of objects down to the nanometer scale. This provides insights into the formation processes and history of the sample.

### **3.7.2. SEM with EDX**

In earth science, SEM and EDX are frequently used together as a powerful analytical combo to investigate the composition of rocks, minerals, and other samples. EDX is an analytical technique attached to SEM that analyzes the elemental composition of a sample area. When the electron beam from the SEM strikes the sample, it excites electrons in the atoms, causing them to emit X-rays with specific energies characteristic of each element. EDX detects and measures these X-ray energies, allowing identification and quantification of the elements present in the sample. By combining SEM's high-resolution imaging with EDX's elemental analysis, earth scientists can gain valuable insights into the composition of the specimen.

### **3.7.3 . SEM for heavy minerals**

For heavy minerals, the SEM is used to inspect general morphological characteristics (Robson 1984, Mallik 1986). However, the majority of studies focus on the examination of surface textures. These revealed by the SEM in great detail, mirror the effects of subaerial or subsurface dissolution processes and aid the assessment of post-depositional diagenetic modifications. Heavy mineral surface textures have received far less attention (see Stieglitz 1969, Setlow & Karpovich 1972, Lin et al. 1974, Gravenor 1979), even though the morphology and surface patterns of first-cycle heavy minerals may provide better information on environmental processes that can be obtained from quartz, which is usually polycyclic. For SEM inspection the grains are mounted on standard aluminum stubs which are covered with double-sided adhesive tape.

The selected grains were mounted on studs and were coated with a gold layer as gold is a good conductive material. Pictures were taken of the grains along with the EDX data.



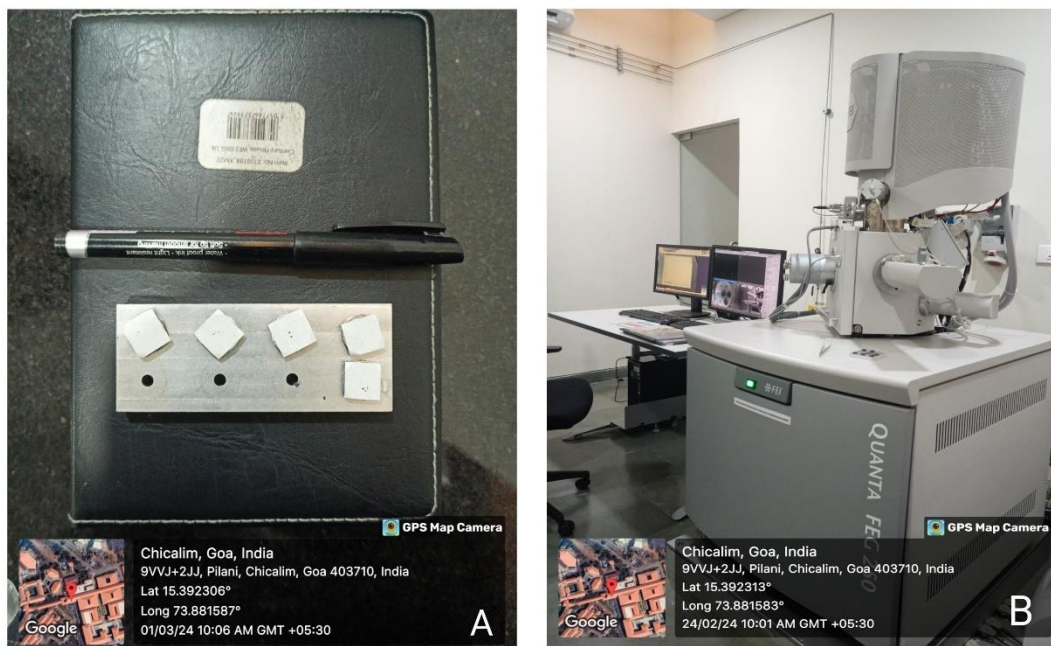


FIGURE 21 A- samples were placed on Studs . B- Quanta FEG 250

### 3.8 XRD Analysis

X-ray diffraction (XRD) is an analytical technique used to analyze physical properties such as phase composition of powder, crystal structure, and orientation of powder, solid, and also liquid samples. It is a non-destructive technique used in many different streams and areas to research the physical properties of materials; that is, it does not require the sample to be altered or damaged to be evaluated.

#### 3.8.1 . Principle of XRD

The principle of X-ray diffraction (XRD) is based on the constructive interference of monochromatic X-rays and a crystalline sample. X-rays are electromagnetic radiation with a wavelength that is similar to the interatomic spacing in crystals. When a beam of X-rays is directed at a crystal, the X-rays interact with the electrons in the atoms and are diffracted in

different directions. The diffraction pattern is determined by the arrangement of atoms in the crystal and can be used to determine the crystal structure.

The diffraction of X-rays by a crystal can be described by Bragg's law:

$$2d \cdot \sin(\theta) = n\lambda$$

where:

$d$  is the interatomic spacing

$\theta$  is the angle of incidence of the X-rays

$n$  is an integer

$\lambda$  is the wavelength of the X-rays

### 3.8.2. XRD in Earth Science

A powerful instrument used widely in geology to examine the mineralogical makeup of rocks, sediments, and soils is X-ray diffraction (XRD). It works by directing a beam of X-rays at a crystalline sample and measuring the angles at which the X-rays diffract. Because each mineral has a distinct diffraction pattern, geologists can identify the minerals in a sample.

- a) Mineral identification: a primary method for identifying unknown crystalline minerals. It is fast, reliable, and can be used to identify a wide range of minerals, including clays, carbonates, oxides, and sulfates.
- b) Quantitative analysis: XRD can be used to determine the relative abundance of different minerals in a sample. This information is essential for Quantification.

- c) Clay mineral identification: Clays are a group of important minerals that play a significant role in the physical and chemical properties of soils and sediments. XRD is a valuable tool for identifying the types of clay minerals present in a sample.

In heavy mineral analysis XRD can also be useful for identifying opaque grains (Harrison 1973) and for obtaining a general knowledge of bulk heavy mineral composition (Pryor & Hester 1969). The X-ray method requires finely ground crystal powder of the minerals.

### 3.8.3. Sample preparation for XRD

1. Once the heavy minerals are separated from the lighter minerals, the heavy minerals need to be finely ground using an agate mortar.
2. The powdered samples were then mounted onto a sample holder appropriate for the PXRD instrument. This involves pressing the powder into a small cavity.
3. Samples were then inserted into the XRD machine and were kept for the scan.
4. Magnetic minerals were analyzed under a standard scan of 15 min and using the researched 2theta value magnetic minerals were identified. Identification was done on Origin Lab software.
5. The heavy minerals were kept for a longer scan of 45 minutes to archive better and more accurate information. Also, the sample was analyzed for phase analysis and quantification analysis.

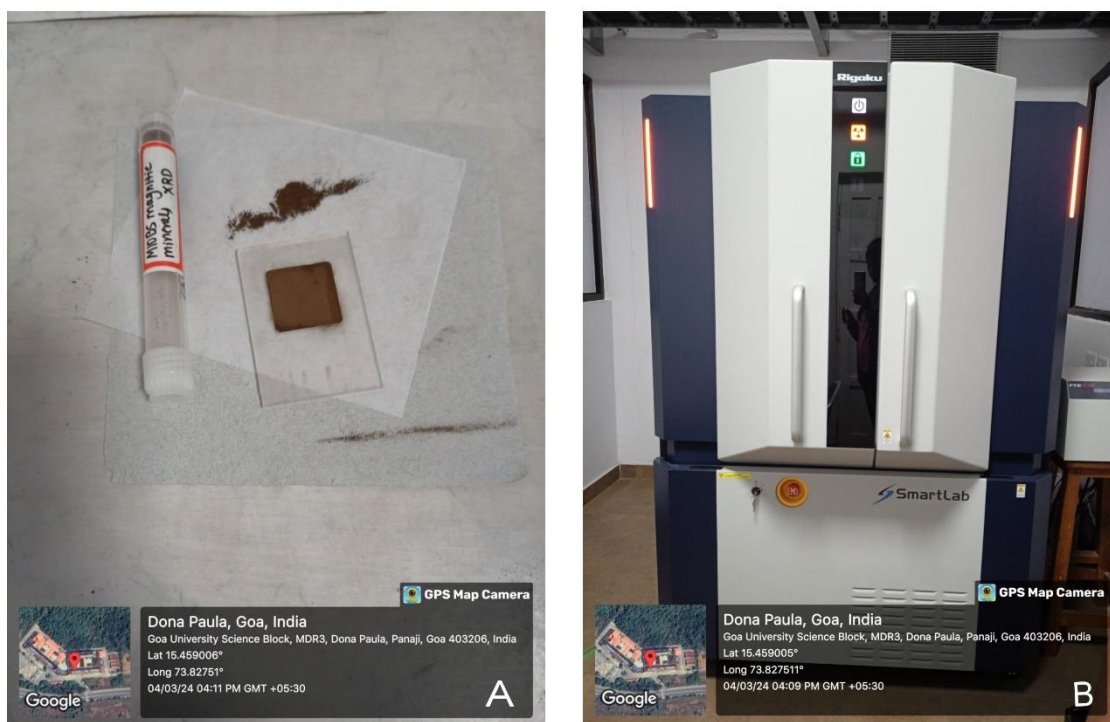


**FIGURE 22 A. powdered samples were placed in rectangular cavity sample holder of dimension 2x1.5 x0.2cm2. B. Rigaku XRD machine.**

# CHAPTER IV

## OBSERVATION AND RESULT

## 4.1 Observation and Result

### 4.1.1 Sieve size analysis

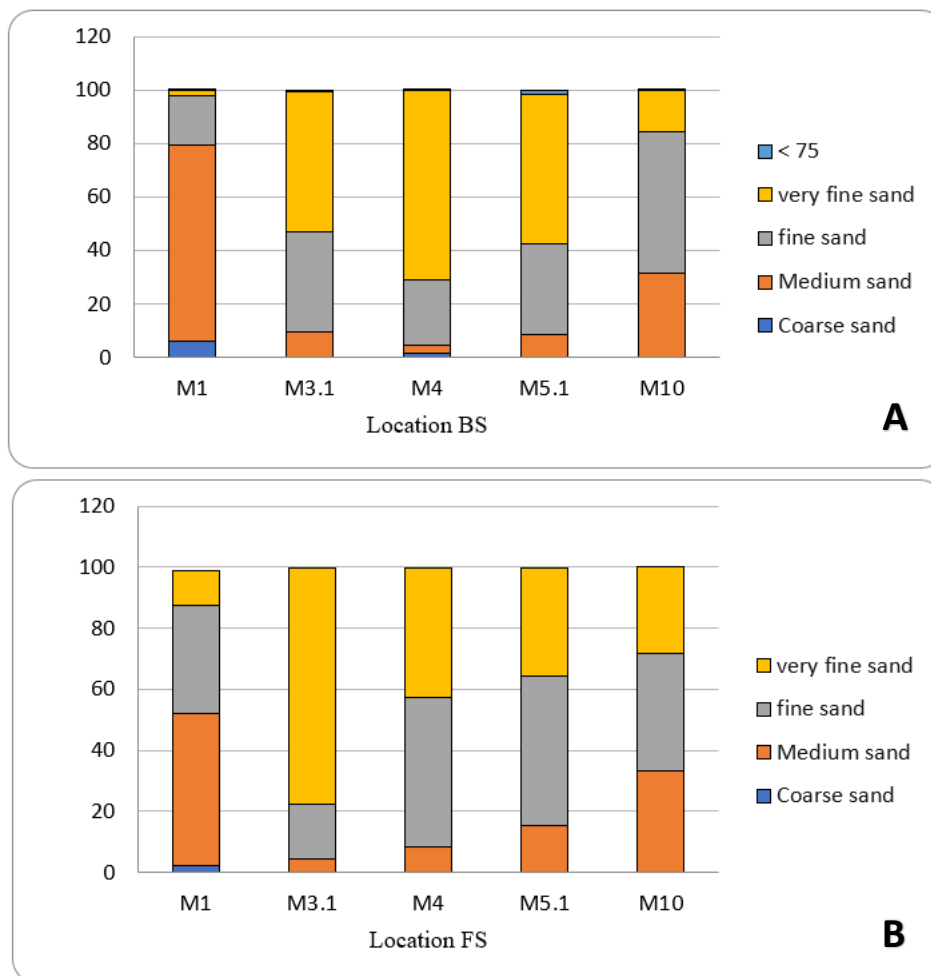


FIGURE 23 Grain size distribution in A - Backshore sample, B- foreshore sample

The grain size distribution pattern was analyzed using samples collected from Polem – Caanaguinium Beach in south Goa, focusing on variations between backshore (BS) and foreshore (FS) profiles Figure 23 and Table 4. Sample M1 BS from Polem Beach exhibited a predominant medium sand fraction of 73.341%, followed by fine sand at 18.34%, coarse sand at 6.13%, and minimal very fine sand. In contrast, M1 FS showed a decrease in medium

sand dominance (50.11%) with an increase in fine sand (34.95%) and very fine sand (11.47%), while coarse sand remained low at 2.18%. This shift suggests an influence of wave action and deposition energy on sand size distribution. The

Sample 3.1 BS from Galgebag Beach displayed a different profile with a dominant very fine sand fraction of 52.67%, along with fine sand (37.26%), medium sand (9.49%), and negligible coarse sand. Its corresponding FS sample M3.1 FS exhibited a higher percentage of fine sand (77.52%) and very fine sand (17.64%) with reduced medium sand (4.59%) and coarse sand(0.04%). figure 23 and table 5

At Talpona Beach (sample M4 BS), very fine sand prevailed at 70.45%, followed by fine sand(24.76%), and minor amounts of medium and coarse sand. In M4 FS, fine sand was predominant (49.02%), followed closely by very fine sand (42.48%), with medium sand (8.09%) and coarse sand (0.27%) present in smaller proportions. Figure 23 and Table 6

Sample M5.1 BS from Rajbag Beach showed a majority of very fine sand (55.81%) and fine sand (34.32%), while M5.1 FS exhibited higher fine sand (49.20%) and very fine sand (35.44%) proportions, with medium sand (15.12%) and minor coarse sand (0.11%). Figure 23 and table 7 Lastly, M10 BS from Cab de Ram featured a dominant fine sand fraction (52.87%) and significant medium sand content (31.56%), with very fine sand (15.39%) and coarse sand (0.11%) in smaller amounts. M10 FS showed a more balanced distribution of fine sand (38.79%) and medium sand (32.85%), with notable very fine sand (28.05%) and minor coarse sand (0.2%). These observations highlight the complex interplay of wave dynamics and deposition energies in shaping sand size distributions along the Goa coastline. Figure 23 and Table 8.

M1BS				
Sieves size	Grain size	Wt retained (gm)	Wt%	Cumulative Wt %
850	Coarse sand	0.002	0.000665177	0.000665177
710		0.219	0.072836845	0.073502022
600		18.234	6.064415709	6.137917731
500	Medium sand	56.044	18.63958067	24.7774984
300		164.473	54.7018013	79.4792997
250	fine sand	40.068	13.32614943	92.80544913
180		15.083	5.016429864	97.82187899
106	very fine sand	6.242	2.07601639	99.89789538
90		0.112	0.037249894	99.93514527
75		0.162	0.05387931	99.98902458
PAN	<75	0.033	0.010975415	100
	<b>Total</b>	300.672	100	

M1FS				
Sieves size	Grain size	Wt retained (gm)	Wt%	Cumulative Wt %
850	Coarse sand	0.001	0.000329295	0.000329295
710		0.068	0.022392065	0.02272136
600		6.577	2.165773728	2.188495089
500	Medium sand	26.827	8.833999058	11.02249415
300		125.351	41.27746733	52.29996147
250	fine sand	68.169	22.44771617	74.74767765
180		37.997	12.51222508	87.25990273
106	very fine sand	31.632	10.41626191	97.67616463
90		1.485	0.489003191	98.16516783
75		1.735	0.57132696	98.73649479
PAN	<75	3.837	1.263505214	100
	<b>Total</b>	303.679	100	

Table 4 M1BS and M1FS table for grain size distribution

M3.1BS				
Sieves size	Grain size	Wt retained (gm)	Wt%	Cumulative Wt %
850	Coarse sand	0	0	0
710		0.004	0.001315011	0.001315011
600		0.062	0.020382668	0.021697679
500	Medium sand	0.831	0.273193504	0.294891183
300		28.055	9.223157341	9.518048524
250	fine sand	49.7	16.3390098	25.85705832
180		63.64	20.92182261	46.77888093
106	very fine sand	149.88	49.27345651	96.05233743
90		2.853	0.937931488	96.99026892
75		7.486	2.461042804	99.45131172
PAN	<75	1.669	0.548688277	100
	<b>Total</b>	304.18	100	



M3.1FS				
Sieves size	Grain size	Wt retained (gm)	Wt%	Cumulative Wt %
850	Coarse sand	0.004	0.0013351	0.0013351
710		0.016	0.0053404	0.006675501
600		0.1	0.033377503	0.040053003
500	Medium sand	0.864	0.288381625	0.328434628
300		12.89	4.302360123	4.630794752
250	fine sand	20.06	6.695527081	11.32632183
180		32.796	10.94648585	22.27280768
106	very fine sand	223.379	74.55833219	96.83113988
90		3.907	1.304059038	98.13519891
75		4.978	1.661532094	99.79673101
PAN	<75	0.609	0.203268993	100
	<b>Total</b>	299.603	100	

Table 5 M3.1BS and M3.1FS grain size distribution

M4BS				
Sieves size	Grain size	Wt retained (gm)	Wt%	Cumulative Wt %
850	Coarse sand	0.018	0.005913835	0.005913835
710		4.546	1.493571989	1.499485825
600		0.051	0.016755867	1.516241692
500	Medium sand	0.199	0.065380736	1.581622428
300		8.53	2.802500895	4.384123323
250	fine sand	25.154	8.26425645	12.64837977
180		50.213	16.49730099	29.14568076
106	very fine sand	207.762	68.25945967	97.40514044
90		3.024	0.99352435	98.39866479
75		3.673	1.206750972	99.60541576
PAN	<75	1.201	0.394584241	100
	<b>Total</b>	304.371	100	

M4BS				
Sieves size	Grain size	Wt retained (gm)	Wt%	Cumulative Wt %
850	Coarse sand	0.018	0.005913835	0.005913835
710		4.546	1.493571989	1.499485825
600		0.051	0.016755867	1.516241692
500	Medium sand	0.199	0.065380736	1.581622428
300		8.53	2.802500895	4.384123323
250	fine sand	25.154	8.26425645	12.64837977
180		50.213	16.49730099	29.14568076
106	very fine sand	207.762	68.25945967	97.40514044
90		3.024	0.99352435	98.39866479
75		3.673	1.206750972	99.60541576
PAN	<75	1.201	0.394584241	100
	<b>Total</b>	304.371	100	

Table 6 : M4BS and M4FS grain size distribution

M5.1BS				
Sieves size	Grain size	Wt retained (gm)	Wt%	Cumulative Wt %
850	Coarse sand	0.014	0.004603643	0.004603643
710		0.014	0.004603643	0.009207286
600		0.177	0.058203198	0.067410484
500	Medium sand	1.731	0.569207549	0.636618032
300		23.526	7.736092888	8.372710921
250	fine sand	34.996	11.50779167	19.88050259
180		69.399	22.82058618	42.70108876
106	very fine sand	165.545	54.43643191	97.13752068
90		1.824	0.59978889	97.73730957
75		2.355	0.774398485	98.51170805
PAN	<75	4.526	1.48829195	100
	<b>Total</b>	304.107	100	

M5.1FS				
Sieves size	Grain size	Wt retained (gm)	Wt%	Cumulative Wt %
850	Coarse sand	0.005	0.001647745	0.001647745
710		0.029	0.009556921	0.011204666
600		0.322	0.106114782	0.117319448
500	Medium sand	3.804	1.253604442	1.370923891
300		42.098	13.87335431	15.24427821
250	fine sand	62.471	20.58725634	35.83153454
180		86.848	28.62067261	64.45220715
106	very fine sand	105.89	34.8959449	99.34815205
90		0.805	0.265286955	99.61343901
75		0.846	0.278798464	99.89223747
PAN	<75	0.327	0.107762527	100
	<b>Total</b>	303.445	100	

Table 7: M5.1BS and M5.1FS Grain size distribution

M10BS				
Sieves size	Grain size	Wt retained (gm)	Wt%	Cumulative Wt %
850	Coarse sand	0.011	0.003657876	0.003657876
710		0.033	0.010973627	0.014631502
600		0.314	0.104415721	0.119047223
500	Medium sand	5.658	1.881478181	2.000525404
300		89.257	29.681	31.6815254
250	fine sand	96.48	32.08289411	63.76441951
180		62.533	20.79435756	84.55877707
106	very fine sand	45.282	15.05781106	99.61658813
90		0.602	0.200185554	99.81677369
75		0.423	0.140661942	99.95743563
PAN	<75	0.128	0.04256437	100
	<b>Total</b>	300.721	100	

M10FS				
Sieves size	Grain size	Wt retained (gm)	Wt%	Cumulative Wt %
850	Coarse sand	0	0	0
710		0.031	0.010332403	0.010332403
600		0.78	0.259976602	0.270309006
500	Medium sand	8.586	2.861742443	3.132051449
300		89.988	29.9933006	33.12535205
250	fine sand	69.719	23.23757528	56.36292734
180		46.673	15.5562666	71.91919394
106	very fine sand	82.017	27.33653971	99.25573365
90		1.268	0.42262863	99.67836228
75		0.886	0.295306756	99.97366904
PAN	<75	0.079	0.026330964	100
	<b>Total</b>	300.027	100	

**Table 8: M10BS and M10FS grain size distribution**

#### **4.1.2 Range selection for heavy mineral**

The research observed a correlation between sand color and heavy mineral content, noting that darker sands tend to contain more heavy minerals, while lighter sands are richer in lighter minerals. During sand sieve size analysis, a higher concentration of dark-colored sand was observed in finer sand sizes, particularly in the very fine sand fraction. However, it was acknowledged that heavy minerals may also be present in other size fractions, indicating the need for a comprehensive analysis.

To avoid bias and ensure a thorough examination of heavy minerals, the research focused on the total sand size fraction ranging from 0.50 mm to 0.075 mm, encompassing coarse to very fine sand. This approach was chosen to capture the entire range of heavy minerals present in the sample, including potentially valuable finer grains. By analyzing this broader spectrum, a more comprehensive understanding of the sample's mineralogy was achieved, minimizing the risk of overlooking important mineral components.

#### **4.1.3 Observation in distribution**

Observations during heavy mineral separation revealed a notable difference in heavy mineral concentration between backshore and foreshore samples, with backshore generally exhibiting higher concentrations. However, instances were also noted where foreshore samples displayed elevated heavy mineral levels. The research encompassed the entire sand size range, precluding definitive conclusions regarding heavy mineral distribution across specific size fractions. Nevertheless, a correlation emerged during sieve size analysis, indicating that finer sand fractions, particularly very fine sand, exhibited darker colors, suggesting a potential association with higher heavy mineral content.

## 4.2 Heavy Mineral Distribution

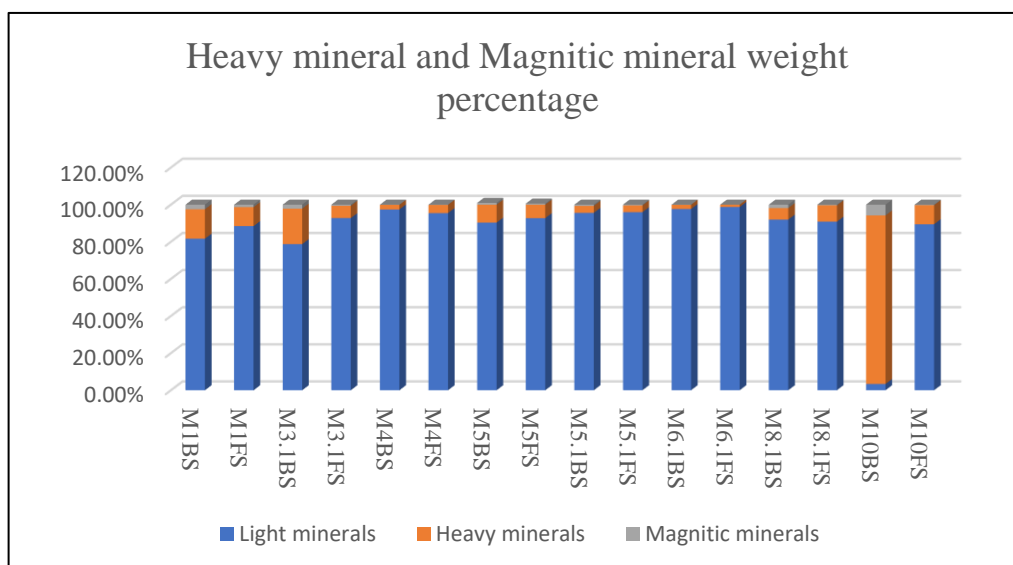


**FIGURE 24** Bar graph showing Heavy minerals and Magnetic mineral Weight percentage

Sample number	Light minerals	Heavy minerals	Magnitic minerals
M1BS	81.64%	15.88%	2.47%
M1FS	88.44%	10.23%	1.33%
M3.1BS	78.73%	19.16%	2.11%
M3.1FS	92.78%	6.64%	0.58%
M4BS	97.43%	2.47%	0.10%
M4FS	95.49%	4.38%	0.13%
M5BS	90.35%	9.65%	0.98%
M5FS	92.72%	7.28%	0.58%
M5.1BS	95.57%	3.80%	0.63%
M5.1FS	95.95%	3.63%	0.42%
M6.1BS	97.68%	2.27%	0.05%
M6.1FS	98.77%	1.21%	0.02%
M8.1BS	91.99%	6.20%	1.82%
M8.1FS	90.84%	8.80%	0.35%
M10BS	3.37%	90.86%	5.78%
M10FS	89.47%	10.25%	0.28%

**Table 9:** Heavy mineral and magnetic mineral weight percentage

### 4.3 Stereozoom observation

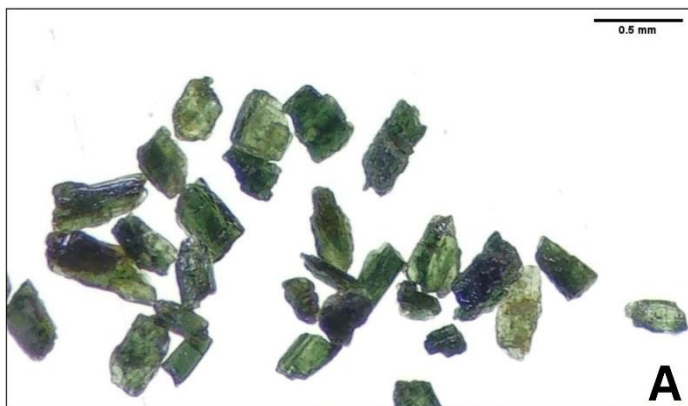


FIGURE 25 :- Diopside image from sample M1BS



FIGURE 26:- Tourmaline images from sample M3.1BS

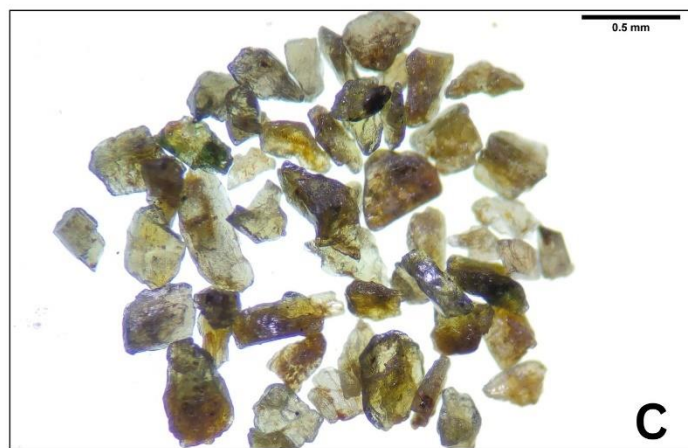


FIGURE 27 :- Mg Hornblende Images from sample M1BS



**FIGURE 28 :- Rutile Grain from sample M5BS**



**FIGURE 29 :- The Garnet grain from the sample M3.1BS**



**FIGURE 30 :- Epidote grain from sample M3.1BS**



FIGURE 31 :-Staurolite grain from sample M3.1BS

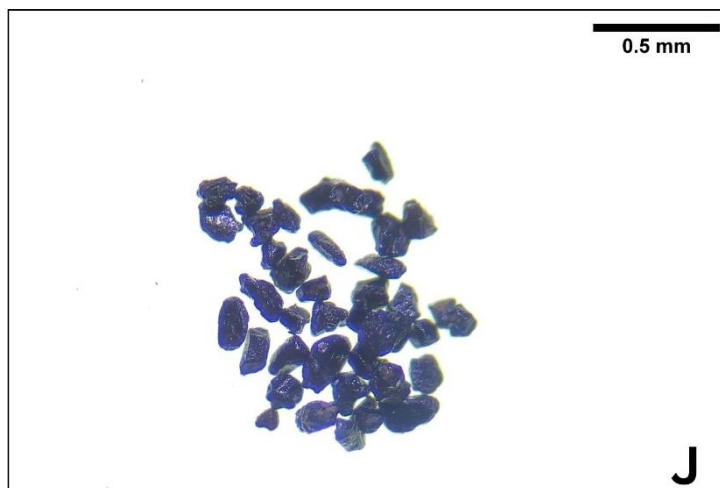


FIGURE 32:- Actinolite grain from Sample M4BS

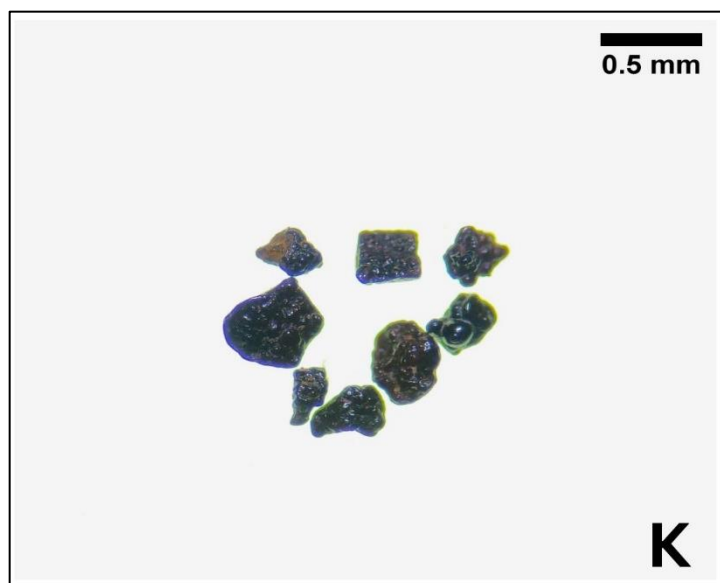


FIGURE 33 :- Tremolite Grain from Sample M5BS





**FIGURE 34: Goethite Grains from sample M10BS**



**FIGURE 35: Goethite Grains from sample M3.1BS**

A stereo microscope offers approximately 40X magnification, enabling detailed observation of mineral grains that are not visible to the naked eye. Its capability to provide a three-dimensional view aids in visualizing and identifying the shapes and features of grains more effectively compared to a standard microscope. Utilizing properties such as color, shape, cleavage, inclusions, and texture, observations made with a stereo microscope help narrow down potential mineral species and allow for comparison with known characteristics found in reference guides, particularly focusing on hand specimens rather than optical properties. Considering that rocks are aggregates of minerals, their density reflects a combination of the densities of the constituent minerals. During stereo zoom identification, three main types of fragments are recognized: transparent/translucent heavy minerals, opaque heavy minerals, and rock and other lithic fragments. This classification aids in distinguishing and analyzing the mineralogical composition of samples under examination.

The minerals identified are:-

1) Diopside is characterized by its green coloration and widespread presence across the samples. It exhibits two distinct sets of cleavage, showcasing conchoidal fractures in new locations. The crystal structure of diopside tends to be blocky in shape as shown in figure 25.

2) Tourmaline grains are typically prismatic and display vertical striations or random inclusions seen in Figure 26, often with irregular terminations. Fractured tourmaline grains are frequently encountered. The predominant color is brown, with variations in size observed, including elongated pipe structures. While tourmaline is present in most samples, it is more abundant toward the backshore but occurs in relatively low numbers overall.

3) Hornblende minerals are characterized by their brown coloration seen in Figure 27 and widespread distribution across the samples. They exhibit varying degrees of translucency, ranging from translucent to near-opaque. Hornblende crystals often form sub-conchoidal surfaces and typically display a massive habit.

4) Rutile is a mineral that occurs in very limited quantities, observed only in sample M5.1Bs. It is classified as a high-temperature and high-pressure mineral commonly found in igneous rocks. Rutile exhibits a color range from blood-red to brownish-red, and its fractures appear uneven seen in figure 28.

5) Garnet is relatively uncommon, observed solely in samples M1BS and M3.1Bs, present in both backshore and foreshore locations but predominantly in the former. The garnet crystals display a pink coloration and range from transparent to translucent figure 29. They exhibit brittleness and tend to exhibit conchoidal fractures. Identifying garnet was challenging due to its appearance, which did not appear pink under bright lighting conditions.

6) Epidote is the most abundant mineral observed throughout the extent of my study area. It possesses a lime green coloration figure 30 and typically exhibits a uniform shape. Epidote grains are characterized by their equidimensional and irregular morphology.

7) Staurolite grains exhibit colors ranging from yellow and gold to brown. Some grains, upon alteration, display a dull to earthy luster figure 31. They have irregular and somewhat platy shapes. Staurolite is not universally present in all samples and is found in limited quantities.

8) Actinolite minerals typically display shades ranging from green to dark green and possess one set of perfect cleavage. They are predominantly translucent to nearly transparent. Actinolite exhibits a splintery fracture pattern, characterized by thin elongated fractures. Its

fibrous and radial nature is notable in Figure 32. Actinolite is observed in varying quantities across samples, ranging from major to minor occurrences. In sample M4, it is notably abundant.

9) Tremolite is primarily observed in the M1BS sample and is scarce in all other samples. It typically exhibits two sets of cleavage and is predominantly transparent Figure 33.. Tremolite appearance can vary, appearing either white or exhibiting coloration in a colloidal state.

10) Goethite is primarily observed in almost all samples but is seen more in M10Bs Figures 34 and 35. Goethite typically crystallizes in the orthorhombic crystal system, forming prismatic or needle-like crystals. These crystals are often grouped in radial clusters, giving them a brush-like appearance.

#### 4.4.1 XRD Analysis for Non-Magnetic

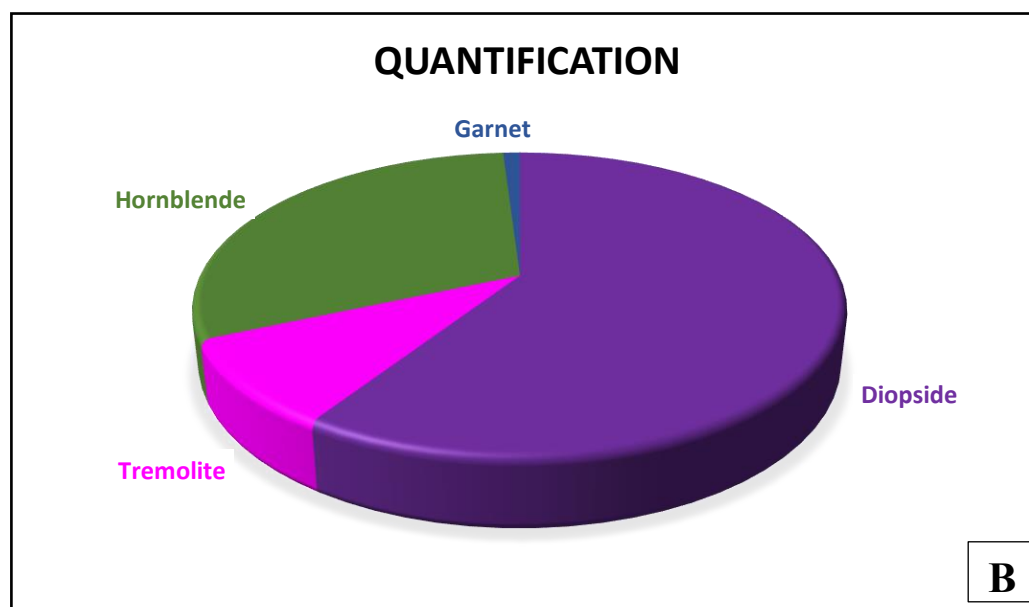
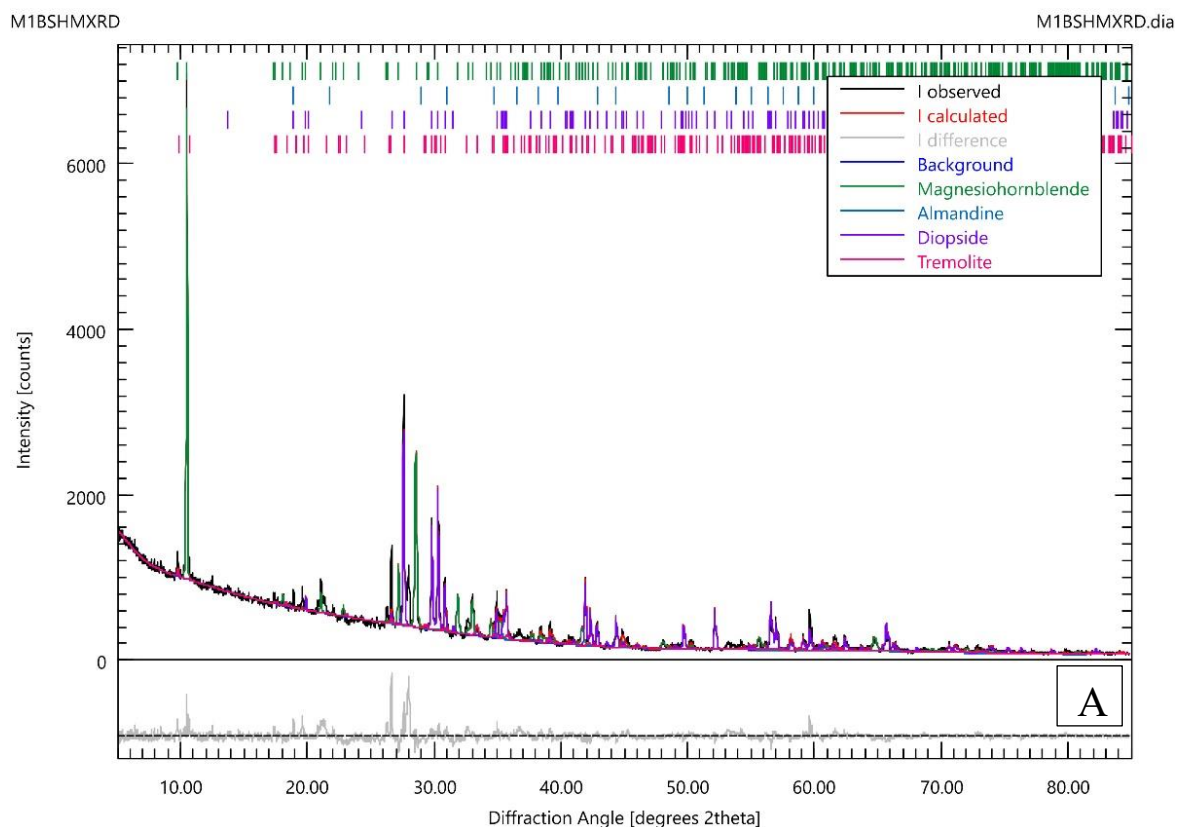


FIGURE 36 : A- XRD graph for M1BS , B- Quantification Pie chart for M1BS

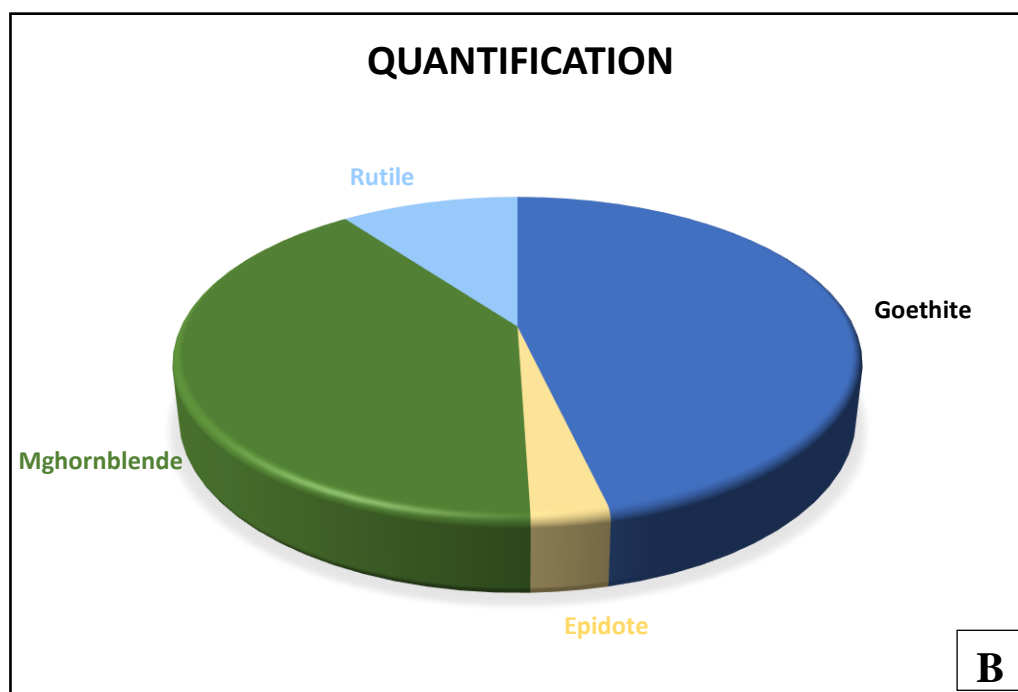
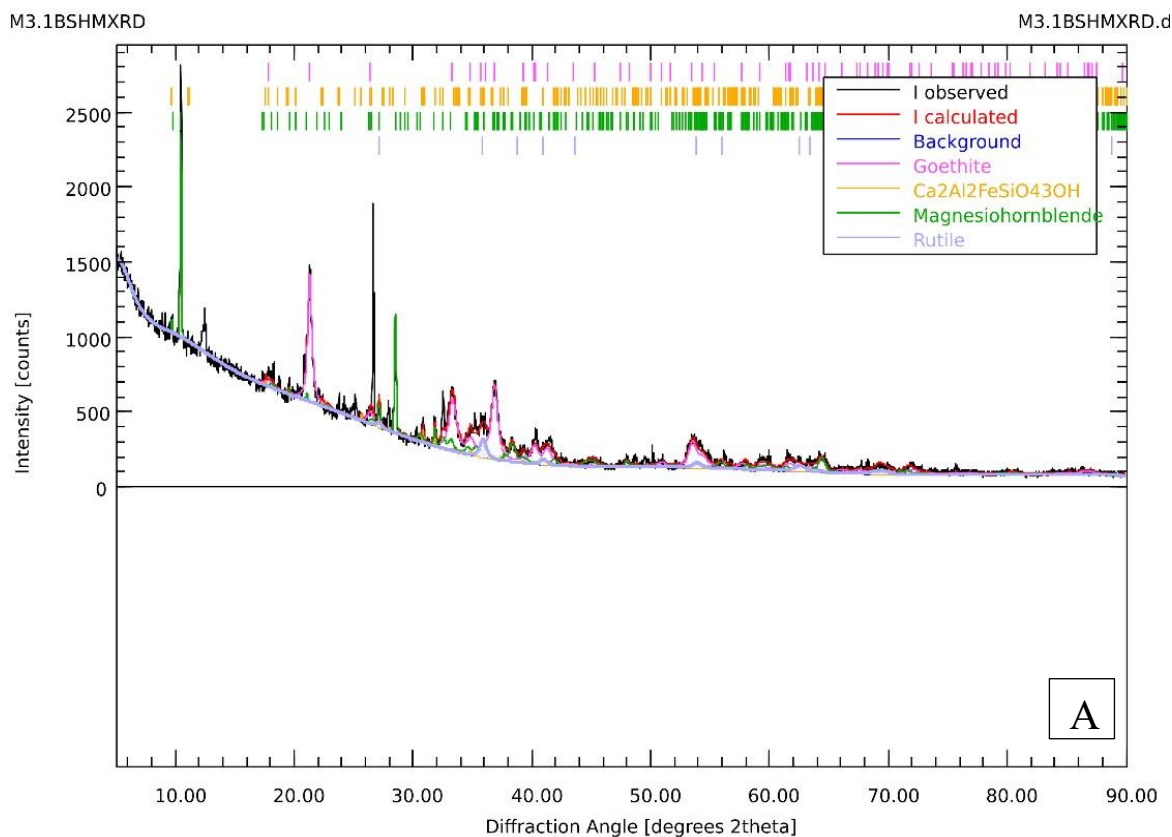


FIGURE 37 : A- XRD graph for M3.1BS , B- quantification Pie chart for M3.1BS

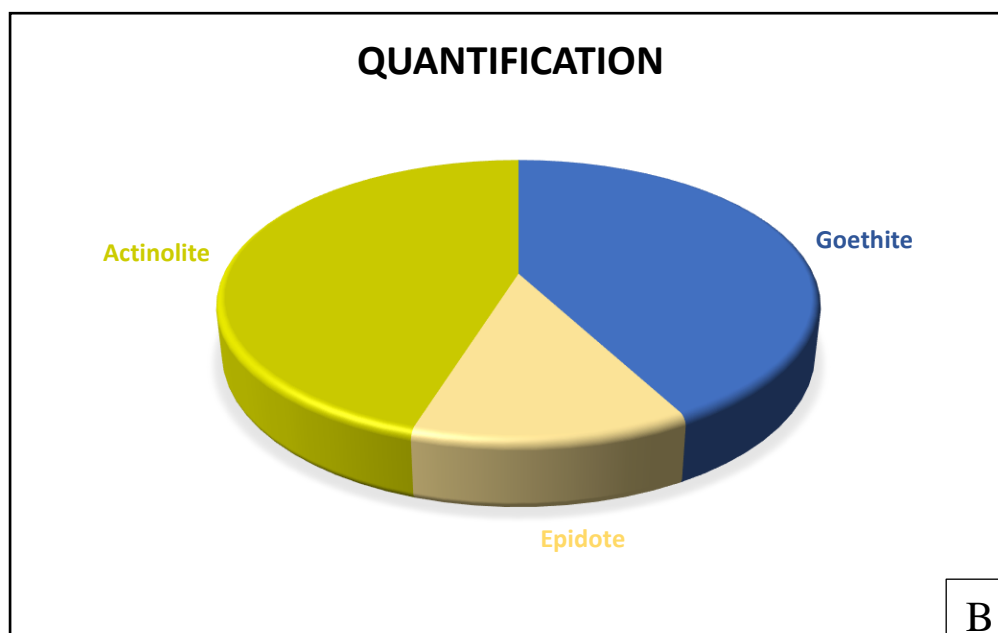
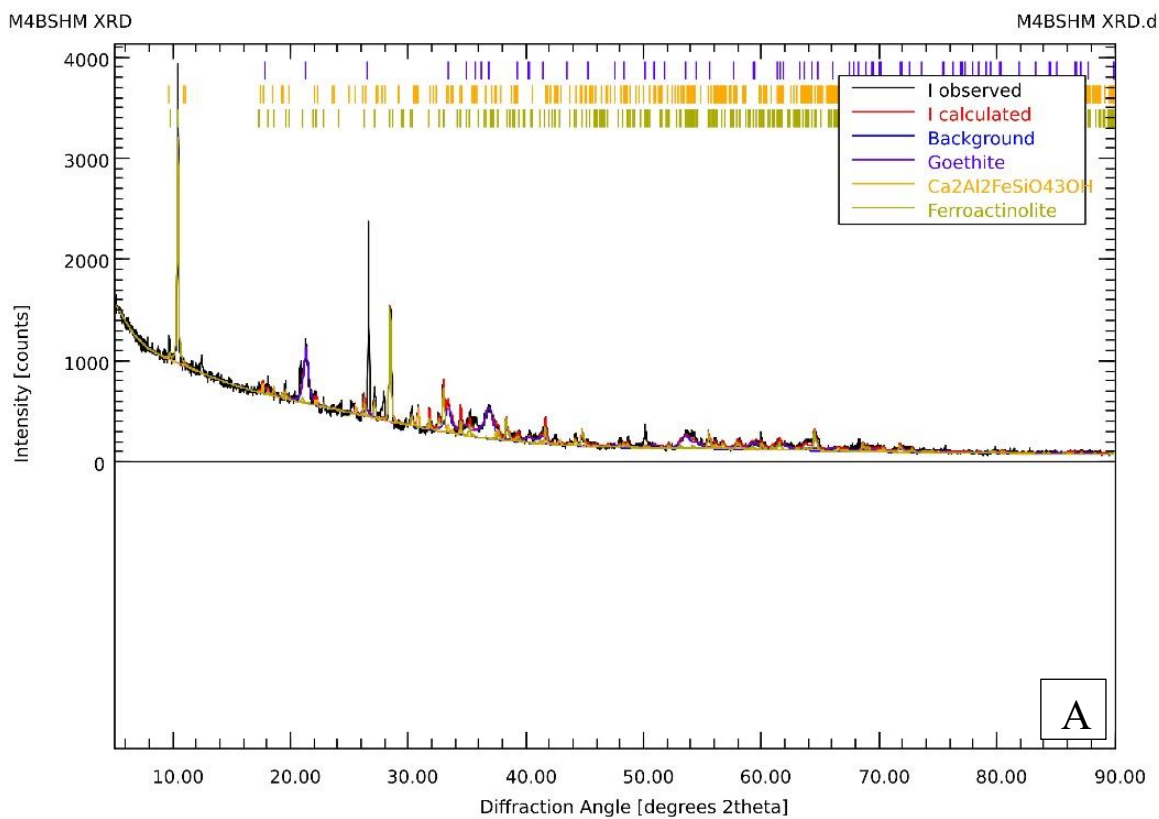


FIGURE 38 : A - XRD data for M4BS , B- quantification Pie Chart

M5.1BSHMXRD

M5.1BSHMXRD.d

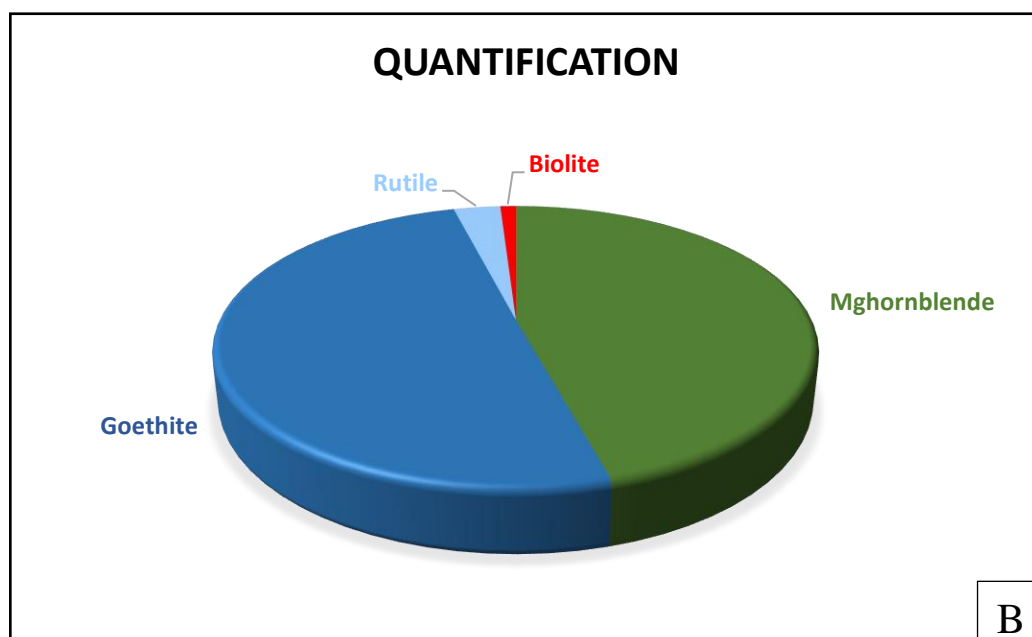
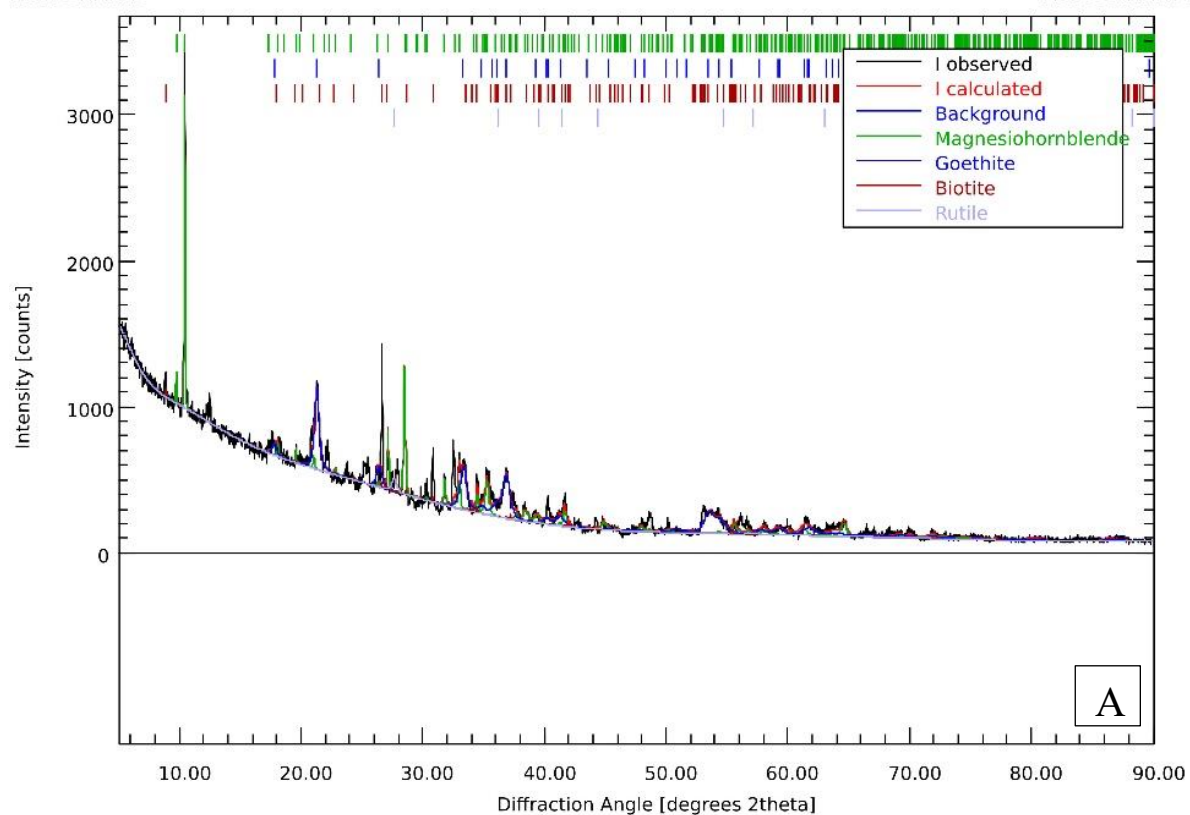


FIGURE 39 : A- XRD data for M5.1BS , B- Quantification pie chart for M5.1BS



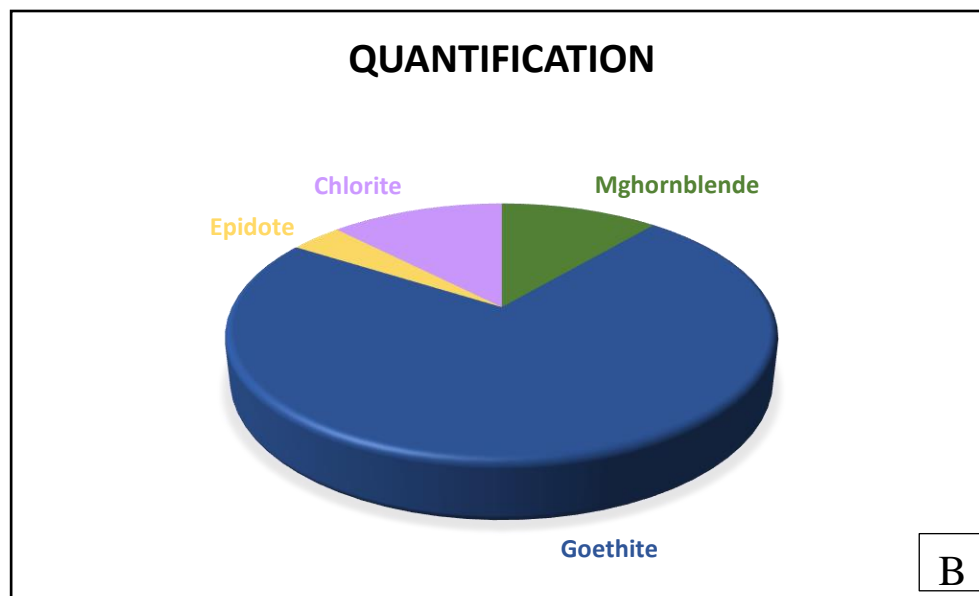
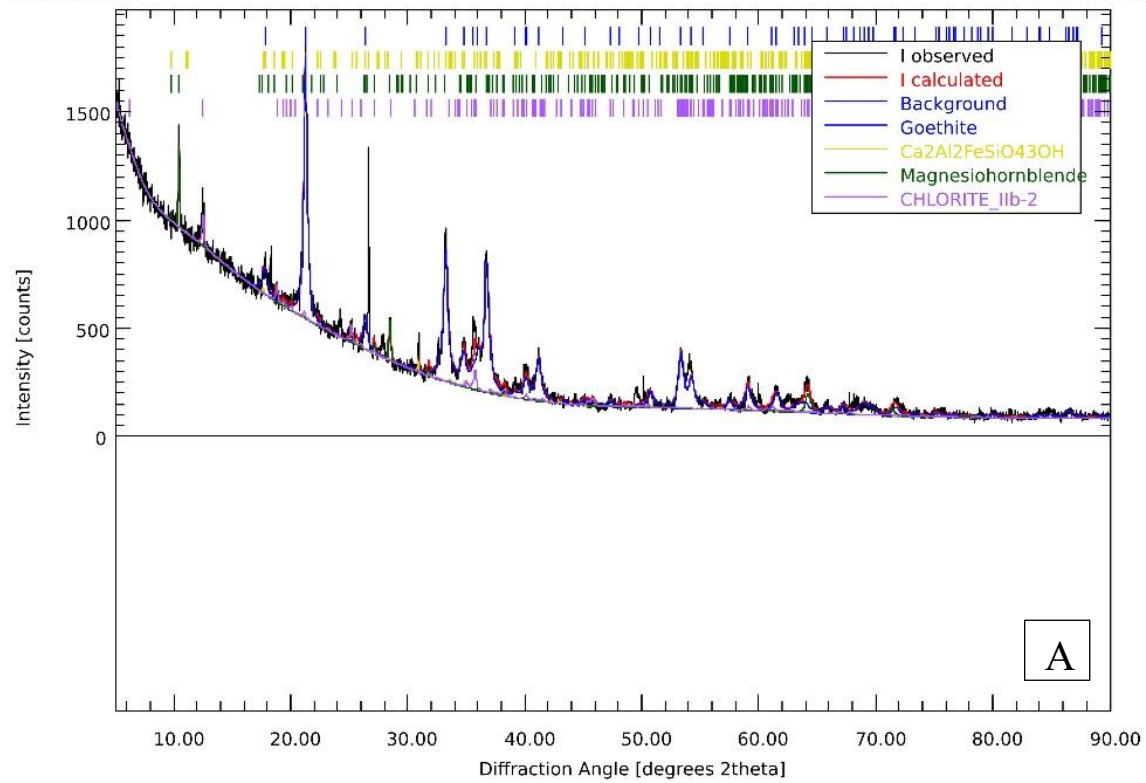


FIGURE 40 : A- XRD garph of M10BS , B- Quantification chart of M10BS

#### 4.4.2 XRD Analysis for Magnetic Minerals

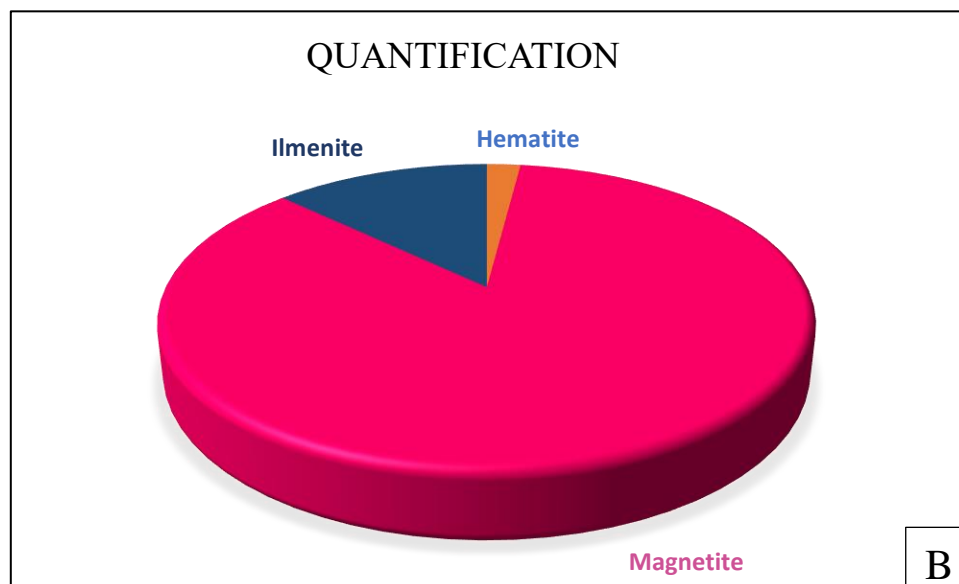
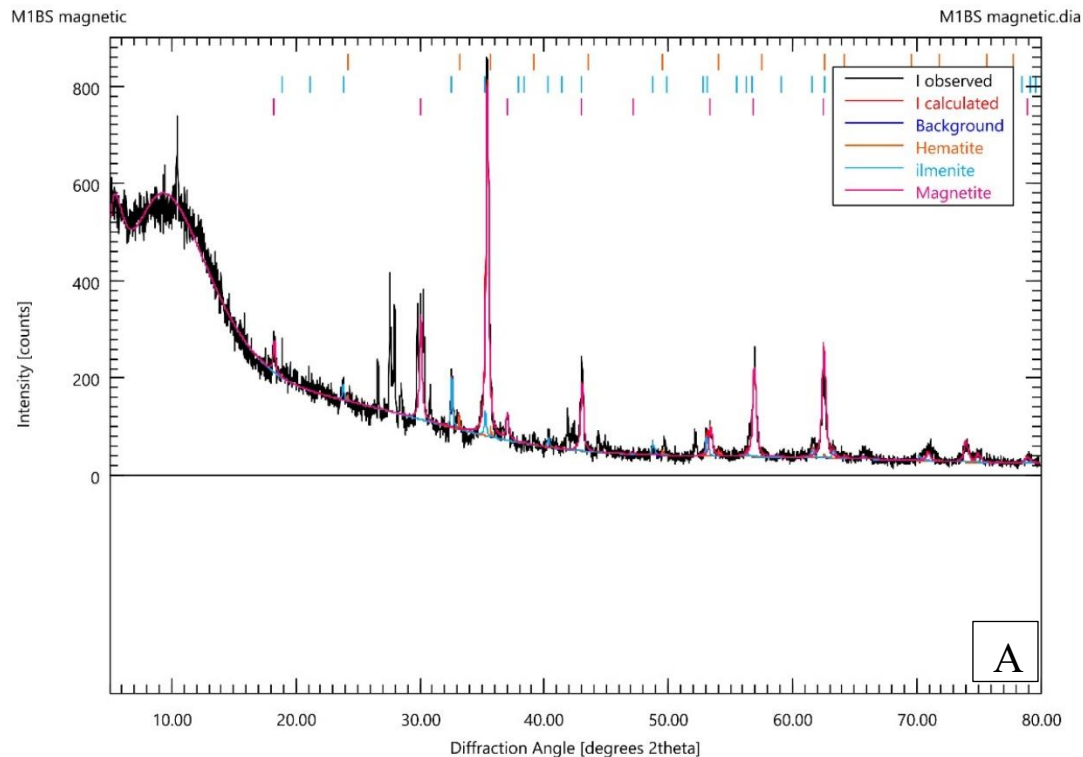


FIGURE 41 : A- XRD of M1BS magnetic minerals, B- Quantification Pie Chart

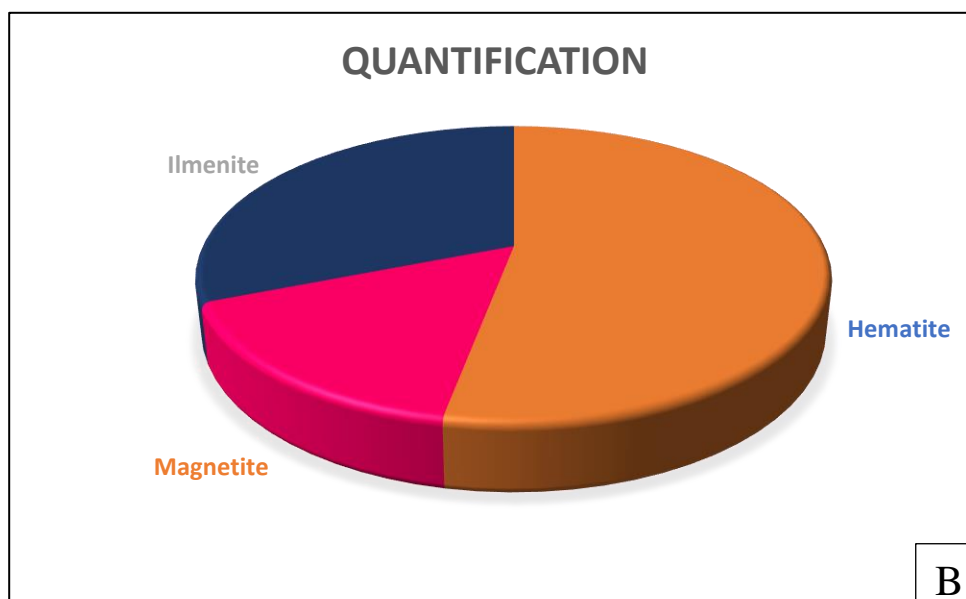
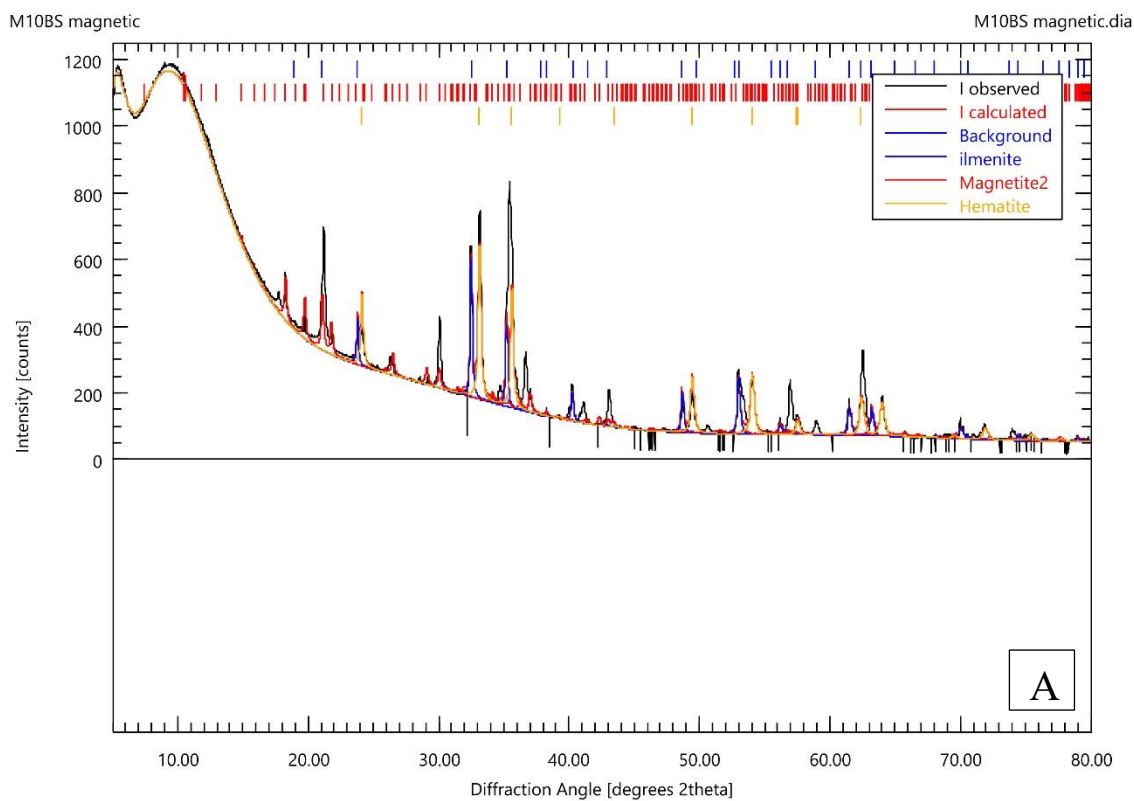


FIGURE 42 : A-XRD of M10BS magnetic minerals , B- Quantification Pie chart of M10BS magnetic minerals

The X-ray diffraction (XRD) analysis of various samples from different locations yielded significant insights into the mineral composition and possible geological origins. The M1BS Figure 36 sample exhibited prominent peaks of Hornblende and Diopside, indicating metamorphic source rocks such as schist. The quantified values, illustrated in a pie chart, showed Diopside at 59%, Hornblende at 30.6%, Tremolite at 9.2%, and Almandine at 1%. This higher concentration of Diopside further corroborates the metamorphic origin, supported by the presence of Hornblende and Tremolite.

In contrast, the M3.1BS sample Figure 37 displayed major peaks of Hornblende and Goethite, indicative of metamorphosed crystalline igneous rocks. The pie chart percentages showed Goethite at 45.9%, Hornblende at 40.8%, Rutile at 10.2%, and Epidote at 3.1%. The prevalence of Goethite suggests potential replacement processes, possibly originating from iron-rich minerals like BHQ (Banded Hematite Quartzite).

Moving on to the M4BS sample Figure 38, Actinolite and Goethite were the major peaks observed, along with Epidote. The pie chart indicated Goethite at 45.2%, Actinolite at 42.2%, and Epidote at 12.7%. The high Goethite content could be attributed to hematite replacement from BHQ or other iron-rich minerals, while Epidote and Actinolite may have originated from igneous or gneiss bodies.

Similarly, the XRD plot of the M5.1BS figure 39 sample exhibited prominent peaks for Goethite and Mg Hornblende, along with Rutile and Biotite. The pie chart percentages showed Goethite at 50.3%, Hornblende at 45.3%, Biotite at 1%, and Rutile at 3%. These mineral suites pointed towards metamorphic rocks as the probable source, with Goethite likely originating from hematite replacement in BHQ and other iron-rich minerals.

Lastly, the XRD data of the M10BS sample figure 40 indicated major peaks of Hornblende and Goethite, followed by Epidote and Chlorite. The pie chart percentages revealed Goethite at 72.8%, Hornblende at 11.2%, Epidote at 11.2%, and Chlorite at 12.3%. The mineralogical suites suggested a potential provenance from granite gneisses, with Goethite concentrations again linked to hematite replacement from BHQ and other iron-rich minerals.

XRD data for Magnetic minerals M1BS sample figure 41 indicate major peaks of Magnetite followed by ilmenite and Hematite. The pie chart percentages show Magnetite as highest at 85.10%, ilmenite at 12.87%, and Hematite at 2.01 %.

XRD data for Magnetic minerals M10BS sample figure 42 indicate Major peaks of Hematite followed by ilmenite and Magnetite. The Pie chart Percentage shows Hematite at the highest at 53.0%, Magnetite at 16% and Ilmenite at 31%.

## 4.5 SEM-EDX Analysis

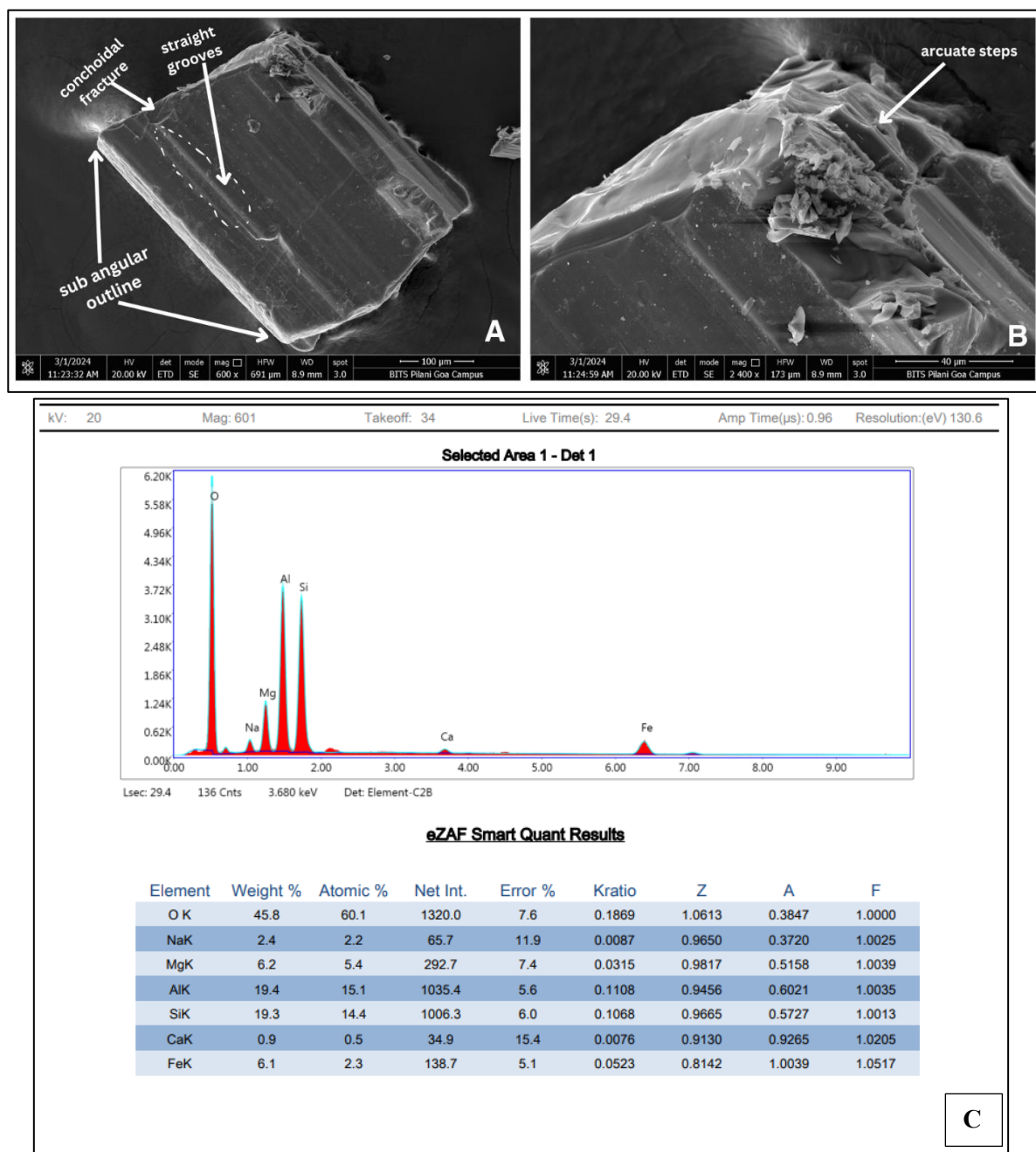


**FIGURE 43 : FSEM image of Tourmaline in Image (A and B), Image C - EDX Graph of tourmaline showing Element composition**

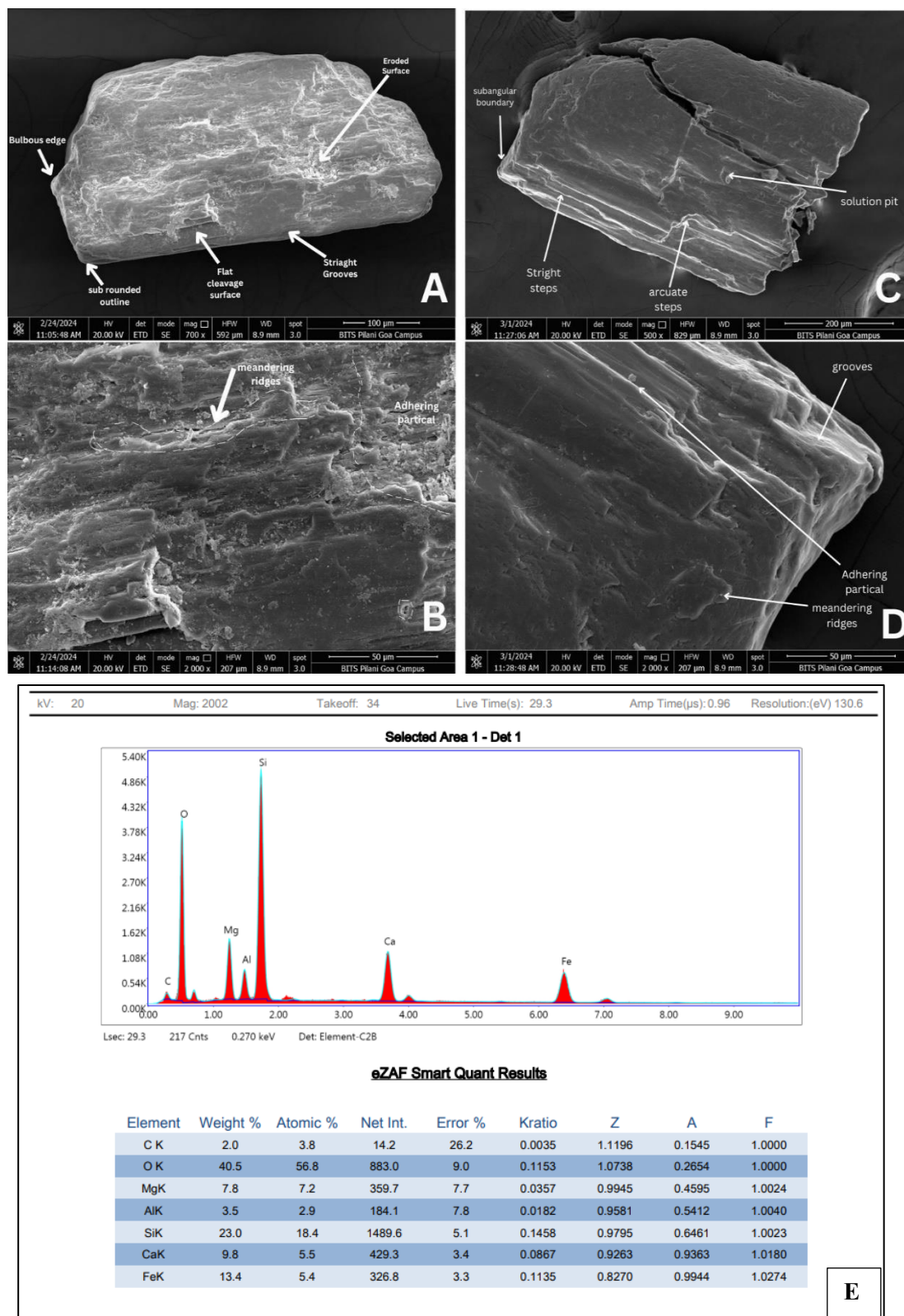


**FIGURE 44 FSEM image of Hornblende in Image (A,B,C&D), Image E - EDX Graph of Hornblende showing Element composition**



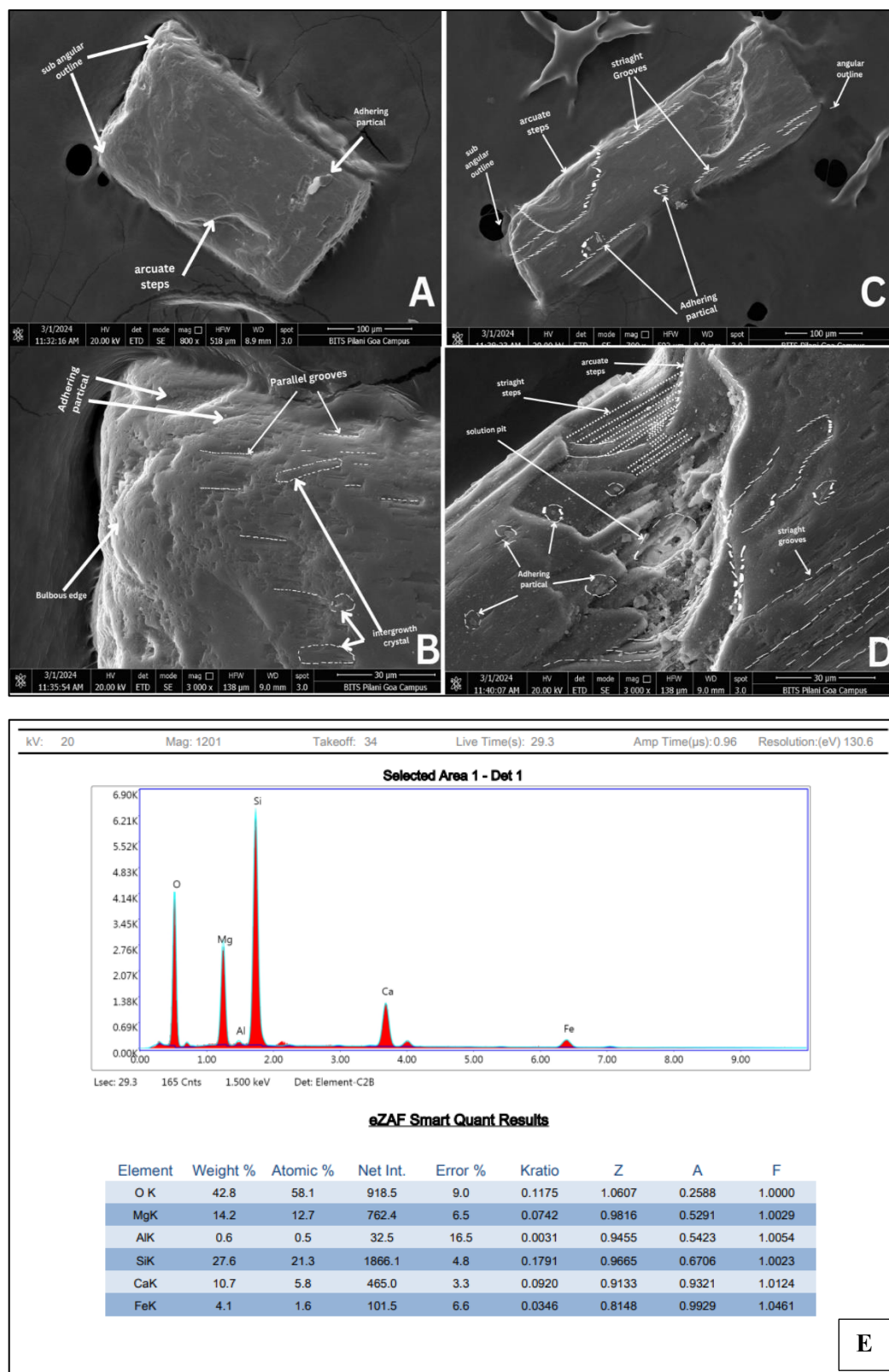


**FIGURE 45 FSEM image of Tremolite in Image (A,B, C&D), Image E - EDX Graph of Tremolite showing Element composition**



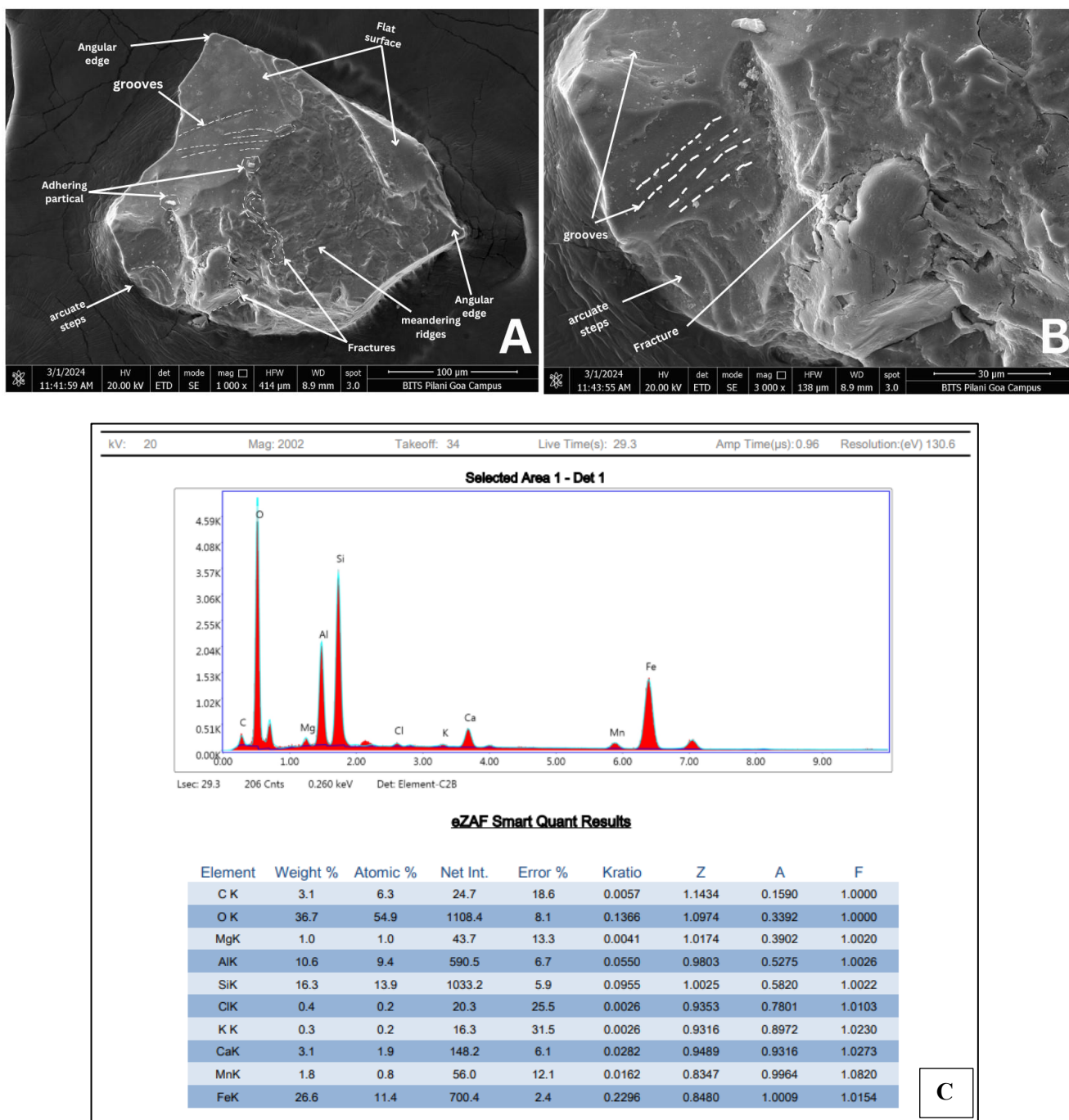


**FIGURE 46 FSEM image of Garent in Image (A,&B), Image C - EDX Graph of Garnet showing Element composition**

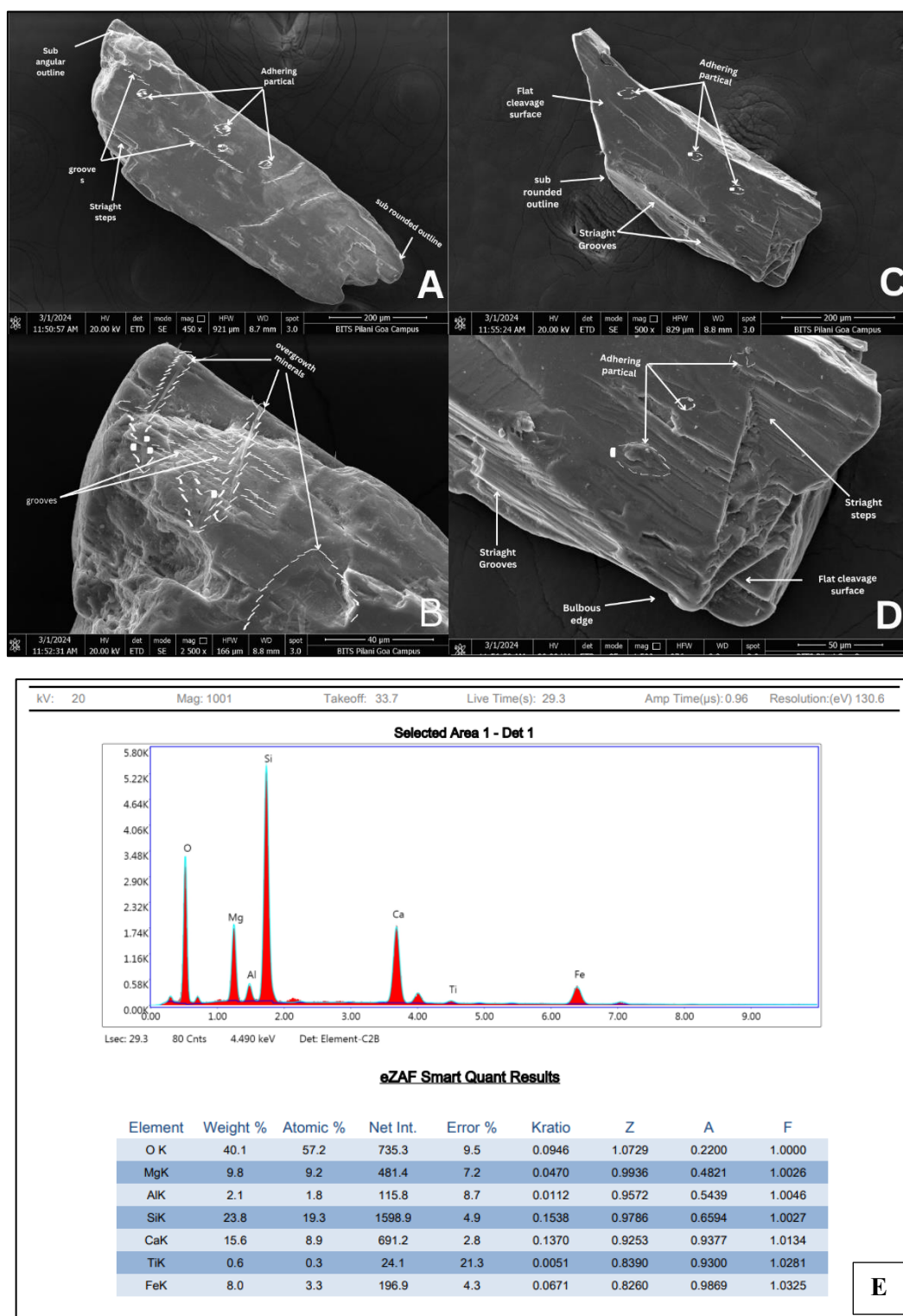


**FIGURE 47 FSEM image of Actinolite in Image (A,B,C,D) , Image E - EDX Graph of Actinolite showing Element composition**

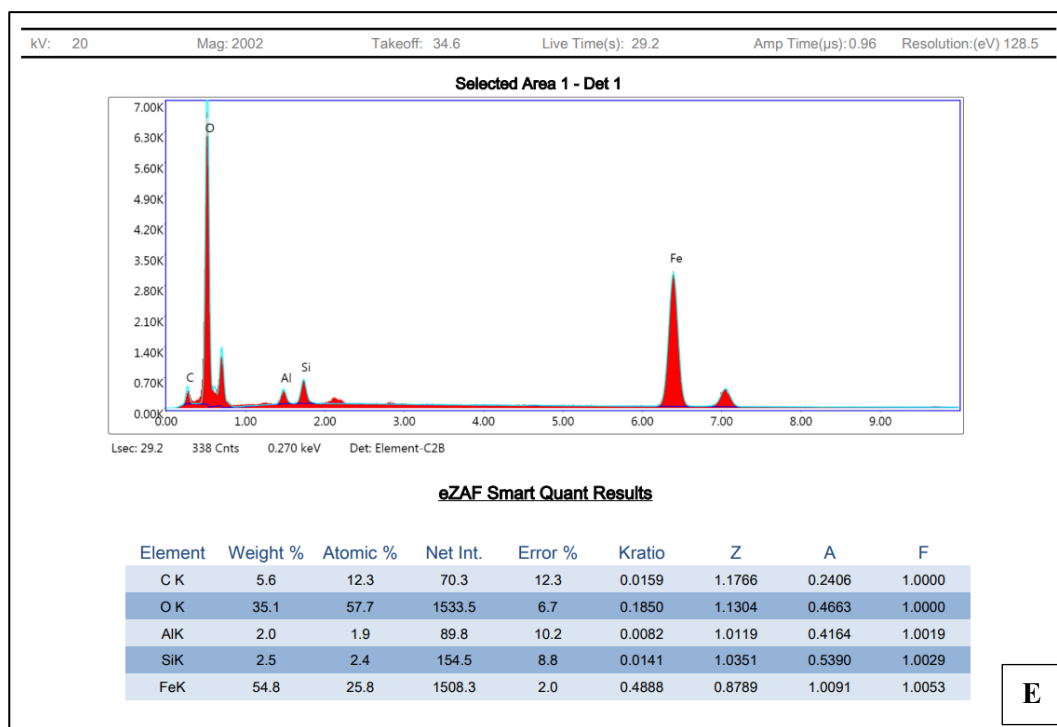
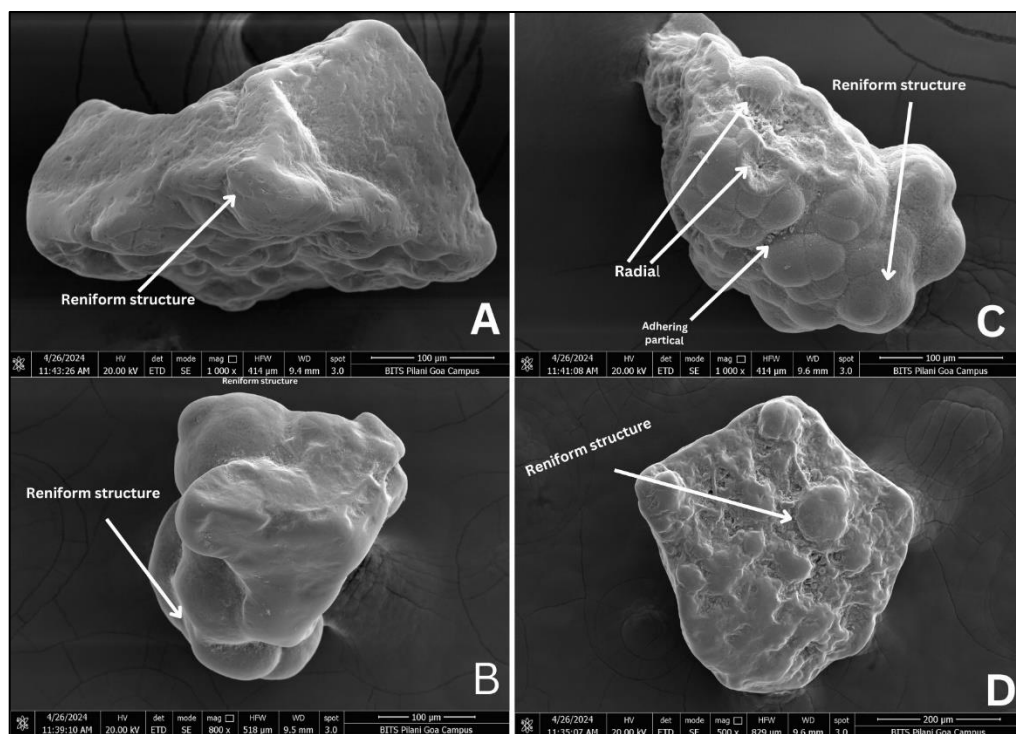


**FIGURE 48 FSEM image of Goethite in Image (A,B,C,D), Image E - EDX Graph of Goethite showing Element composition**

Provenance investigations of heavy minerals have been extensively explored by researchers such as Callender & Folk (1958), Dill (1998, 2007), Dill et al. (2007), Morton (1985, 1991), Morton & Hallsworth (1999), Statteger (1987), among others. Surface microtextures of heavy mineral grains serve as valuable indicators for understanding their transport history, processes, and depositional environments. The utilization of scanning electron microscopy (SEM) stands out as a highly effective auxiliary tool (Dill, 2007; Krinsley & Donahue, 1968; Vos et al., 2014) for discerning surface microtexture and grain morphology at the micron scale.

The microtexture of mineral grains, both heavy and light, is categorized into three types based on their formation origin: mechanical, chemical, and mechanical/chemical (Krinsley & Donahue, 1968). Surface textures observed on heavy-mineral grains have been thoroughly analyzed using SEM analysis, with grains selected from four key locations within the study area: M1BS, M3.1 BS, M4BS, M5 BS, and M10BS

The investigation of heavy minerals from M1BS revealed a prevalence of mechanical features, suggesting extensive transportation of the grains over long distances. The tourmaline grains exhibited rounded to sub-rounded edges, straight grooves, and conchoidal fractures, primarily indicating mechanical abrasion (refer to Figure 43 ). The mineral typically displayed short prismatic or granular morphologies, often appearing sub-angular or sub-rounded in shape (see Figure 43 ). The crystal surfaces of tourmaline were generally flat with clear edges, showcasing minimal alteration or dissolution due to chemical factors( Figure 43 ).

Hornblende grains exhibited pronounced mechanical features such as straight steps, arcuate steps, and meandering ridges, alongside a few solution pits as chemical indicators.

Additionally, some adhering particles were observed on the grain surfaces (refer to Figure 44).

Similarly, tremolite grains showed prominent mechanical features including straight and parallel grooves, meandering ridges, fractures, steps, and bulbous edges, with occasional solution pits and adhering particles. The grains appeared angular to subangular and elongated in nature. (refer to Figure 45)

SEM analysis of garnet from M3.1BS indicated the dominance of mechanical processes, with features like grooves, arcuate steps, angular edges, flat cleavage surfaces, and meandering ridges. The grains were sub-angular to subrounded, suggesting moderate transportation distances, with limited chemical impact observed on their surfaces. Adhering particles were also noted.(refer to Figure 46)

Actinolite from M4BS exhibited mechanical features like grooves, arcuate steps, flat surfaces, and overgrowth features, both on the grain surfaces and within hollows. Medium-sized grains appeared elongated and angular to subangular, with some adhering particles observed ( refer to Figure 47)

Lastly, Goethite from M10BS has a reniform shape and radial texture. Goethite crystals tend to be acicular (needle-shaped). During growth, these acicular crystals often radiate outward from a central nucleation point. This preferred growth direction creates a radial pattern, like spokes on a wheel, visible as a texture within the goethite mass. (refer to Figure 48).

#### **4.6. Discussion and Interpretation**

The research scope encompasses a 40-kilometer stretch extending from Canaguinim to Polem, focusing on the identification, characterization, and origin elucidation of heavy minerals in the area. Heavy minerals can be classified into four main groups based on their physical and chemical characteristics as outlined by Folk (1974, p.96): opaque, micas, ultra-stable, and metastable minerals.

Opaque minerals are distinguished by their high iron content and typically exhibit a notable specific gravity. This group encompasses minerals such as magnetite, ilmenite, pyrite, hematite, limonite, and leucoxene. While opaque minerals are often grouped without differentiation, for this analysis, a differentiation attempt will be made.

Micas demonstrate variability in specific gravity due to compositional variances and hydraulic behavior differences attributed to particle shape discrepancies. Additionally, mica particles may not settle in bromoform, leading to their exclusion from heavy mineral assessments.

The ultra-stable group encompasses minerals like zircon, tourmaline, and rutile. Zircon and tourmaline are chemically inert and exceptionally durable, enabling them to endure multiple erosion and transportation cycles. They are also polyvarietal, making them valuable indicators of sediment provenance.

The metastable group includes olivine, apatite, amphibole, pyroxene, garnet, epidote, clinozoisite, zoisite, kyanite, sillimanite, andalusite, staurolite, along with various other minerals.

The grain size distribution patterns were analyzed across various beaches in south Goa, focusing on backshore (BS) and foreshore (FS) profiles. At Polem Beach (M1 BS), BS samples were dominated by medium sand (73.341%), contrasting with FS samples that showed reduced medium sand (50.11%) and increased fine sand (34.95%). Galgebag Beach (Sample 3.1 BS) exhibited a prevalence of very fine sand (52.67%) in BS, shifting to higher fine sand (77.52%) in FS. Talpona Beach (M4 BS) had a predominant very fine sand fraction (70.45%) in BS, while FS displayed more fine sand (49.02%) and very fine sand (42.48%). Rajbag Beach (M5.1 BS) showed a majority of very fine sand (55.81%) and fine sand (34.32%) in BS, shifting to higher fine sand (49.20%) and very fine sand (35.44%) in FS. Cab de Ram (M10 BS) exhibited dominant fine sand (52.87%) and medium sand (31.56%) in BS, with FS showing a balanced distribution of fine sand (38.79%) and medium sand (32.85%). Variations in grain size distribution among different locations may stem from differences in wave energy levels experienced at each sampling site, alongside variations in beach morphology (Dora et al 2011; Bryant 1982).

The average grain size measured along the FS (Foreshore) area was 2.3, contrasting with the average grain size of 2.16 observed along the BS (Backshore) region.

High-energy waves are crucial for the transportation and concentration of heavy minerals compared to lighter minerals, primarily due to their elevated specific gravity (Rajganapathi et al., 2013). The occurrence of heavy minerals is closely linked to factors such as the type of weathering, mode and distance of transportation, and the depositional environment's nature (Pettijohn, 1984). The heterogeneous distribution of heavy minerals within the study area is governed by a multitude of factors, encompassing wave-induced processes,

provenance variability, depositional settings, intrinsic mineral properties, and subsequent diagenetic modifications.

The total weight percentage of heavy minerals derived from bromoform analysis serves as a valuable metric for assessing heavy mineral deposits within the study area, providing insights into the source nature of these strategic minerals. Samples were collected from eight locations spanning the foreshore and backshore areas. Table 8 presents the results of heavy mineral analysis conducted on beach sediments (M1 BS, M1 FS; M3.1 BS, M3.1 FS; M4 BS, M4 FS, M5 BS, M5 FS, M5.1 BS, M5.1 FS, M6.1 BS, M6.1 FS, M8.1 BS, M8.1 FS, M10 BS, M10 FS) in the study area.

The highest total heavy mineral weight percentage (THM %) with Sum of magnetic mineral was observed at sample location M10 BS (96.64%), followed by M3.1 BS (21.26 %), M1 BS (18.33%), M1 FS (11.56%), M10 FS (10.53%), M5 BS (10.6 %), M8.1 FS (9.11%), M5 FS (7.86%), M3.1 FS (7.22%), M8.1 BS (8.02%), M4 FS (4.51%), M5.1 BS (4.05%), M5.1 FS (4.05%), M4 BS (2.57%), M 6.1 BS (2.268%), and M.6.1 FS (1.24%), in descending order of abundance. Notably, the Cab de Ram area (M10 BS) exhibited the highest heavy mineral content.

The heavy mineral suite predominantly comprises opaque minerals like magnetite, ilmenite, Hematite, and Goethite alongside transparent minerals such as diopside, tourmaline, hornblende, actinolite, epidote, garnet, tremolite, rutile. Light minerals, mainly quartz and feldspars, exhibit opaque concentrations ranging from 0.03 to 5.78 percent and nonmagnetic concentrations from 1.21 to 90 percent. Variability in heavy mineral suites across locations suggests diverse source rocks and the involvement of geochemical factors in their accumulation. Heavy minerals are more abundant in grain size from very fine to fine sand.



It is generally observed that heavy mineral concentration increases with a decrease in grain size.

The mineralogical analysis results, depicted in Figures 34 and 35 through stereo zoom microscopy, reveal Goethite as the most prevalent heavy mineral across all 16 examined samples. With XRD quantification analysis Goethite content varies from 72.8% wt% (M10BS) to 45.9 wt% (M3.1Bs), averaging at 53.27%. Following Mg hornblende, is observed with an average content of 9.0 wt%, ranging from 31.7% (M10BS) to 45.5 % (M5.1BS), and Diopside at 59.2% at (M1BS). Rutile has an average content of 6.5 %, ranging from 3 % (M5.1BS) to 10.2 % (M3.1BS). and garnet 1% (M1BS ) in decreasing order of abundance.

For the microtexture analysis of heavy minerals using scanning electron microscopy (SEM), seven minerals were chosen from specific locations. Numerous heavy mineral grains (ranging from 10 to 30 grains for each mineral) were meticulously selected using a stereo-zoom microscope. Each grain was identified before being securely fixed onto the SEM stage. To enhance sample imaging, a gold coating procedure was performed on every individual grain.

The SEM analysis of various grains such as tourmaline, tremolite, garnet, actinolite, , hornblende, and Goethite, reveals a diverse array of microtextures shaped by mechanical and chemical processes within the coastal region. Mechanical forces contribute to the formation of conchoidal fractures, pitted surfaces, grooves, and furrows, while chemical processes result in concavities, solution pits, silica precipitation, and overgrowth in certain instances as seen in SEM images from Figure 43-48.

Predominant mechanical features observed include straight grooves, flat cleavage surfaces, arcuate steps, brittle fractures, meandering ridges, conchoidal fractures, and subangular, and rounded grain boundaries. Notably, the presence of sub-rounded grains with high impact marks signifies high-energy conditions characteristic of coastal areas. Additionally, mechanically induced breakage blocks suggest a nearby sediment source, while arc-shaped furrows indicate a fluvial environment. The observed microfractures are likely outcomes of either grain-to-grain collisions during sediment transportation or diagenetic processes. The grains predominantly exhibit sharp euhedral crystals with prismatic shapes and anhedral fragment imprints.

The highest concentrations of heavy minerals within the study area are found in fine fractions. Nonmagnetic heavy minerals exhibit varying degrees of transformation and sizes, ranging from euhedral to subhedral forms. These observations offer valuable insights into the dynamic processes and environmental conditions shaping the mineralogy of coastal sediments. The heavy mineral analysis of samples from M1BS revealed significant mechanical features, indicating extensive transportation over long distances. Tourmaline grains displayed rounded to sub-rounded edges, straight grooves, and conchoidal fractures, indicative of mechanical abrasion. Hornblende grains exhibited pronounced mechanical features like straight and arcuate steps, while tremolite grains showed angular to subangular and elongated shapes with mechanical characteristics.

SEM analysis of garnet from M3.1BS showed the dominance of mechanical processes, with features such as grooves, angular edges, and meandering ridges. Actinolite from M4BS exhibited similar mechanical features, including grooves and overgrowth, suggesting transport and deposition dynamics.

Goethite, a prevalent heavy mineral in the study area, is a naturally occurring iron oxy-hydroxide mineral commonly associated with various mineral deposits such as iron, manganese, and bauxite ores. It typically forms under oxidizing conditions as a weathering product of iron-bearing minerals, either through inorganic chemical processes or organic precipitation. Goethite exhibits diverse shapes, sizes, and morphologies.

Goethite formed by replacing hematite tends to be free of deleterious elements, while re-precipitated goethite often contains adsorbed alumina, silica, and/or phosphorus. In the present study, goethite may be predominantly the result of the replacement of hematite from the BIF. Different microstructures of goethite such as Reniform and radial texture are noticed in sample M10BS.

Garnet and tourmaline are favored choices for provenance studies due to their prevalence in sediments, diverse chemical and mineralogical compositions, origins from various rock types, and resilience to harsh geological conditions (Garzanti et al., 2013).

Tourmaline exhibits a variable habit, typically with rounded triangular cross-sections and notable inclusions (figure 26). These minerals appear vitreous, transparent to translucent, and pleochroic, displaying hues ranging from yellow-brown to pale yellow, indicating possible iron or magnesium content (Mange & Maurer, 1992).

Rutile, characterized by dominantly red-wine coloration, non-rounded shapes, and euhedral forms with pyramidal terminations, suggests a source from high-grade metamorphic areas. Rutile grains also display irregular or conchoidal breakage patterns (Figure 28).

The observed mineral assemblage on the surface features collectively suggests the derivation of source rocks like mixtures of igneous and metamorphic rocks, crystalline gneisses, and

schists. The limited diversity and high abundance of heavy mineral assemblages are governed by both provenance and diagenetic mechanisms. These factors pose challenges in precisely reconstructing the paleo-history of lithologic units solely through heavy mineral analysis.

The XRD analysis of samples from multiple locations revealed distinct mineral compositions indicative of varied geological origins. In M1BS, Hornblende and Diopside peaks suggested a metamorphic source like schist, supported by Tremolite and Almandine presence. Conversely, M3.1BS displayed Hornblende and Goethite peaks, pointing to metamorphosed crystalline igneous rocks with possible BHQ involvement. M4BS showcased Actinolite and Goethite peaks, possibly from iron-rich minerals and igneous or gneiss sources. M5.1BS indicated metamorphic rocks as a source with Goethite from BHQ replacement. Lastly, M10BS hinted at granite gneisses as a provenance, with notable Goethite concentrations from BHQ and iron-rich minerals. These findings provide crucial insights into the geological evolution and mineralization processes in the studied areas. Goethite emerges as a dominant mineral in four samples (M10, M5.q, MS4, MS3.1) in descending order of abundance, accompanied by other minerals like epidote, amphiboles, etc

The potential source rocks for all five locations include metabasalt, metasediments, TTG (Tonalite-Trondhjemite-Granodiorite), Quartz sericite, phyllite, and Banded Iron Formation (BIF). Geologically, the study area exhibits a wide lithological variation, encompassing metabasalt, metasediments, TTG, Quartz sericite, phyllite, and BIF. Stratigraphically, these formations are associated with the Ponda and Barcem groups within the Goa group of rocks.

## 4.7 Conclusions

The study encompassed an investigation from Canaguinim to Polem, focusing on the heavy mineral distribution and geological origins along the coastal expanse. Specifically, heavy mineral fractions ranging from fine to coarse sand were meticulously identified using a stereo zoom microscope. Analysis of grain size distribution patterns underscored variations in sediment composition across diverse beach profiles, likely influenced by wave dynamics and beach morphology.

Comprehensive analyses integrating heavy mineral analysis, XRD characterizations, and SEM observations unveiled a low-diversity and abundant heavy mineral composition. This composition was primarily influenced by provenance factors, diagenetic processes, and the replacement of dominant minerals by iron oxyhydroxides minerals along a north-to-south lateral gradient within the study area.

The predominant heavy mineral identified throughout the study area was Goethite (M10 BS; 72.8%), accounting for an average of 53.6% of the total heavy mineral concentration from Galgebag Beach to Cab de Ram Beach (measured in kilometers). Notably, there was a negligible presence or absence of unstable heavy minerals. The prevalence of ultra-stable heavy minerals suggested a probable derivation from granitic and metamorphic source rocks, particularly from intensely weathered regions.

These findings contribute significantly to our understanding of coastal sediment dynamics, heavy mineral distribution patterns, and the geological processes shaping the studied coastal stretch. The study sheds light on the interplay between provenance, diagenesis, and mineral stability, providing valuable insights into the geological evolution of coastal environments.

## 4.8 References

- Al-Saady, Y. I., Othman, A. A., Mohammad, Y. O., Ali, S. S., Ali, S. A., Liesenberg, V., & Hasan, S. E. (n.d.). *Composition of rare earth elements in fluvial sediments of the lesser Zab river basin, Northeastern Iraq: Implications for tectonic setting and provenance*. Research Online. <https://ro.uow.edu.au/test2021/10258/>
- Anitha, J. K., Joseph, S., Rejith, R. G., & Sundararajan, M. (2020, April 4). Monazite chemistry and its distribution along the coast of Neendakara–Kayamkulam Belt, Kerala, India - SN applied sciences. SpringerLink. <https://link.springer.com/article/10.1007/s42452-020-2594-6>
- Bryant, E., Behaviour of grain size characteristics on reflective and dissipative foreshores, Broken Bay, Australia. *Journal of Sedimentary Petrology*, 52 (2), (1982) 431-450
- Cardona, J. P. M., Mas, J. M. G., Bellón, Á. S., Domínguez-Bella, S., & López, J. M. (2005). Surface textures of heavy-mineral grains: a new contribution to provenance studies. *Sedimentary Geology*, 174(3–4), 223–235. <https://doi.org/10.1016/j.sedgeo.2004.12.006>
- De Souza, A., & Filho, A. P. (2022). Scanning Electron Microscopy (SEM) in the surficial cover analysis of the low fluvial-marine terraces in the southern coast of São Paulo state, Brazil. *Revista Brasileira De Geomorfologia*, 23(1). <https://doi.org/10.20502/rbg.v23i1.1959>
- Dessai, A. G. (n.d.). *The geology of Goa Group: Revisited*. Geological Society of India. <https://www.geosocindia.org/index.php/jgsi/article/view/58235>

- Dora, G. U, Kumar, V. S, Philip, C. S., Johnson, G., Vinayaraj, P., Gowthaman, R., Textural characteristics of foreshore sediments along Karnataka shoreline, west coast of India. *International Journal of Sediment Research*, 26 (3), (2011), 364-377.
- Encyclopædia Britannica, inc. (n.d.). *Placer deposit*. Encyclopædia Britannica. <https://www.britannica.com/science/placer-deposit>
- Gandhi, M. S., Gayathri, G. S., Panicker, M., & Paul, S. S. (2023). Sediment Properties and Provenance Study of heavy minerals along Chinnavilai and Erayumanthurai Beach, south west coast of India. *Journal of Geosciences Research*, 8(1), 7–11. <https://doi.org/10.56153/g19088-021-0047-14>
- Garzanti, E., Padoan, M., Andò, S., Resentini, A., Vezzoli, G., & Lustrino, M. (2013). Weathering and relative durability of detrital minerals in equatorial climate: Sand petrology and geochemistry in the East African Rift. *The Journal of Geology*, 121(6), 547–580
- Gazi, M. Y., Tafhim, K. T., Ahmed, M. K., & Islam, A. K. M. S. (2019). INVESTIGATION OF HEAVY-MINERAL DEPOSITS USING MULTISPECTRAL SATELLITE IMAGERY IN THE EASTERN COASTAL MARGIN OF BANGLADESH. *Earth Science Malaysia*, 3(2), 16–22. <https://doi.org/10.26480/esmy.02.2019.16.22>
- Grain size analysis and depositional environment ... (n.d.-a). <https://www.ijstr.org/paper-references.php?ref=IJSTR-0816-14987>
- Grain size parameters and heavy minerals as indicators of depositional ... (n.d.). [https://www.researchgate.net/publication/268805633\\_Grain\\_size\\_parameters\\_and\\_heavy\\_minerals\\_as\\_indicators\\_of\\_depositional\\_environment\\_A\\_case\\_study\\_of\\_beach\\_sediments\\_from\\_Goa\\_India](https://www.researchgate.net/publication/268805633_Grain_size_parameters_and_heavy_minerals_as_indicators_of_depositional_environment_A_case_study_of_beach_sediments_from_Goa_India)

- Heavy Mineral Studies of beach sands of Vagathor, North Goa, India - IJMER. (n.d.-b). [http://www.ijmer.com/papers/Vol4\\_Issue8/Version-1/I0408\\_01-7078.pdf](http://www.ijmer.com/papers/Vol4_Issue8/Version-1/I0408_01-7078.pdf)
- Heavy minerals I N Alaskan beach sand deposits ... (n.d.-a). [https://dggs.alaska.gov/webpubs/mirl/report\\_no/text/mirl\\_n20.pdf](https://dggs.alaska.gov/webpubs/mirl/report_no/text/mirl_n20.pdf)
- *Heavy minerals*. Sandatlas. (n.d.). <https://www.sandatlas.org/heavy-minerals/>
- Kumar, M. P., Nagalakshmi, K., Prasad, T. L., Praveena, B., Thejovanth, Y., & Jayaraju, N. (2023). A study on seasonal dynamics of heavy mineral distribution and surface micro-textures of Beach sediment from Govindampalli – Durgarajupatnam Coast, East Coast of India. *Results in Earth Sciences*, 1, 100008. <https://doi.org/10.1016/j.rines.2023.100008>
- M. Suresh Gandhi, & AbstractThe main objectives of the present study are to understand the heavy mineral distribution. (2014, June 20). *Heavy Mineral Distribution and geochemical studies of coastal sediments between Besant Nagar and Marakkanam, Tamil Nadu, India*. Journal of Radiation Research and Applied Sciences. <https://www.sciencedirect.com/science/article/pii/S1687850714000557>
- Mange, M. A. (1991, January 1). *Heavy minerals in color*. AbeBooks. <https://www.abebooks.co.uk/9780412439100/Heavy-Minerals-Colour-Mange-Maria-0412439107/plp>
- Mange, M. A., & Maurer, H. F. W. (1992). *Heavy minerals in colour* (pp. 147). London: Chapman and Hall
- Mejía-Ledezma, R., Kasper-Zubillaga, J. J., Álvarez-Sánchez, L. F., Mendieta-Lora, M., Arellano-Torres, E., Tetlalmatzi-Martínez, J., González-Bermúdez, A., Patiño-Andrade, D., & Armstrong-Altrin, J. S. (2020). Surface textures of quartz and ilmenite grains from dune and beach sands of the Gulf of Mexico Coast, Mexico: Implications for fluvial,



aeolian and marine transport. *Aeolian Research*, 45, 100611.  
<https://doi.org/10.1016/j.aeolia.2020.100611>

- Microtextures of quartz grain surface from recent sedimentary environments along the Al-Khowkhah-al-Mokha coastal area, Southern Red Sea, Yemen | request PDF. (n.d.-c).  
[https://www.researchgate.net/publication/286390022\\_Microtextures\\_of\\_quartz\\_grain\\_surface\\_from\\_recent\\_sedimentary\\_environments\\_along\\_Al-khowkhah-Al-mokha\\_coastal\\_area\\_southern\\_Red\\_Sea\\_Yemen](https://www.researchgate.net/publication/286390022_Microtextures_of_quartz_grain_surface_from_recent_sedimentary_environments_along_Al-khowkhah-Al-mokha_coastal_area_southern_Red_Sea_Yemen)
- Natural Resources of Goa: A geological perspective. (n.d.-a).  
[https://www.researchgate.net/publication/274391057\\_Natural\\_Resources\\_of\\_Goa\\_A\\_Geological\\_Perspective](https://www.researchgate.net/publication/274391057_Natural_Resources_of_Goa_A_Geological_Perspective)
- panelMaria Augusta M. Da Silva, AbstractThe sands in the fore- and backshore zones between Rio Grande and Chui (Rio Grande do Sul State, Asmus, H. E., Bigarella, J. J., Butler, L. W., Carraro, C. C., Cordani, U. G., Gardner, D. E., Jost, H., Lambert, R., Martins, L. R., & MacColl, P. (2003, April 8). The provenance of heavy minerals in Beach Sands, southeastern Brazil: From Rio Grande to Chui (Rio Grande do sul state). *Sedimentary Geology*. <https://www.sciencedirect.com/science/article/pii/0037073879900332>
- panelMustafa Ergin a b, a, b, c, AbstractBackshore sediment samples from 22 beaches along the Antalya and Finike Gulfs have been studied for their grain size, Abuodha, J. O. Z., Dill, H. G., Frihy, O. E., Hounsflow, M. W., İşler, F. I., Jennings, R., Mange-Rajetzky, M. A., Morton, A. C., Okay, N., Schwartz, M. O., Anfuso, G., Berquist, C. R., Bridge, J. S., Chaudry, M. A., ... Gent, M. R. (2007, February 24). Grain size and heavy mineral distribution as related to the hinterland and environmental conditions for modern beach

sediments from the Gulfs of Antalya and Finike, Eastern Mediterranean. *Marine Geology*.

<https://www.sciencedirect.com/science/article/abs/pii/S0025322707000564>

- Perera, U., Ratnayake, A. S., Weerasingha, W. a. D. B., Subasinghe, H., & Wijewardhana, T. D. U. (2023). Grain size distribution of modern beach sediments in Sri Lanka. *Anthropocene Coasts*, 6(1). <https://doi.org/10.1007/s44218-023-00025-7>
- Pettijohn FJ (1984) *Sedimentary rocks*, 3rd edn. Harper and Row, New York, pp 1–614
- Principles of sedimentology and stratigraphy (4th edition): Boggs Jr., Sam: 9780131547285: Amazon.com: Books. (n.d.-f). <https://www.amazon.com/Principles-Sedimentology-Stratigraphy-4th-Boggs/dp/0131547283>
- R.S. Chaudhri 1, 1, 2, 3, AbstractSedimentological studies of 390 samples from Dwarka, Shepard, F. P., Allen, J. R. L., Asseez, L. O., Bagnold, R. A., Bascom, W. N., Bird, E. C. F., Chakrabarti, A., Chappell, J., Chaudri, R. S., Duane, D. B., Folk, R. L., Fraser, G. S., Friedman, G. M., Fuller, A. O., ... Inman, D. L. (2003, April 8). *Sedimentology of beach sediments of the West Coast of India*. *Sedimentary Geology*. <https://www.sciencedirect.com/science/article/abs/pii/0037073881900142>
- Rajganapathi VC, Jitheshkumar N, Sundararajan M, Bhat KH, Velusamy S (2013) Grain size analysis and characterization of sedimentary environment along Thiruchendur coast, Tamilnadu, India. *Arab J Geosci* 6(12):4717–4728
- Sakuna, D., Szczuciński, W., Feldens, P., Schwarzer, K., & Khokiattiwong, S. (2012, October 24). *Sedimentary deposits left by the 2004 Indian Ocean tsunami on the inner continental shelf offshore of Khao Lak, Andaman Sea (Thailand) - earth, planets and space*. SpringerOpen. <https://earth-planets-space.springeropen.com/articles/10.5047/eps.2011.08.010>

- Shalini, G., Hegde, V. S., Soumya, M., & Korkoppa, M. M. (2019, October 9). Provenance and implications of heavy minerals in the beach sands of India's Central West Coast. Allen Press. <https://meridian.allenpress.com/jcr/article/36/2/353/427116/Provenance-and-Implications-of-Heavy-Minerals-in>
- Singh, Y. (2020, April 18). *Rare earth element resources: Indian context: Ebook*. Barnes & Noble. <https://www.barnesandnoble.com/w/rare-earth-element-resources-yamuna-singh/1136166171>
- world thorium occurrences, deposits, and resources. (n.d.). [https://www.researchgate.net/publication/333999449\\_World\\_Thorium\\_Occurrences\\_Deposits\\_and\\_Resources](https://www.researchgate.net/publication/333999449_World_Thorium_Occurrences_Deposits_and_Resources)
- Yue, Y., Yue, Y., Panwar, Zhang, B., & Jin, J. (2019). The Chemical Composition and Surface Texture of Transparent Heavy Minerals from Core LQ24 in the Changjiang Delta. *Minerals*, 9(7), 454. <https://doi.org/10.3390/min9070454>